

I give permission for public access to my thesis and for copying to be done at the discretion of the archives' librarian and/or the Mount Holyoke College library.

Signature

Date

DIFFERENTIAL EXPRESSION OF AN ENDOGENOUS RETROVIRUS IN
MAIDS SUSCEPTIBLE (C57BL/6) *VERSUS* RESISTANT (BALB/C) MICE

By

Amanda Socha

A Paper Presented to the
Faculty of Mount Holyoke College in
Partial Fulfillment of the Requirements for
the Degree of Bachelors of Arts with
Honor

Department of Biological Sciences
South Hadley, MA 01075

May, 2006

This paper was prepared
under the direction of
Professor Sharon Stranford
for twelve credits

For my parents—My two best friends
and unwavering supporters

ACKNOWLEDGMENTS

First, I would like to thank my advisor Sharon Stranford for all of her guidance and encouragement. I am grateful to her for her faith in me and for giving me the opportunity to become a better scientist. The knowledge and experience I gained in her lab will benefit me throughout my scientific career.

I must also thank all of the women of the Stranford lab 2005-2006 for being such wonderful people. Their friendship and support has been invaluable. I am especially grateful to Smita for sharing her Real Time-PCR expertise and for always being willing to answer questions (even after midnight).

I would also like to thank Professor Craig Woodard for assisting me with the technicalities of DNA sequencing, Professor Sarah Bacon for the use of the Robocycler, and Professor Amy Springer for providing me with the tools to isolate DNA. I am very appreciative of all of the time and advice that they have given me throughout the year.

NIH and the Biology department of Mount Holyoke College should also be credited for their generosity in providing me with the funds to carry out my research project.

I must also thank all of my friends for putting up with me and supporting me through the years. Finally, I must thank my family for always being proud of me.

TABLE OF CONTENTS

	Page
List of Figures	vii
List of Tables	ix
Abstract	x
Introduction	1
MAIDS Small Animal Model System	3
Murine AIDS <i>versus</i> Human AIDS	3
Murine Leukemia Virus.....	5
Susceptibility to MAIDS	9
Microarray Data	10
Endogenous Retroviruses.....	14
The Retroviral Life Cycle	17
Categories of Endogenous Retroviruses	21
MCF Polytropic Virus Sequences.....	22
Human Endogenous Retroviruses.....	24
Tolerance.....	25
Real Time PCR	26
Research Objective	28
Materials and Methods	29
Animals	29
RNA Isolation from Spleen and Lymph Node	29

RNA Isolation from LP-BM5 Infected Mouse Fibroblast Cells.	32
RNA Concentration and Integrity Measurements.....	34
DNA Isolation from Naïve Mice	37
Creating PCR Primers.....	39
cDNA Synthesis.....	40
Reverse Transcriptase-Polymerase Chain Reaction (RT-PCR)...	41
PCR with Genomic DNA.....	42
Sequencing PCR Products	43
Quantitative Real Time PCR	45
Results	51
Confirming cDNA Synthesis	51
Primer Selection and Optimization.....	53
Naïve Mouse Genomic DNA.....	62
Non-Quantitative RT-PCR.....	64
Real Time PCR	73
Sequencing Data	88
Discussion	94
Optimizing RT-PCR Protocols and Primers.....	94
MCF-like Sequences in the Mouse Genome	97
Expression of MCF-like Sequences.....	97
Quantitation of MCF Expression using Real Time PCR.....	99
MCF Sequencing Analysis	104

Future Research	106
Conclusions.....	107
References	108
Appendix I	
Appendix II	

List of Figures

	Page
Figure 1. General Structure of a retrovirus virion and genome	7
Figure 2. A General Overview of a DNA-based Microarray Assay...	13
Figure 3. Illustration of a Typical Retrovirus Lifecycle	19
Figure 4. Integration of Viral DNA into Host Chromosomal DNA ...	20
Figure 5. Examples of RNA Samples with Good versus Poor Integrity	36
Figure 6. Real Time PCR Plate Design	47
Figure 7. RT-PCR of LP-BM5 Infected SC-1 Cells using β -actin Primers.....	52
Figure 8. RT-PCR of LP-BM5 Infected SC-1 Cells using Three MCF Primer Sets	57
Figure 9. RT-PCR of LP-BM5 Infected SC-1 Cells using MCF PS2 and MCF PS3 over a Range of Annealing Temperatures...	59
Figure 10. RT-PCR of RNA from Three Different Species	61
Figure 11. PCR using Genomic DNA.....	63
Figure 12. Electrophoretic Gel Showing Integrity of BALB/c and BL/6 mouse RNA	65
Figure 13. Histograms Showing Integrity of BALB/c and BL/6 RNA mouse RNA	66

Figure 14.	Bioanalyzer Results of RNA Isolated from LP-BM5 Infected SC-1 Cells.....	68
Figure 15.	RT-PCR using MCF Primer Set 1	70
Figure 16.	RT-PCR using MCF Primer Set 3	72
Figure 17.	RT-PCR with Varying Primer Concentrations.....	74
Figure 18.	Plot of Log Template Input <i>versus</i> the Ct of β -actin.....	77
Figure 19.	Plot of Log Template Input <i>versus</i> the Ct of MCF PS1	78
Figure 20.	Plot of Log Template Input <i>versus</i> the Ct of MCF PS3	79
Figure 21.	Plot of the MCF PS1 Validation Experiment.....	81
Figure 22.	Plot of the MCF PS3 Validation Experiment.....	82
Figure 23.	Fold Differences in Expression of MCF in BALB/c and BL/6 mouse Lymphoid Tissues	87
Figure 24.	Comparison of PCR Product Sequences using MCF PS1 Forward.....	90
Figure 25.	Comparison of PCR Product Sequences using MCF PS1 Reverse	91
Figure 26.	Comparison of PCR Product Sequences using MCF PS3 Forward.....	92
Figure 27.	Comparison of PCR Product Sequences using MCF PS3 Reverse	93

List of Tables

	Page
Table 1. Forward and Reverse Primer Sequences for β-actin, MCF PS1, MCF PS2, and MCF PS3	54
Table 2. Raw Data Regarding Integrity and Concentration of Naïve Mouse RNA	67
Table 3. qRT-PCR Validation experiment data	76
Table 4. Ct Values for the Reference Gene used in the Experimental Plate	84
Table 5. Real Time PCR Data using MCF PS1 and MCF PS3	85

ABSTRACT

Murine acquired immunodeficiency syndrome (MAIDS) is a retrovirus-induced disease in mice that results from infection with a specific mixture of Murine Leukemia Virus (MuLV) known as LP-BM5. The two strains of mice used in this research are either the disease susceptible strain (C57BL/6 or BL/6) or the disease resistant strain (BALB/c). The Tepsuporn thesis in the Stranford lab at Mount Holyoke College generated differential gene expression data from a DNA-microarray based assay of MAIDS susceptible *versus* resistant mice that were either injected with virus or mock supernatant. One gene in particular, mink cell focus-forming virus (MCF), had a 55-fold higher expression in disease susceptible mice when compared to resistant mice under any conditions. MCF is a component of LP-BM5 MuLV and was originally used to track virus expression in host cells. The objective of this research is to utilize Reverse-Transcriptase PCR and Real-Time RT-PCR to determine whether or not MCF is found in the genome of mice and expressed as mRNA. Data shows that both BL/6 and BALB/c mice, when naïve from injection with virus or mock supernatant, expressed MCF mRNA in both the spleen and the lymph node and contained MCF in their genomes. Real time RT-PCR data analysis suggests that naïve mice express higher levels of MCF-like mRNA in the BL/6 mice when compared to the BALB/c mice; this information contradicts the microarray data. It is possible that prior to infection with virus or mock supernatant, MCF-like sequences are suppressed in BALB/c mice and upregulated in BL/6 mice. Future studies of MCF and its implications disease pathogenesis may lead to a better understanding of the immune response to HIV and discover new factors that contribute to human susceptibility to AIDS.

INTRODUCTION

Acquired immune deficiency syndrome (AIDS) is a widespread epidemic that has plagued the world for over 20 years (Mosier, 1996). In 2004, close to 3 million people worldwide were known to have died from AIDS. As of 2005 there are approximately 40 million people living with human immunodeficiency virus (HIV), the retrovirus shown to induce onset of AIDS in humans (Jolicoeur et al., 1991; UNAIDS fact sheet, 2005). Sub-Saharan Africa is home to 60 percent of those infected with HIV despite it holding only 10 percent of the world's population. Alarming, East Asia, Eastern Europe, and Central Asia have seen a 9-fold increase in HIV infection in just 10 years (UNAIDS fact sheet, 2005).

Since the identification of HIV in the early 1980s, various antiretroviral drugs have been developed in order to decrease viral loads in the blood and control virus spread in humans by interfering with the replication of the virus (AIDSinfo, 2005). However, there is currently no cure or vaccine for the retrovirus. Much of the delay in developing a functional curative agent for HIV is due to limited knowledge of the molecular and cellular mechanisms by which the retrovirus induces immunodeficiency (Jolicoeur et al., 1991). Many studies regarding HIV have focused on the patients who are able to naturally combat HIV infection in hopes of developing new treatment techniques. A group of HIV infected individuals, clinically known as long-term nonprogressors (LTNR), comprise approximately 5-10% of those living with HIV (Lange and Lederman, 2003). The LTNR phenotype is characterized by the patient's ability to suppress

viral replication, thereby decreasing viral titers in the blood. In addition, the immune system can remain functional for more than 10 years without the assistance of antiretroviral therapy. It should be noted that while LNTRs do not progress to AIDS, they lack the ability to eradicate HIV (Miedema et al, 1988; Lange and Lederman, 2003; Sankaran et al, 2005).

In hopes of better understanding the differential immune response that provides certain individuals with the ability to combat HIV, various animal models have been developed. Studies of the various animal models and the identification of effective and ineffectual immune responses to infection can help contribute to eliciting a successful antiretroviral immune response in humans. The goal of this research is to examine unique features that distinguish between AIDS susceptible and resistant organisms. Data from a previously completed DNA-based microarray assay, which provided information regarding differential gene expression patterns early in the immune response between disease resistant *versus* disease susceptible mice, were analyzed. From these data one highly differentially expressed gene that structurally resembles the AIDS inducing retrovirus was chosen for further study in hopes of elucidating certain factors that designate susceptibility or resistance to AIDS.

MAIDS Small Animal Model System

Due to the continuing threat of HIV and AIDS, animal models using similar but not identical viruses have been used. Some examples of animal models for AIDS include simian immunodeficiency virus (SIV), feline immunodeficiency virus infection (FIV) and infection of immunodeficient transgenic mice (SCID mice) with HIV-1 (Jolicoeur, 1991; Jolicoeur, et al., 1991). However, such animal models require high levels of biohazard control and special animal training to utilize. Mice are arguably the most popular organisms chosen for study due to the extensive knowledge of their genome and immune system (Mosier, 1996). In this study, the model system of choice is murine AIDS (MAIDS), which remains one of the most extensively studied and convenient model systems for human AIDS.

Murine AIDS versus human AIDS

Human AIDS is a disease induced by infection with a retrovirus from the lentivirus family known as HIV. MAIDS, on the other hand, is caused by a unique mixture of pathogenic, defective, and helper viruses designated the LP-BM5 isolate of Murine Leukemia Virus (MuLV) (Jolicoeur, 1991; Morse, et al., 1992; Mosier, 1996). MAIDS acquired its name due to the prominent similarities of the MuLV induced disease and human AIDS, along with its induction by a retrovirus (Mosier et al., 1987). Such similarities include increased lymphoproliferation, polyclonal B cell expansion, and enlargement of lymphoid

organs such as the spleen and lymph node (Morse et al., 1992). The effects of MuLV and HIV lead to uncontrolled virus spread, impairment of the immune system, and increased susceptibility to opportunistic infections (Jolicoeur, 1991; Liang et al., 1996).

While the MAIDS model system is an excellent animal model for studying the immune system pathways in response to retroviral infection, it is not without faults: the retroviruses that cause MAIDS and AIDS differ. HIV is a retrovirus from the lentivirus family, while MuLV is a C-type retrovirus from the oncornavirus family (Mosier, 1996). Also, the cells targeted by HIV infection are CD4⁺ T cells and macrophages, while MuLV targets primarily B cells and macrophages (Morse et al., 1992; Mosier 1996).

Despite the previously mentioned differences, the MAIDS model is still important because it is practical, cost effective and simple to work with. MuLV is not easily transmitted between mice and has not been found to infect humans, resulting in a lower biohazard level required to work with the virus. In addition, the comparable clinical symptoms of HIV and MuLV could be due to similar pathways utilized by the immune system. As a result, a better understanding of the immune response to MuLV infection could provide information regarding the immune pathways used during HIV infection. Other animal models, such as the Simian Immunodeficiency Virus (SIV) model can be used to study AIDS. However, while SIV may be a lentivirus like HIV, the disease it induces has greater dissimilarities to human AIDS than does MAIDS (Jolicoeur et al., 1991).

Therefore, while MAIDS and AIDS may have differences, their striking similarities have made a valid model system of MAIDS.

Murine Leukemia Virus

Murine Leukemia Virus (MuLV) was first discovered in the early 1900s when isolated from the mammary carcinomas (Ehrlich's carcinomas) of female mice (reviewed in Clark et al., 2001). In 1962, Laterjet and Duplan recognized that a specific laboratory isolate of the virus, when injected into a specific strain of mouse caused a disease, now termed MAIDS, in nearly 100% of infected mice (Jolicoeur, 1991; Laterjet and Duplan, 1962). The specific virus utilized by Laterjet and Duplan was a radiation induced MuLV line, termed RadLV-R, which underwent further manipulations to produce LP-BM5 MuLV (Mosier et al., 1985).

The MuLV genome consists of three main structural genes: *gag* (core proteins), *pol* (polymerase), and *env* (envelope) (See figure 1). The *gag*, or group specific antigen, gene is responsible for encoding proteins that make up the viral matrix, capsid and nucleoproteins, which constitute the viral core (Taruscio and Mantovani, 2004; Nolan, 2006). The *pol* gene allows for reverse transcription of viral RNA into viral DNA and integration of the viral DNA into the host genome by encoding for reverse transcriptase, protease and integrase enzymes (Taruscio and Mantovani, 2004; Nolan, 2006). The *env* gene codes for surface glycoproteins and transmembrane polyproteins. The transmembrane protein will

eventually be altered to form the glycoprotein present on the viral envelope (Taruscio and Mantovani, 2004; Nolan, 2006). Long terminal repeats (LTR) are also an important component of the genomic structure of a retrovirus. LTRs are repeating sequences of DNA, which are several hundred nucleotides long and located at the 5' and 3' ends of the proviral genome (Taruscio and Mantovani, 2004; Nolan, 2006). The LTRs contain regulatory regions, such as a promoter, enhancer binding motifs, and polyadenylation signals in their structure, which allow them to direct viral expression and viral replication (Chattopadhyay et al., 1991; Taruscio and Mantovani, 2004; Nolan, 2006).

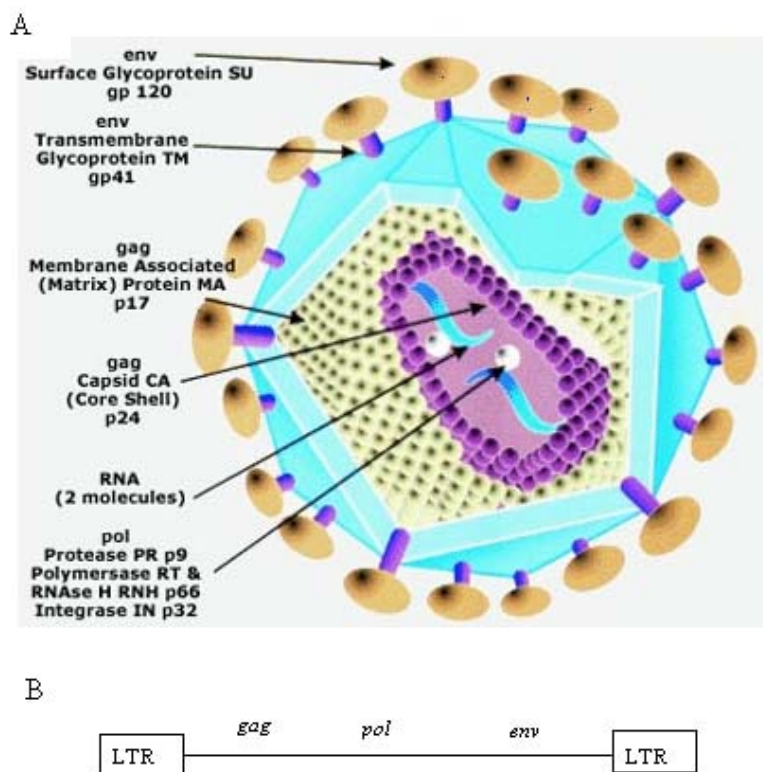


Figure 1: (A) General structure of a retrovirus virion, emphasizing the products of the three main viral genes: *gag*, *pol*, and *env*. The *gag* gene encodes for viral core proteins such as the matrix, nucleoproteins and capsid. *Env* is responsible for synthesis of transmembrane and glycoproteins of the viral envelope, and *pol* encodes for essential enzymes such as reverse transcriptase, protease and integrase.

(B) Typical structure of the retroviral genome, showing the locations of the LTR, *pol*, *env*, and *gag* genes relative to one another. (Adapted from:

<http://www.stanford.edu/group/nolan/tutorials/ret_6_gpedesc.html>).

The specific mixture of MuLV used in these studies, termed LP-BM5, is comprised of three distinct types of viruses: ecotropic (a retrovirus that can only replicate in the species in which it was originated), mink cell focus forming (MCF), and defective (BM5d). The first component mentioned is a non-pathogenic, replication competent, B-tropic ecotropic full-length viral sequence (BEV). The B-tropic designation of the ecotropic portion of LP-BM5 is significant due to the fact that the virus can only grow in mice homozygous for the B allele at the *Fv-1* locus (Risser et al., 1983; Amadori and Cjiec-Bianchi, 1989; Morse et al., 1992). N-tropic viruses will show efficiency of replication in cells from mouse strains with the N allele at the *Fv-1* locus as opposed to the B allele at the *Fv-1* locus (Risser et al., 1983; Morse et al., 1992). Interestingly, cells heterozygous for the B and N allele will restrict viral replication of both N-tropic and B-tropic viruses due to the co-dominance of the B and N alleles. The mice used in this study are homozygous for the B allele, therefore B-tropic sequences can enter and grow in their cells (Risser et al., 1983; Amadori and Cjiec-Bianchi, 1989; Morse et al., 1992).

The second virus component of the LP-BM5 viral mixture is the B-tropic mink cell focus-inducing virus (MCF). MCF is a polytropic virus, which means that it can replicate in various host tissues (Morse et al., 1992). An ecotropic portion of another virus that recombines with a yet unidentified noncotropic MuLV-like sequence encodes the MCF viral sequence. Through the act of recombination, a new virus species (MCF), with a more extensive host range and

cell binding specificity, is produced (Khan, 1984). The MCF portion of LP-BM5 serves a helper virus to allow for spread of infection in host cells along with enhanced virus replication (Cook et al., 2002; Morse et al., 1992).

The BM5d viral fragment of LP-BM5 is a defective virus sequence devoid of the *pol* and *env* genes along with a truncated *gag* sequence from the original ecotropic MuLV. The resulting BM5d is a 4.9 kb replication incompetent defective virus fragment that can cause disease. The defective portion of LP-BM5 is dependent on MCF to facilitate virus intake by the host cells and subsequent viral proliferation (Cook et al., 2002; Morse et al., 1992). Therefore, while BM5d is responsible for inducing MAIDS, the defective virus requires helper viruses such as BEV and MCF to facilitate transmission and spread of MuLV in the host cells (Liang et al., 1996; Morse et al., 1992).

Susceptibility to MAIDS

The two mouse strains most often used to study MAIDS are C57BL/6, or BL/6 (BL/6/disease susceptible) and BALB/c (disease resistant). BL/6 mice are susceptible to developing MAIDS after being infected with LP-BM5 MuLV (Hartley et al., 1989; Morse, 1992). The susceptible strain will exhibit symptoms similar to human AIDS and eventually die from opportunistic infection or pulmonary compromise as a result of enlarged lymph nodes blocking the air passage. (Hartley et al., 1989; Morse, 1992). However, the BALB/c disease resistant mice mount an effective immune response to MuLV, eradicate the virus

and eventually become resistant to further challenges by the virus (Jolicoeur, 1991; Panoutsakapoulou et al., 1998). Comparisons of BALB/c and BL/6 strain responses to MuLV are important because these animals could reveal particular factors that allow one mouse strain to be more susceptible to disease while the other remains resistant.

Microarray Data

One of the hypotheses of the Stranford lab at Mount Holyoke College is that strain-specific gene expression patterns early on in the immune response may distinguish MAIDS susceptible *versus* resistant animals. A DNA-microarray based assay, which generates an organized array where each gene of a specific organism's genome is represented as a distinct spot, was used to compare differential gene expression between disease susceptible mice and disease resistant mice at 3 and 7 days post infection (Tepsuporn, 2005).

A microarray experiment requires RNA isolated from two distinct cell types (i.e. MuLV-infected cells and mock-infected cells or infected BALB/c versus BL/6 cells), which is used as a template for cDNA synthesis (See figure 2) (Young, 2000). The cDNA is then labeled with a dye, one for each cell type (either red or green), and combined in equal amounts to hybridize to the array of genome probes. Each probe is composed of oligonucleotides located on the surface of the microarray slide (Young, 2000; Tepsuporn, 2005). In addition to the standard probes used in microarray analysis, our arrays include 4 additional

probes specific to sequences from each of the three virus components (MCF, BM5d, and BEV) and an endogenous mouse ecotropic virus sequence control (ECO) (Tepsuporn, 2005). The microarray is scanned using a two-wavelength laser scanner once hybridization is complete in order to detect fluorescence intensity. If a probe hybridizes to only red or only green, then the specific mRNA transcript is only expressed in one of the two samples, while a yellow color concludes that the mRNA transcript is present in both cell types (Tepsuporn, 2005). Abundance of the original mRNA transcript can also be detected since the mRNA concentration is directly proportional to fluorescent intensity (Young, 2000; Tepsuporn, 2005).

Data from a previously performed DNA-microarray experiment compared MuLV- infected disease susceptible (BL/6) mouse gene expression to MuLV- infected disease resistant (BALB/c) gene expression. Another set of microarrays compared mock-infected disease susceptible and disease resistant mice (Tepsuporn, 2005). From analysis of these microarray experiments, genes that showed significantly different levels of expression between the two mouse strains can be chosen for further study.

For my research project, I chose to study the most highly differentially expressed gene between the two mouse strains: MCF. Disease susceptible mice, either infected with MuLV or mock infected, had a near 55-fold increase in expression of mink cell focus forming virus in comparison to disease resistant mice under any conditions (Tepsuporn, 2005). The MCF probe was originally

added to the microarray to track expression of the virus in host cells. However, it appears that an MCF-like sequence may be present in disease susceptible mice and is hypothesized to be an endogenous “MCF-like” retrovirus present in the BL/6 genome.

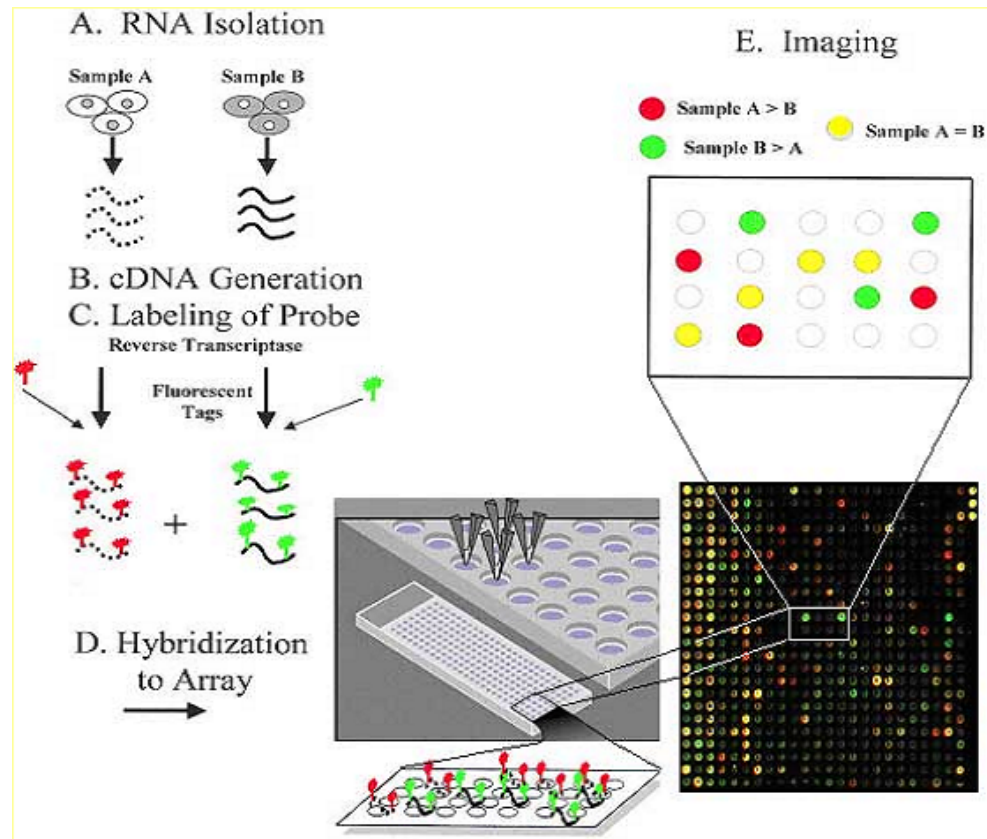


Figure 2: A general overview of a DNA-microarray based assay. RNA is isolated from two distinct cell types and used as templates for cDNA synthesis. The cDNA from the two cells types is labeled with a red or green dye and hybridized to an oligonucleotide probe on the surface of a microarray slide overnight. The microarray is scanned using a two-wavelength laser scanner once hybridization is complete in order to detect fluorescence intensity of each distinct gene spot. A green or red spot indicates that the mRNA is specific to only one of the cell types, while a yellow spot indicate that the mRNA transcripts can be found within both cell types. (Adapted from:

<http://www.fao.org/DOCREP/003/X6884E/x6884e00.jpg>)

Endogenous Retroviruses

Endogenous retroviral-like elements (ERVs) are estimated to comprise between 5-10% of all organism's genomes (Fine and Sodroski, 1981; Taruscio and Mantovani, 2004). ERVs are defined as transposable genetic elements that are highly homologous to retroviruses and utilize RNA intermediates and reverse transcriptase during their replication cycles (Fine and Sodroski, 1981; Blatt et al., 1983; Stevens et al., 1999; Taruscio and Mantovani, 2004). A typical ERV exhibits significant structural similarities to exogenous (coming from outside of the body) retroviruses with LTRs at the 3' and 5' ends, which flank *gag*, *env*, and *pol* in the internal coding region.

As mentioned previously, LTRs regulate gene expression, thus endogenous (originating from within an organism) retroviruses have the ability to be transcribed into mRNA or retrovirus-like particles (Taruscio and Mantovani, 2004). The probability of spontaneous expression appears to be regulated by location of ERVs in the genome. One hypothesis is that when DNA surrounding ERVs are activated by mitogens, the secondary effect is the subsequent expression of nearby genes (Risser et al., 1983; Krieg et al., 1988). Another theory suggests that gene expression is intrinsic to the viral genome; therefore varying levels of ERV mRNA are governed by distinct ERV regulatory sequences (Risser et al., 1983). In addition, ERV expression can also be attributed to factors such as inflammation due to injury, radiation, toxic chemicals, and activation of the immune system (Stevens et al., 1999). It should be noted that while ERVs

have been demonstrated to be transcribed and translated like other genes, they lack introns, and can be translated without undergoing splicing (Gourley, et al., 1990)

While many ERVs can be transcribed and translated, most are not infectious or functional due to structural defects (Fine and Sodroski, 1981). Defects include deletion of the entire coding region, leaving only the LTR intact. However, more subtle flaws in the ERV structure include frameshift mutations, point mutations and deletions in the gag and env initiation codons that have occurred during integration or have accumulated over time. As a result, most ERVs are not full length and have an incomplete retroviral structure. Stop codons are also known to be present in ERV open reading frames, thus halting complete gene expression (Fine and Sodroski, 1981; Krieg et al., 1992; Taruscio and Mantovani, 2004).

While most retroviruses integrated into the genome are not pathogenic, a few examples exist in which ERVs are responsible for causing disease. Mouse mammary tumor virus (MMTV) is a type B ERV that induces mammary cancer in mice through insertional mutagenesis. Insertional mutagenesis occurs when a “silent” region of genomic DNA is mutated due to insertion of nucleotides. The presence of the additional base pairs alters the function of the previously “silent” gene, which in the case of MMTV mutagenesis causes breast cancer.

Another pathogenic ERV is found in ARK mice, in which complex recombination of the endogenous retroviral sequences will lead to T-cell

lymphoma followed by death of the mice by the age of 2 (Pogo et al., 1997; Stewart et al., 2000; Stewart 2002). However, replication competent pathogenic ERVs are uncommon for the obvious reason that they are evolutionarily unfavorable and the organism would most likely not survive to pass on the gene. Since most ERVs are not harmful it is highly plausible that they would survive in the gene pool (Krieg et al., 1992).

The popular hypotheses regarding initial ERV integration into the mammalian genome is that they originated due to transposition and recombination of ancestral retroelements or by infection of ancient germ-cells by an exogenous retrovirus (Obata and Khan, 1988; Taruscio and Mantovani, 2004). Then, during evolution, ERVs spread throughout the genome as a result of amplification and repeated events of reintegration of the reverse-transcribed provirus mRNA (a process called retrotransposition) (Seifarth et al., 2005). Whether pathogenic or defective, ERVs were integrated into genomic DNA through an integrase-mediated process, which is demonstrated by the junction between the LTR of the retrovirus and the host DNA. Once the ERVs become a part of an organism's genome they are inherited vertically between generations. Due to the variation between type and abundance of ERVs between species, whether closely or distantly related, it is believed that integration of viral DNA occurred later during evolution and after divergence of closely related species (Fine and Sodroski, 1981).

The Retroviral Life Cycle

As mentioned previously, the derivation of ERVs from exogenous retroviruses is due to an integrase-mediated process, which happens to occur during infection of a host with a retrovirus. While the actual lifecycle of a retrovirus is extraordinarily complex and not completely understood, a general overview of the process is essential to comprehending the mechanism by which ERVs become inserted into host chromosomal DNA. (See figures 3 and 4 for representations of the retroviral lifecycle and viral DNA integration into host DNA).

A retrovirus is a small virion with a genome that consists of two RNA molecules (See figure 1A). The glycoproteins located on the viral envelope act as ligands, which specifically bind to a surface molecule of a cellular membrane (LP-BM5 MuLV uses B-tropic *FV-I* receptors to bind to host cells). After the binding of the retrovirus to the surface of a cell, fusion of the virus-cell membrane occurs, which allows the contents of the virion to enter the cell's cytoplasm (Fine and Sodroksi, 1981; White and Fenner, 1994). Once the virion has penetrated the cell surface it is stripped of its membrane coat (Fine and Sodroksi, 1981; White and Fenner, 1994). The RNA from the retrovirus is reverse transcribed using an RNA-dependent DNA polymerase (i.e. reverse transcriptase enzyme) carried by the virus and encoded by the virus's *pol* gene, into a double stranded DNA-RNA molecule (Krieg et al. 1992). Reverse transcriptase then acts as a nuclease to remove the RNA and synthesize a double stranded DNA molecule. The double

stranded viral DNA is then transported to the nucleus and integrated into the host cell chromosomal DNA using a viral protein known as integrase (Krieg et al. 1992). Once the viral DNA is inserted into the host cell DNA it is known as a provirus and becomes a stable and permanent part of the host genome, which can be transcribed, translated, and inherited (if integration occurs in germ cells) like all other genes (Krieg et al. 1992).

Replication of the viral DNA is dependant on the activity of the cell; therefore a provirus can remain dormant for long periods of time. As previously described, the cellular enhancer sequences within the provirus LTR can be activated by other exogenous signals such as infectious agents (Fine and Sodroksi, 1981; White and Fenner, 1994). Once provirus expression is initiated, the sequence will be transcribed by the host cell's RNA polymerase II (Fine and Sodroksi, 1981; White and Fenner, 1994). Then, RNA for the viral genome is created along with translation of the mRNA essential to production of the viral components (such as envelope glycoproteins, transmembrane proteins, and proteins essential to the viral core) (Fine and Sodroksi, 1981; White and Fenner, 1994). Viral proteins are subsequently glycosylated and cleaved using host cell enzymes (Fine and Sodroksi, 1981; White and Fenner, 1994). Afterwards, the virus is assembled, using the host cell's plasma membrane as its new envelope (Fine and Sodroksi, 1981; White and Fenner, 1994). Newly formed viruses exocytose from the cell in a process called "budding"; cell death can result from an excess of virus budding (Fine and Sodroksi, 1981; White and Fenner, 1994).

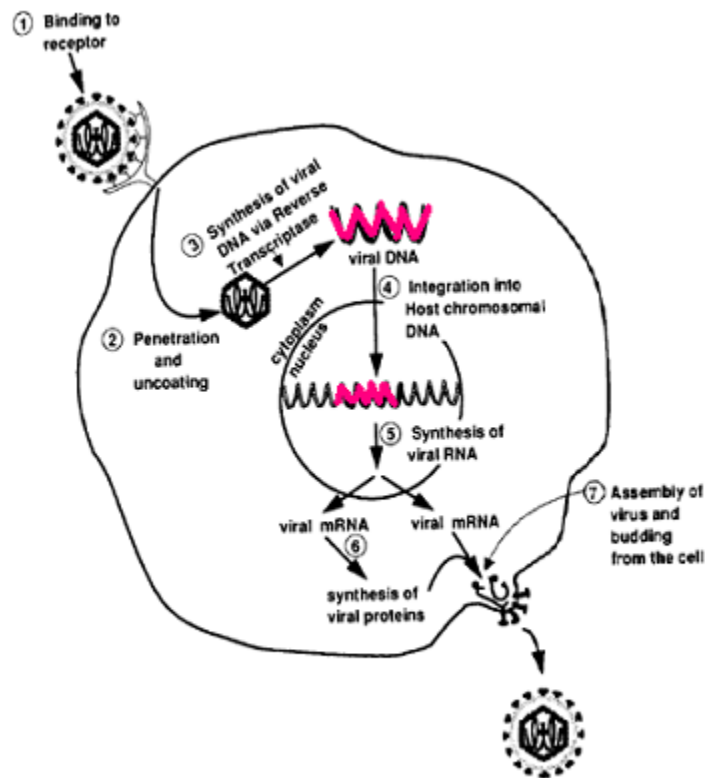


Figure 3: Illustration of a typical retrovirus lifecycle. First, the virus binds to a specific receptor on a host cell and is subsequently integrated into the cytoplasm and stripped of its surface coating. An RNA-dependant DNA polymerase reverse transcribes the retrovirus's RNA genome into double stranded viral DNA. Integrase transcribed from the virus initiate integration of the viral DNA into host cell chromosomal DNA. Retroviral transcripts formed using transcriptional machinery of the host cell will synthesize viral proteins. Viral proteins will be assembled into new virions that will exocytose from the cell in a process called budding. (Adapted from:

http://www.chem.wisc.edu/~newtrad/CurrRef/AIDStopic/AIDSfig/1_10.gif)

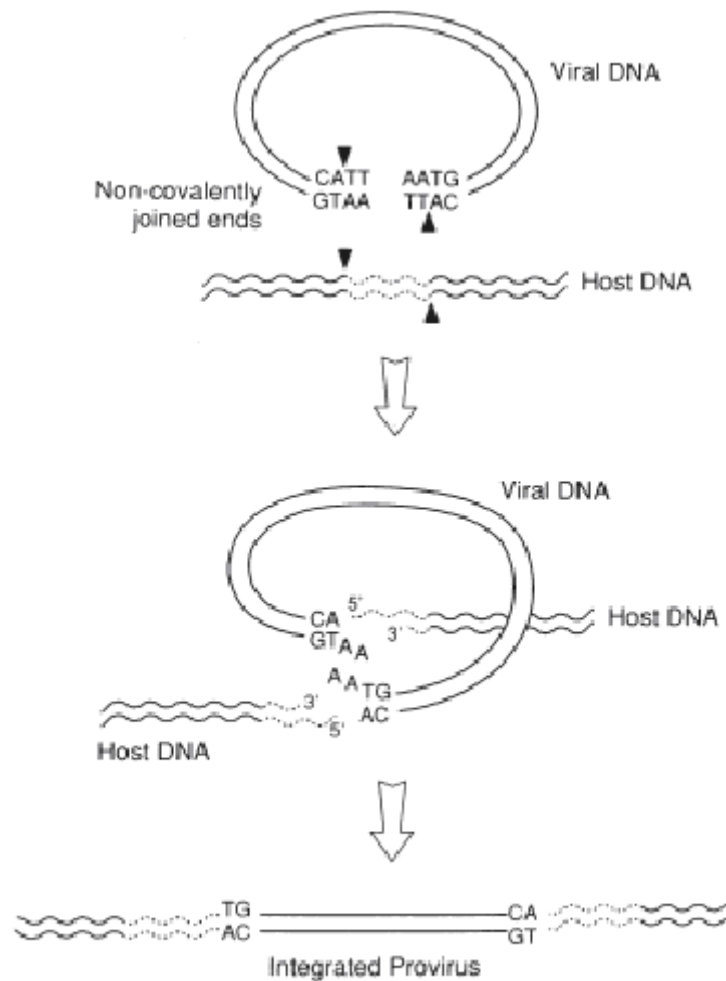


Figure 4: Integration of viral DNA into host chromosomal DNA. Double stranded viral DNA, reverse transcribed from viral RNA along with a piece of the host DNA are cleaved by the integrase enzyme produced by the *pol* gene of the retrovirus. Two base pairs are deleted from the retroviral DNA and four to six base pairs of are duplicated from the host DNA. The result is a stably integrated viral sequence in the host genome, called a provirus. (Adapted from Fine and Sodroski, 1981)

Categories of Endogenous Retroviruses

Inbred strains of laboratory mice are just one of the organisms known to contain ERVs in their genome. The ERVs within mouse DNA resemble the type C MuLV that is used in the MAIDS model system. These MuLV-like sequences are categorized into two main groups by their different host ranges (i.e. infectivity), which are determined by the viral envelope surface glycoproteins: the two groups are ecotropic and nonecotropic. The ecotropic virus sequence, which infects only murine cells, is present in one to five copies in most laboratory mice (Tomonaga and Coffin, 1999). The disease resistant mice are known to be a low ecotropic strain, with only one complete copy of the ecotropic provirus in their genome. However, the level of ecotropic virus in disease susceptible mice is yet to be determined (Chattopadhyay et al., 1980).

The nonecotropic groups of endogenous MuLVs are divided into the three subgroups of xenotropic, polytropic and modified polytropic. The xenotropic viral sequences can only infect cells from species other than the mouse, such as human, mink, duck, and rabbit. Polytropic and modified polytropic virus sequences can infect both mouse and non-mouse cells. Each of the nonecotropic viruses exhibit limited genetic variation between sequences and are prevalent throughout the genome (Tomonaga and Coffin, 1999; Krieg et al, 1998). The three nonecotropic virus groups are distinguishable in the mouse genome due to polymorphisms found in the *env* and LTR gene regions (Tomonaga and Coffin,

1999). The *gag* and *pol* genes are the most conserved between the endogenous MuLVs (Risser et al., 1985; Gourlet, et al., 1990).

MCF Polytropic Virus Sequences

The possible presence of MCF-like polytropic endogenous virus sequence in the mouse genome is the basis for my research based on microarray data in the Stranford lab. The microarray assay suggests MCF is the most highly differentially expressed gene between disease susceptible and resistant mice under any conditions (Tepsuporn, 2005). The MCF detected in the microarray is thought to be an endogenous MCF-like sequence, since they are highly homologous to the infectious retrovirus and are expressed in mice that are not exposed to the virus (Blatt et al., 1983; Krieg et al., 1988).

Previous studies, which mapped the chromosomal locations of various MCF-like sequences, show that these genes are located near genes involved in the immune response. Such genes include those of the heavy and light chains of immunoglobulin (Ig) molecules, genes encoding lymphocyte antigens and the allotype determinants on B and T lymphocytes (Blatt et al., 1983; Krieg et al., 1988). However, the regulation of expression of these endogenous MCF-related sequenced remains unknown and the biologic significance of endogenous MCF-like sequence expression prior to immune system activation is unclear (Obata and Khan, 1988; Krieg et al., 1988; Krieg et al., 1989). Although, some studies have shown that B and T cell mitogens (agents that induce cell division) could be

involved in inducing expression of the retroviral proteins in the lymphoid tissues of mice (Obata and Khan, 1988; Krieg et al., 1988; Krieg et al., 1989).

Studying the function of ERVs such as MCF-like sequences in host cells along with their interactions with the immune system is an arguably important research topic. This is because the analysis of the role of ERVs in physiology and disease can provide valuable insight into the normal cellular activation mechanisms, regulation of gene activation, co-evolution of ERVs in a host, and the interactions between host and retrovirus (Krieg et al, 1988; Tomonaga and Coffin, 1999). In addition, understanding ERVs is important in the study of MAIDS due to their plausible relationship to disease pathogenesis as a result of their structural similarities to LP-BM5 MuLV (Blatt et al. 1983).

Some ERVs have been found to have beneficial effects in certain strains of mice. One endogenous retrovirus in mice is known to encode surface glycoproteins that can defend against a specific retrovirus (Cas BrE MuLV) infection by blocking the binding of the infectious retrovirus to receptor molecules on host cells (Fine and Sodroski, 1981; Krieg et al., 1992). Also, Gardner and colleagues (1991) studied feral mice resistant to retrovirus infection, which they attributed to a truncated provirus within the mouse genome. Immunity against infection is a possible reason for the conservation of ERVs throughout evolution (Krieg et al., 1992).

However, ERVs have also been found to be detrimental to an organism's survival. One proposed theory links endogenous MCF expression to the

suppression of lymphocyte activation, thus delaying the immune system from mounting an effective immune response (Krieg et al., 1989; Krieg et al., 1992). The transmembrane and surface glycoproteins in particular are thought to trigger inhibition of lymphocyte activation. These proteins could induce a negative feedback mechanism involved in immune homeostasis that turns off immune cells when MCF mRNA is translated (Krieg et al., 1989; Krieg et al., 1992). Therefore, expression of the *env* portion of endogenous MCF-like sequence is thought to have inhibitory effects since the *env* gene is responsible for encoding the inhibitory proteins (Krieg et al., 1989; Krieg et al., 1992).

Human Endogenous Retroviruses

Human endogenous retroviruses (HERVs) are similar to other endogenous retroviruses, except they tend to not be as active and to show less homology to infectious retroviruses (Taruscio and Mantovani, 2004). However, there are HERVs that are similar to HIV. As a result, extensive research has been done to determine whether HERVs behave similarly to ERVs in mice. Since defective exogenous retroviruses have been demonstrated to recombine with ERVs in animals such as mice and form new infectious retrovirus, researchers have theorized that HIV may recombine with HERVs (Krieg et al. 1992; Taruscio and Mantovani, 2004). Yet, to date, there are no known infectious HERVs and further research is required to determine whether they affect the immune system (Krieg et al. 1992; Taruscio and Mantovani, 2004).

HERVS are expressed in various human tissues such as those of the reproductive tract, lymphocytes, and monocytes, which suggest that HERV LTRs are functional and allow for transcription (Seifarth et al., 2005). As with other known ERVs, HERV expression is assisted when the endogenous retrovirus is located in a transcriptionally active genome locus (Seifarth et al., 2005). In 1999, a study was conducted that correlated increased anti-HERV antibodies in urine with later stages of HIV disease progression. Interestingly, asymptomatic patients and LTNP showed no HERV antibodies in their urine (Stevens et al., 1999). There are also HERVs that are capable of inhibiting or downregulating the immune system, much like MCF-like sequences are suspected to hinder immune activation in mice (Urnovitz and Murphy, 1996).

Tolerance

Tolerance is the ability of the body's lymphocytes to ignore self proteins and antigen but respond to foreign entities such as viruses and bacteria. Immune cell tolerance is essential to an organism's health because recognition of self as foreign would lead to autoimmune disease (Parham, 2005). The deletion of immune cells that would attack self occurs in the thymus early during development. A class of lymphocytes known as helper T cell (because they help activate other lymphocytes) will come in contact with self proteins that circulate through the thymus (Parham, 2005). If the T cell binds to a protein it will be deleted from the T cell repertoire in a process called clonal deletion (Parham,

2005). If proteins translated from MCF-like sequences were present within the thymus during creation of the T cell repertoire, then MCF could be recognized as self, causing the animal to ignore the MCF component of LP-BM MuLV.

According to Khan (1984), ERVs are expressed in the thymus, which could implicate them in autoimmune diseases or even thymic lymphomas. In cases involving thymic lymphomas, the LTR of endogenous MCF appears to remain functional and will facilitate enhanced transcription and translation of the ERVs in cells of the thymus (Khan, 1984). Of particular interest is whether or not MCF-like proteins in the thymus could also impact development of T cells by inducing tolerance of immune cells to antigens that resemble these MCF proteins (Krieg et al., 1992).

Real Time PCR

Real-Time Polymerase Chain Reaction (qRT-PCR) is a method of quantitative amplification used to compare levels of gene expression between mouse strains (Dorak, 2004). qRT-PCR requires RNA isolated from two different cell types (i.e. disease susceptible versus disease resistant mice) to be reverse transcribed into cDNA. The cDNA will then undergo amplification during PCR. The advantage of qRT-PCR is that it measures cycle by cycle amplification of template, not just the endpoint product. Quantitation of initial template is made possible by fluorescently labeling the amplicons generated during the reaction and extrapolating back to a relative starting concentration (Dorak, 2004; ABI, 2006).

There are different methods of fluorescently labeling the amplicons, the most common being intercalating dyes or fluorescent probes. SYBR Green is an example of an intercalating dye, which nonspecifically binds to double stranded DNA molecules in a sample mixture (Dorak, 2004). Once binding between the fluorescent dye and DNA occurs fluorescence is emitted and can be measured using a laser scanner. Theoretically, the amount of fluorescence should double during each PCR cycle (Dorak, 2004). However, since SYBR Green is non-specific, extensive optimization of primers is required in order to eliminate primer dimer and other non-specific double stranded DNA that is not the desired amplicon (Dorak, 2004; ABI, 2006).

A more expensive method of quantitative analysis utilizes a probe in addition to two primers. The probes, known as TaqMan probes, are 20-30 bp oligonucleotides with a fluorescent dye (called a reporter) attached at the 5' end and a quenching dye (such as TAMRA) at the 3' end (Dorak, 2004). Fluorescence Resonance Energy Transfer (FRET) occurs when the two dyes are in close proximity, which allows energy transfer from the fluorescent molecule to the quencher and prevents release of fluorescence and signal (Dorak 2004).

The probe specifically attaches to the desired template in a qRT-PCR reaction mixture. During PCR, the probe is degraded and the reporter and quencher are no longer in close proximity (loss of FRET), thus allowing the release of fluorescence during each cycle, proportional to the rate of probe

cleavage. As a result of probe specificity, less optimization of primers and protocol are required (Dorak, 2004; ABI, 2006).

Research Objective

The goal of this research is to study MCF-like endogenous sequences in mice and attempt to account for the differential expression of the gene within MAIDS susceptible and resistant mice. One of the methods utilized is Reverse Transcriptase Polymerase Chain Reaction (RT-PCR). RT-PCR can determine whether or not MCF is expressed in one or both strains of mice. Additionally, qRT-PCR will quantitative the different levels of expression of MCF-like sequences within the two mouse strains. Sequencing of PCR products is also utilized in order to compare sequence homology between the detected MCF in the mouse genome and infectious MCF from LP-BM5 MuLV.

Further study of endogenous MCF could provide clues regarding the role, if any, of specific endogenous MCF-like sequences in MAIDS pathogenesis. Questions regarding whether or not ERVs have inhibitory affects on the immune system or are recognized as self are of particular importance. In addition, parallels between MCF-like sequences and HERVs could help us to better understand the progression of HIV to AIDS in humans.

MATERIALS AND METHODS

Animals

The two mouse (*Mus musculus*) strains used in the study were cared for in the Mount Holyoke College Animal Facility according to the National Institutes of Health Guidelines for the Care and Use of Laboratory Animals. Six BALB/c (disease resistant strain) and six C57BL/6 (disease susceptible strain) mice were kept naïve to challenge with mock or MuLV infection. The naïve mice were subsequently sacrificed using carbon dioxide inhalation. All protocols in this study received IACUC (Institutional Animal Care and Use Committee) approval and adhere to the guidelines of the National Institutes of Medicine animal care and use guidelines.

RNA Isolation from Spleen and Lymph Node

A modified Invitrogen TRIzol protocol for tissues was used to isolate RNA. Spleen and lymph nodes were removed from the naïve disease resistant and susceptible mice using sterile surgical instruments. Half of the spleen and a lymph node pool consisting of axillary¹, brachial², inguinal³, and mesenteric⁴ lymph nodes were submerged respectively in 10 mL RNase free round bottom plastic tubes containing 1 mL of TRIzol reagent (Invitrogen). One mL of TRIzol

¹ Found at the armpit

² Located under the pectorals on the bicep muscle

³ On the tissue of the groin

⁴ Found at the mesentery of the pancreas and small intestines (Ward et al., 1999).

was used for every 50-100 mg of tissue. A sterile power homogenizer (Polytron) was used to homogenize the tissues in the round bottom tubes until the tissues were completely fractured and the sample was homogenous. To clean the Polytron between homogenizations, alternating aliquots of water and TRIzol (in that order) were run under the polytron probe. Fresh water and TRIzol aliquots were used when homogenizing tissues from a different mouse strain.

The cell lysate was transferred into a phase lock gel tube (Eppendorf) pre-spun at 15,000 x g for 30 seconds. After a 5 minute incubation at room temperature, which allows additional time for complete dissociation of nucleoprotein complexes, 200 μ L of chloroform (0.2 mL for every 1 mL of TRIzol) was added to each tube. Tubes were inverted vigorously for 15 seconds to allow sufficient mixing of the sample with chloroform and then allowed to incubate at room temperature for 5 minutes. Each tube was subsequently centrifuged at 12,000 x g for 10 minutes at 4 °C.

Following centrifugation, the phenol-chloroform layer became trapped underneath the gel matrix in the phase lock gel tubes, while the clear aqueous layer was located above the gel matrix. This allowed for the easy transfer of the aqueous layer, which contained RNA, to a fresh RNase free 1.5 mL microfuge tube. RNA was precipitated from the aqueous phase through the addition of 500 μ L of room temperature 100% isopropyl alcohol (0.5 mL for every 1 mL TRIzol previously used.) Tubes were gently inverted and then allowed to incubate at room temperature for 10 minutes. A centrifugation at 12,000 x g for 10 minutes

at 4 °C followed in order to pellet the precipitated RNA. The supernatant was decanted and the pellet was washed with 1 mL of room temperature 75% ethanol (1 mL of 75% ethanol for every 1 mL of TRIzol.) The microfuge tubes were briefly vortexed to remove the gel like pellet from the bottom of the tubes. The samples were centrifuged once again at 7,500 x g for 5 minutes at 4 °C.

Following centrifugation, all of the ethanol was removed and the pellets were allowed to dry. In order to allow the ethanol to evaporate quickly, the tubes were uncapped and placed at a 45° angle on strategically placed Kimwipes in the laminar flow hood. Pellets were allowed to dry for approximately 10-20 minutes until all of the ethanol had evaporated. However, pellets were not allowed to over dry and become opaque, as this inhibited their solubility. Between 100-200 µl (depending on the size of the pellet) of Molecular-Grade Nuclease-free water (Ambion) was added to the tubes. The tubes were vortexed and the water-pellet mixture was pipetted up and down (without pipetting the pellet into the pipette tip) until the pellet appeared to be dissolved. In order to ensure that the pellet had completely dissolved, the samples were then incubated in a 60 °C heat block for 10 minutes. Three microliters of each sample was removed and aliquoted for future analysis of the RNA. All RNA samples were placed in the -80 °C freezer for long-term storage.

RNA Isolation from LP-BM5 Infected Mouse Fibroblast Cells

In order to have a positive control for Mink Cell Focus Forming Virus, RNA was isolated from the LP-BM5-MuLV infected mouse fibroblast cell line (SC-1). Cells frozen in DMSO for 69 days were obtained from a cryovial stored in a liquid nitrogen tank. After thawing cells in 37 °C water for approximately 30 seconds, the 1.5 mL of cells in DMSO were quickly transferred to a 15 mL conical tube containing 10 mL of standard complete culture media⁵. A 10 µl aliquot of cells in suspension was removed and mixed with 10 µl of 0.4% trypan blue stain (GibcoBRL). The mixture of cells and dye was added to a hemocytometer to count the number of live cells *versus* dead cells under a microscope. The thawed cells were shown to have 86% viability with approximately 2 million live cells total in the conical tube.

At this stage, the Invitrogen protocol for isolating RNA from cells in suspension was followed. After the cells were pelleted by centrifugation at 1200 rpm for 5 min at 4 °C, the supernatant was removed and 0.5 mL of TRIzol was added (1 mL of TRIzol for every 5-10 million cells). Cells were lysed in TRIzol by repetitive pipetting and the lysate was transferred to a phase lock gel tube to incubate at room temperature for 5 minutes. Next, 100 µl of chloroform (used 0.2 mL for every 1 mL of TRIzol) was added to the tube and mixed vigorously for 15

⁵ Complete media is comprised of 10% Heat inactivated Fetal Bovine Serum (Sigma), 100 µg/mL Penicillin-Streptomycin (Cellgro), and 2mM L-Glutamine (HyClone) in RPMI media (Cellgro).

seconds. After a 5 minute incubation at room temperature, the tube was centrifuged at 12,000 x g for 10 minutes at 4 °C.

The upper aqueous layer was transferred into an RNase free 1.5 mL microfuge tube. To precipitate the RNA, 250 µl of 100% isopropyl alcohol (used 0.5 mL for every 1 mL TRIzol previously added) was pipetted into the microfuge tube. The isopropanol and sample were mixed by repeated inversions, followed by incubation at room temperature for 10 minutes and then centrifugation at 12,000 x g for 10 minutes at 4 °C. After the supernatant was decanted, the pellet was washed with 0.5 mL of room temperature 75% ethanol (1 mL of 75% ethanol for every 1 mL of TRIzol.) The microfuge tube was briefly vortexed until the pellet was dislodged and centrifuged at 7,500 x g for 5 minutes at 4 °C. The supernatant was once again decanted and the pellet was allowed to dry in the laminar flow hood. Once the pellet was fairly dry it was resuspended in 200 µl of Nuclease-free water (Ambion) and then heated in a heat block at 60 °C for 10 minutes to ensure complete dissolution of the RNA. An aliquot of three microliters was removed and the sample was stored at -80 °C.

RNA Concentration and Integrity Measurements

The NanoDrop ND-1000 Spectrophotometer (NanoDrop Technologies) was utilized to quantify the collected RNA. In order to ensure that the spectrophotometer was clean, 7 μ l of a 5% bleach solution was pipetted onto the lower pedestal, and the upper pedestal was lowered. The solution was allowed to sit for 3 minutes and then removed with a Kimwipe. To remove remaining traces of bleach, 7 μ l of deionized water was placed on the pedestal for 3 minutes. Once the apparatus has been cleaned, between 1.5 and 2 μ l of the previously aliquoted RNA samples was pipetted onto the Nanodrop apparatus and UV readings were taken at 260 and 280 nm wavelengths. The Nanodrop software uses the 260 nm absorption numbers to calculate the concentration of RNA in each sample. The formula utilized by the program multiplies the 260 nm absorbance, by a dilution factor (not applicable in this case), and the conversion factor for single stranded RNA⁶. The Nanodrop also provided a 260:280 absorbance ratio. While the 260 nm absorbance reading is specific to nucleic acids, the 280 nm reading can detect proteins. If the 260:280 ratio is between 1.8 and 2.0, there is little to no protein contamination within the sample.

In order to determine the integrity of the isolated RNA, each sample was analyzed on the Bioanalyzer (Agilent). The previous RNA aliquots along with the RNA concentration data obtained from the Nanodrop were used to dilute the samples to approximately 200 ng/ μ l concentrations. The RNA 6000 Nano Chip

⁶ RNA concentration in ng/ μ l = 260 Absorption x dilution factor x 40

and 1 μ l of diluted RNA per well was used. One of the wells is designated to contain 1 μ l of the ladder (150 ng/ μ l) while another well solely contains a fluorescent dye that allows the RNA bands separated by electrophoresis to be detected by the Agilent Bioanalyzer. The bands are detected as a result of a laser located within the Bioanalyzer that scans fluorescent intensity. The 2100 expert software for the Bioanalyzer generated an integrity analysis and allowed for visualization of a histogram and an electrophoretic gel image for each RNA sample. Each lane is specific to a corresponding well on the chip. Two strong ribosomal RNA bands (approximate 2:1 ratio) in each lane without smearing indicated a good quality sample without RNA degradation. The bands can also be seen as peaks on an electropherogram. RNA with high integrity will have two thin ribosomal RNA peaks and no high molecular weight peaks, which indicate the presence of DNA. See Figure 5 for representations of RNA samples with good or poor integrity.

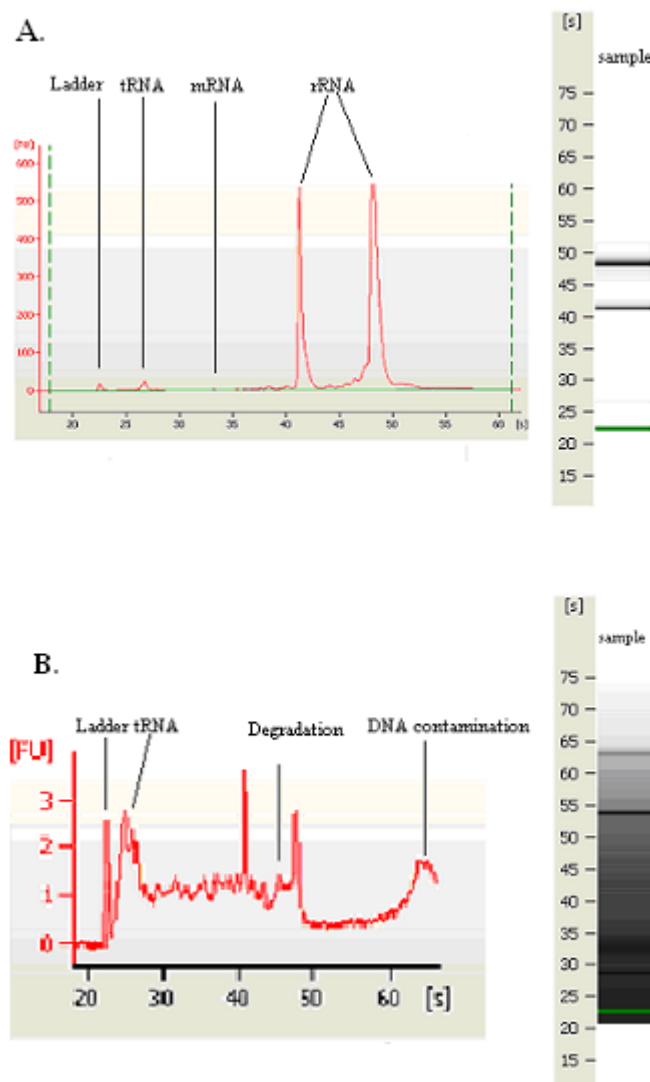


Figure 5: Examples of RNA samples with good *versus* poor integrity through analysis of the histogram and electropherogram generated by the Agilent Bioanalyzer. Figure 5A shows a perfect RNA sample without contamination or degradation. Figure 5B represents an unusable sample with DNA contamination and degraded RNA.

DNA Isolation from Naïve Mice

DNA was isolated from naïve BALB/c (disease resistant) and C57BL/6 (disease susceptible) mice. Samples of liver tissue from the respective strains were removed aseptically and placed in a petri dish. The liver was cut into small pieces, frozen in liquid nitrogen and stored in the -80°C freezer until needed. When removed from the freezer, a tissue fragment was placed into a mortar and pestle to be ground into very small granules. Liquid nitrogen was continually added to the mortar in order to ensure that the tissue remains frozen during the grinding. Once the tissue was sufficiently pulverized, it was placed into a pre-weighed petri dish until there was between 5 and 10 mg of frozen ground tissue.

The Puregene DNA Purification kit and protocol was used to isolate and purify the DNA from the pulverized liver. The 5-10 mg of tissue sample was transferred from the petri dish to a 1.5 mL microfuge tube containing 300 μL of Cell Lysis Solution. A microfuge tube pestle was used to further homogenize the sample, which was subsequently placed in a 65°C water bath for 60 minutes. Proteinase K (20 mg/ml) was then added to the cell lysate, the sample was mixed by inverting the tubes 25 times, and then incubated overnight at 55°C to completely dissolve the tissue.

Once the sample was homogenous, 1.5 μL of 4 mg/mL RNase A Solution was added to each sample and mixed through repeated inversions. The cell lysate was incubated at 37°C for 60 minutes and then cooled to room temperature by being placed on ice for 5 minutes. Once at room temperature, optimum protein

precipitation could be achieved by adding 100 μ l of Protein Precipitation Solution. Samples were vortexed at high speed for 20 seconds and centrifuged at 14,500 x g for 3 minutes to form a protein pellet. The supernatant, which contained DNA, was separated from the pellet and placed into a clean 1.5 mL microfuge tube containing 300 μ l of 100% isopropyl alcohol. The small samples were mixed by gently inverting 50 times and then centrifuged at 14,500 x g for 1 minute to form a DNA pellet. The supernatant was then removed and the pellet was washed with 300 μ l of 70% ethanol, followed by centrifugation at 14,500 x g for 1 minute. Once the DNA was pelleted to the bottom of the tube, the ethanol was removed and the tubes were placed in the laminar flow hood for 10-15 minutes until the pellets were sufficiently dry. Next, 50 μ l of DNA hydration solution was added to the dried pellets, resuspended with a pipette and incubated at 65 °C for 60 minutes to allow for the DNA to completely dissolve. The recovered DNA concentration was evaluated, as described previously, using the Nanodrop spectrophotometer (260 nm)⁷ and the DNA sample was stored at -20 °C.

⁷ DNA concentration in ng/ μ l = 260 Absorption x dilution factor x 50

Creating PCR Primers

Primer sets were created using the Integrated DNA Technologies (IDT) *PrimerQuest* software (<http://scitools.idtdna.com/Primerquest>). A published sequence of MCF *env* gene was found using BLAST and ENSEMBLE searches. Select pieces of the chosen sequence were inserted into the sequence box in the “basic” tab of the web page. In addition, the primer set with probe option was selected and the Real Time PCR parameter was chosen. Under the “standard” tab of the web page, the number of primer sets to return was selected to be 20, optimum primer size was changed to 20 bp, and optimum primer T_m (melting temperature) was set to 55 °C. Product design was automatically set to 80-200 bp. From these parameters, several possible primer sets were returned. Selection was based on each primer pair having the same or similar T_m's and having the smallest primer penalty possible. Primer penalties are calculated by the *PrimerQuest* software, which looks at adherence to the previously set criteria along with general criteria used to pick primers, such as GC content at the 3' end (a high GC content can lead to mispriming) and probability of primer dimer. Primer penalties close to zero are preferred.

In addition to primers for the MCF gene, primers specific to B-actin were created. B-actin is ubiquitously expressed and commonly used to test efficiency of cDNA synthesis by reverse transcription, in addition to serving as the normalizer used in qRT-PCR. B-actin is also utilized because its poly Adenine tail will allow for differentiation between cDNA reverse transcribed from

messenger RNA (mRNA), which has a polyA tail, and cDNA synthesized from ribosomal RNA (rRNA).

All primer sets were ordered from IDT. They were received lyophilized in separate tubes and subsequently made into 100 μ M dilutions by adding 10 μ l of Nuclease-free water for every nanomole of lyophilized primer present. All solubilized primers were stored at -20°C .

Primers were optimized using conventional PCR, varying annealing temperatures and a Robocycler Gradient 96 in the Bacon lab (Stratagene). The Robocycler allowed up to 12 different annealing temperatures during one PCR reaction. The annealing temperatures tested ranged between 44°C and 55°C .

cDNA Synthesis

Synthesis of cDNA was performed using a modified method from Promega. RNA along with reaction components were thawed and vortexed. The concentration of the RNA obtained from the Nanodrop was used to dilute the sample to 1 $\mu\text{g}/\mu\text{l}$. Each RNase-free reaction tube contained 2 μl of 1 $\mu\text{g}/\mu\text{l}$ RNA, 1.5 μl of 0.5 $\mu\text{g}/\mu\text{l}$ random primers (Promega), 1.5 μl of 0.5 $\mu\text{g}/\mu\text{l}$ Oligo dT (Promega) and 5 μl nuclease free water (Ambion). The tubes were heated at 75°C for 5 minutes, and then cooled at 4°C for 5 minutes. After incubation, tubes were briefly centrifuged to ensure that all reactants were located at the bottom of the tube. Next, 4 μl of ImProm-IITM 5x reaction buffer (Promega), 2 μl MgCl_2 (25 mM) (Promega), 3 μl 10mM dNTP mixture (Promega), and 1 μl of 1 unit/ μl

ImProm-II™ reverse transcriptase (Promega) was added to each tube to generate a 20 µl cDNA synthesis reaction. Tubes were incubated in the Genius thermocycler at 42°C for 2 minutes, followed by 37°C for 1 hour, 95°C for 5 minutes and a hold at 4°C. Following cDNA synthesis, all products were stored in the -20 °C freezer until needed.

Reverse Transcriptase-Polymerase Chain Reaction (RT-PCR)

Non-quantitative PCR reactions were performed in 50 µl reactions. A master mix was prepared, which consisted of 35 µl of nuclease free water (Ambion), 5 µl of Magnesium free 10x thermophilic polymerase reaction buffer (Promega), 5 µl of 25mM Magnesium Chloride (Promega), 1 µl of 10mM dNTP mixture (Promega), and 1 µl of 5 units/µl Taq DNA polymerase (Promega) per reaction tube. The appropriate primer set was then added to the master mix: 1 µl of 200nM β-actin primers or 1 µl of 15 µM MCF primer set PS1, PS2 or PS3. Next, 1 µl of cDNA from the original 20 µl cDNA synthesis reaction was added to each tube. Reactions were run in the Genius thermocycler; hot start was used to limit non-specific binding. The thermocycler parameters consisted of initial denaturation at 95 °C for 2 minutes followed by 35 cycles of denaturation at 95 °C for 30 seconds, annealing at 55 °C for 30 seconds, and extension at 72 °C for 30 seconds. There was a final extension at 72 °C for 30 seconds and a 4 °C hold.

Gel electrophoresis was used to visualize the PCR products. A 1.5x agarose gel in 1x TAE containing 2.5 µl of ethidium bromide was made. In a fresh microfuge tube, 10 µl of PCR product was mixed with 2.5 µl of DNA loading buffer and added to the appropriate wells of the gel with 12.5 µl of the exACTGene 50 bp mini DNA ladder (Fisher Scientific) as a reference marker. The gel was immersed in 1x TAE with 2.5 µl of ethidium bromide added to the buffer below the gel. The electrophoresis was run at 95 Volts for approximately 1 hour.

Agarose gels were imaged using the Fujifilm intelligent dark box. The Las-3000 Pro image reader software was set to the UV light (312 nM DIA) option and the sensitivity and resolution remained standard. The precision option was chosen for exposure type with the exposure time manually changed to ¼ seconds.

PCR with Genomic DNA

A PCR reaction was run with MCF primer sets 1 and 3 using genomic mouse DNA. LP-BM5 infected SC-1 cell RNA was reverse transcribed, as described above, into cDNA and used as a positive control. The PCR protocol remained unchanged, except that 1 µg/µl of genomic DNA was used in place of 2 µg/µl of cDNA.

Sequencing PCR Products

For sequencing, 10 μ l of PCR products were run on each lane of 1.5% agarose gels using 1x TAE buffer. Gels were placed on a UV light source, the appropriate bands were excised using sterile tweezers and these gel pieces were placed in labeled 1.5 mL microfuge tubes (10 bands of each sample were pooled together.) In order to ensure maximum efficiency of the QIAquick Gel Extraction Kit (Qiagen), the pooled band weight did not exceed 0.4 g. Subsequent DNA isolation followed the procedures outlined in the kit's QIAquick spin handbook. Briefly, For every 0.1 g of gel, 300 μ l of buffer QG was added to the tubes and then allowed to incubate at 50 °C for 10 minutes, or until the gel was completely dissolved. In order to ensure the optimal pH of the sample, 10 μ l of 3M sodium acetate (pH 5) was transferred into each tube. Next, 100 μ l of room temperature 100% isopropyl alcohol was added to each tube for each 0.1 g of gel and mixed through repeated inversions to allow the DNA to precipitate. In order to collect the DNA, each sample was aliquoted into an appropriate QIAquick spin column (800 μ l at a time) and centrifuged at 13,000 rpm for 1 minute. Flow through was discarded and 500 μ l of buffer QG was added to the column followed by centrifugation at 13,000 rpm for 1 minute to remove all traces of agarose from the DNA. The spin column was washed by adding 750 μ l of buffer PE (ethanol mixture), incubating the tubes for 5 minutes at room temperature and centrifuging for 1 minute at 13,000 rpm. Flow through was discarded, each QIAquick column was placed into a clean microfuge tube, and the centrifugation was repeated to

remove remaining traces of ethanol. Each QIAquick column was once again placed into a clean microfuge tube. To elute DNA, 20 μ l of buffer EB⁸ was added to the center of the QIAquick column membrane and incubated at room temperature for 2 minutes, followed by centrifugation for 1 minute at 13,000 rpm. This step was repeated with an additional 10 μ l of buffer EB added to the center of the QIAquick membrane and the two volumes were pooled together.

Isolated PCR product concentration was determined using the NanoDrop to ensure that more than 5 ng/ μ l was present. A 50 μ l aliquot of primer sets 1 (PS1) and 3 (PS3) were diluted to 3 μ M concentrations. These primers and PCR products were sent to Elim Biopharmaceuticals, Inc. (<http://elimbio.com>.) with the template name, template concentration, template size, primer name, primer concentration, and preferred annealing temperature information provided.

The sequences were received via email in two distinct formats. The ABI file was viewed using a program known as Geospiza's FinchTV (free download available at <http://www.geospiza.com/finchtv/index.htm>). FinchTV allowed viewing of chromatogram files of raw data, DNA sequence trances, and quality values. The other files, viewed using Microsoft Word, had sequences oriented in the 5' to 3' direction. When using a forward primer to sequence the PCR products, the nucleotide following the forward primer is listed. As a result, the complimentary sequence of the reverse primer can be found within the data, oriented in the 3' to 5' direction. The opposite is true when using the reverse

⁸ Buffer EB is 10 mM Tris-Cl, pH 8.5

primer to sequence the PCR products; the complimentary nucleotides of the forward primer can be found oriented in the 3' to 5' direction.

PCR was performed on BALB/c genomic DNA, BL/6 genomic DNA, and RT-PCR was performed on LP-BM5 infected SC-1 RNA using both MCF primer set 1 and 3. Each sample was sequenced using the forward and reverse primer separately, thus generating twelve sequences.

Quantitative Real Time RT-PCR

The 7300 Real Time PCR system (Applied Biosciences) and a modified protocol from ABI (ABI User Bulletin #2) were utilized for quantitative PCR analysis. The Real time PCR experiment was executed using the SYBR Green fluorescent probe, which binds non-specifically to any double stranded DNA. Therefore, primer dimer needs to be limited by using minimal primer concentrations. Through the use of the previously described RT-PCR method, primer dimer and amplicon bands can be viewed with the different forward and reverse primer concentrations of 0.5 μ M, 1.5 μ M, 3 μ M, and 9 μ M in order to determine the ideal primer concentration for qRT-PCR.

Previously synthesized cDNA of naïve disease susceptible mouse lymph node and spleen along with naïve disease resistant mouse lymph node and spleen was calculated to have roughly 100 ng/ μ l concentrations. In order to follow the parameters of qRT-PCR, the cDNA was diluted to approximately 5 ng/ μ l.

Next, a 96 well plate was set up. The cDNA, which was added first, was at a final concentration of approximately 10 ng (2 μ l of the previously diluted cDNA in each well). A master mix was prepared, which contained all essential components of the reaction, save for the cDNA. For each well of the qRT-PCR plate containing 2 μ l of cDNA, 25 μ l of 2x SYBR Green fluorescent probe (ABI) is required. Since the final reaction volume per well was 50 μ l, the SYBR Green concentration was 1x. In addition, a 300 nM concentration of the β -actin primer and 9 μ M concentration of PS1 and PS3 were added to their respective wells. Nuclease-free water is then added to the wells to bring the volume up to 50 μ l. Therefore, wells containing β -actin primer need 11 μ l of water each while the wells containing primer sets 1 and 3 require 21 μ l of water. In addition to wells that contain cDNA, no template controls (NTC) for every primer set were included, which contain all reaction components with 2 μ l of Nuclease-free water (Ambion) in place of template cDNA. It should be noted that each well was only done in duplicate as opposed to the recommended triplicate due to an insufficient volume of SYBR Green reaction mixture (See figure 6 for plate design.)

	1	2	3	4	5	6	7	8	9	10	11	12
A	B16 spleen B-actin	B16 spleen B-actin	B16 ln B-actin	B16 ln B-actin	Balb/c spleen B-actin	Balb/c spleen B-actin	Balb/c ln B-actin	B-actin NTC	B-actin NTC	B-actin NTC		
B	B16 spleen ps 1	B16 spleen ps 1	B16 ln ps 1	B16 ln ps 1	Balb/c spleen ps 1	Balb/c spleen ps 1	Balb/c ln ps 1	Balb/c ln ps 1	ps 1 NTC	ps 1 NTC		
C	B16 spleen ps 3	B16 spleen ps 3	B16 ln ps 3	B16 ln ps 3	Balb/c spleen ps 3	Balb/c spleen ps 3	Balb/c ln ps 3	Balb/c ln ps 3	ps 3 NTC	ps 3 NTC		
D												
E												
F												
G												
H												

Figure 6: Real Time PCR plate design. All three lanes had duplicates of disease resistant (BALB/c) and disease susceptible (BL/6) spleen and lymph node cDNA.

Lane A used β -actin primers, Lane B used MCF primer set 1 and lane C used MCF primer set 3. Columns 9 and 10 are no template (cDNA) controls for each primer set. It should be noted that each well is in duplicate rather than the recommended triplicate. This is because there were limited amounts of SYBR Green reaction mixture available for the experiment.

Thermal cycling parameters for the SYBR Green dye chemistry had an initial step consisting of a 2 minute hold at 50 °C followed by a 10 minutes hold at 95 °C, which allowed for activation of the polymerase. Next, 40 cycles of PCR began with melting at 95 °C for 15 seconds followed by annealing/extension at 55 °C for 1 minute. Once the PCR reaction has finished an amplification plot was generated.

Since SYBR Green reagent chemistry was used, a dissociation assay needed to be performed to determine the number of different bands generated. In order to create a dissociation curve, the PCR products were denatured at 95 °C for 15 seconds. The denatured DNA was then allowed to anneal by slowly ramping down to 55 °C and holding for 30 seconds so that products of significant length will be double stranded. Increasing the temperature to 95 °C and holding for another 15 seconds then collects fluorescent data. All data was collected and analyzed using the SDS 3000 software. The plate study function allowed examination of the plate and the data was exported into Microsoft excel for further calculations and analysis.

Gene expression was detected by determining the point at which fluorescence emitted by SYBR Green crosses an arbitrarily set threshold (known as the Ct or cycle threshold value). To compare differences in gene expression, the comparative Ct method instead of the standard curve method was utilized. The comparative Ct method required a validation experiment to be performed in order to ensure that the efficiencies of the target (MCF PS1 and PS3) and

endogenous control (β -actin) are approximately equal. For the validation experiment the same protocol for qRT-PCR was followed with a few exceptions. Since all of the SYBR Green reaction mixture from ABI was used for the previous plate, SYBR Green reaction mixture from Stratagene was utilized. The reference dye (ROX) provided with the Stratagene SYBR Green kit was diluted 1:50 using nuclease-free water (Ambion), and 0.75 μ l per well was added to the master mix. The volume of nuclease-free water needed in the master mix was altered to accommodate the additional reference dye and ensure that each well contained 50 μ l of reaction mixture. Prior to addition of the master mix, cDNA known to be positive for MCF-like sequence was added to the wells in various concentrations: 1.25 ng, 2.5 ng, 5 ng, 10 ng, 20 ng, 50 ng, and 100 ng. Due to abundance of SYBR Green reaction mixture, samples were added in triplicate to the plate.

The efficiencies for β -actin, MCF PS1, and MCF PS3 reactions were calculated by creating a standard curve, which plots the log input template *versus* the Ct value. A slope of -3.33 ± 0.3 indicates 100% efficiency⁹. More importantly, the slopes generated should show similar efficiencies. Then, the log of the input template *versus* the Δ Ct¹⁰ was graphed in order to compare reaction efficiencies of each primer set. The absolute value of the slope of the line generated in the graph must be less than or equal to 0.1 in order to demonstrate

⁹ Efficiency = $10^{(-1/\text{slope})}$

¹⁰ Δ Ct_{Gene of Interest} = Ct_{Gene of Interest} - Ct_{reference gene}

that the primer set amplifications for the gene of interest are approximately equal to the primer set amplifications of the reference gene.

Once the primer sets were shown to have comparable efficiencies, the $\Delta\Delta C_t$ method of relative quantification can be used to compare the expression of MCF between the two mouse strains. Relative quantification compares the changes in genes expression of a sample relative to another reference sample (i.e. the calibrator). This method was chosen over absolute quantification because the absolute quantification method requires a standard curve to be constructed by amplifying known amounts of cDNA, which was not applicable in these experiments. First, the data was normalized by comparing the C_t value of the gene of interest to the C_t value of the reference gene.¹¹ Following normalization, the fold expression¹² difference relative to the calibrator was calculated.¹³ The fold expression differences were then compared using a bar graph.

¹¹ $\Delta C_t \text{ Gene of Interest} = C_t \text{ Gene of Interest} - C_t \text{ reference gene (i.e. } \beta\text{-actin)}$

¹² $\text{Fold Difference} = 2^{(-\Delta\Delta C_t)}$

¹³ $\Delta\Delta C_t = \Delta C_t \text{ Gene of Interest} - \Delta C_t \text{ Calibrator Sample}$

RESULTS

I. Confirming cDNA synthesis

Before proceeding to additional cDNA synthesis with valuable RNA stocks it was important to ensure that the protocol for reverse transcription was working. The cDNA reverse transcribed from LPBM5 infected mouse fibroblast SC-1 cells was amplified in a previously developed PCR protocol (see Materials and Methods) with β -actin primers. Figure 7 shows the results of the PCR experiment in which β -actin amplicons were visible at the expected molecular weight of 153 bp. A negative control sample that was denied reverse transcriptase (RT) enzyme during cDNA synthesis was included in the PCR reaction and showed no amplification, as expected. In all cases of RT-PCR, cDNA samples were checked in this manner to confirm that synthesis of DNA from RNA was successful.

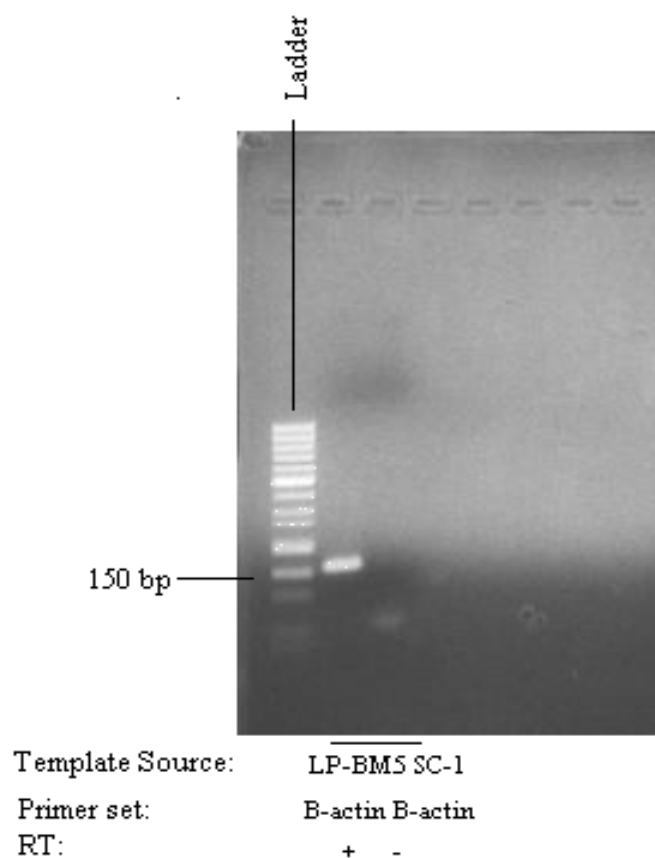


Figure 7: RT-PCR of LP-BM5 infected SC-1 cells using β -actin primers. Ten microliters of PCR products were analyzed in 1.5% agarose gels. The expected amplicon at 153 bp is visible in the reverse transcriptase (RT) positive lane, but not in the RT negative lane. The ladder used was a 50 bp mini ladder from Fischer Scientific.

II. Primer Selection and Optimization

A. Choosing Primer Sets

A primer set specific to the ubiquitous β -actin gene was chosen to serve as a positive control for RT-PCR reactions and as an endogenous control (also known as a reference gene) for qRT-PCR. In addition, three primer sets specific to a published sequence of MCF were ordered. Two of the primer sets contain a portion of the sequence from the 70-mer microarray probe that initially detected MCF (designated PS2 and PS3), while one primer set is just upstream of this region (named PS1) (See table 1 for forward and reverse primer sequences of the 4 primer sets).

Table 1: Forward and Reverse primer sequences for the β -actin reference gene and the three primer sets specific to MCF. The expected size (in base pairs) of the amplicons produced by the respective primer sets is also listed. All sequences are oriented 5' to 3'.

	Forward Primer	Reverse Primer	Amplicon Length
β Actin	CCCAGATCATGTTTGAGACCT	AGAGCATAGCCCTCGTAGAT	153 bp
MCF PS1 (PS1)	ATGCTGTTTCTATGCCGACC	CCACCCTTGTTGGGATTCAA	105 bp
MCF PS2 (PS2)	GGAAGTTTAGTTAAAGAATAAGGC	CCACCCTTGTTGGGATTCAA	146 bp
MCF PS3 (PS3)	GGAAGTTTAGTTAAAGAATAAGGC	CCAGAACTGTTGCTAGTT	138 bp

B. Testing the MCF Primer Sets

In order to determine which primers would bind specifically to MCF-like sequences in the two mouse strains. RT-PCR was performed (see materials and methods). The cDNA synthesized from LPBM5 infected mouse fibroblast SC-1 cell RNA was used to test various annealing temperatures for PCR with the three different MCF primer sets: PS1, PS2, and PS3. The primer sets had varying melting temperatures (T_m), which led to the selection of different annealing temperatures during PCR. Primer set 1 had a forward and reverse primer melting temperature (T_m) of 55.4 °C, so the annealing temperature was chosen to be 55 °C. Primer set PS2 had a forward primer T_m of 49.9 °C and a reverse primer T_m of 55.4°C while PS3 had a forward and reverse primer T_m of 49.9°C. Therefore, the annealing temperatures during PCR for reaction using PS1 and PS3 were 50 °C.

Positive control cDNA along with negative controls (samples without RT enzyme) were prepared for PCR with each primer set. Primer set 1 amplicons were calculated to be 105 bp, which was the location of the band on the agarose gel (See figure 8). The expected molecular weight of primer set 2 was 146 bp, which showed no amplification except for some primer dimer around 25-50 bp. Primer set 3 exhibited a band at the anticipated molecular weight of 138 bp. However, this primer set was less specific due to the additional high molecular weight band seen at approximately 600 bp. All of the negative controls showed no significant amplification except for primer dimers (See figure 8). Due to the

specificity issues with primer sets PS2 and PS3, additional experiments were performed to further optimize the reaction conditions.

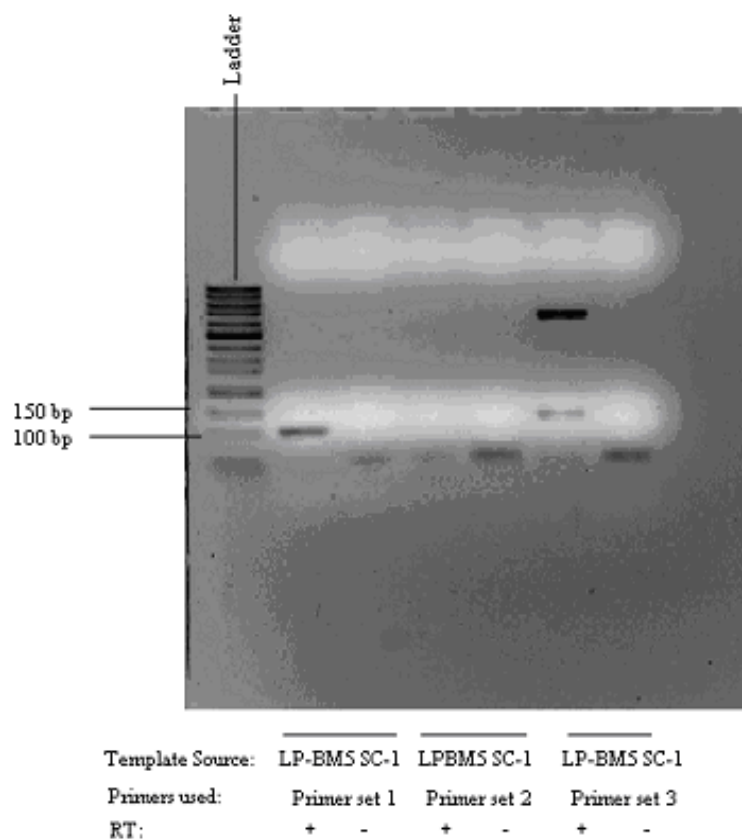


Figure 8: RT-PCR of LP-BM5 infected SC-1 cells using primer sets MCF PS1, MCF PS2, and MCF PS3. Ten microliters of PCR products were analyzed in 1.5% agarose gels. For PS1, the expected band at 105 bp is visible in the reverse transcriptase (RT) positive lane but not in the RT negative lane. The PS2 amplicon at 146 bp is not seen in the positive control lane or the negative control lane. PS3 has a band at the expected length of 138 bp in the RT positive lane, but not in the RT negative lane. The ladder used in the first lane was a 50 bp mini ladder from Fischer Scientific.

B. Optimizing the Annealing Temperatures for MCF Primers

MCF Primer sets 2 and 3 needed revised thermocycler parameters during PCR in order to ensure amplification of only one specific band of the correct molecular weight. Small alterations in the annealing temperature can have a significant effect on primer annealing specificity. If annealing temperature were decreased there was a chance that one or both primers will anneal to a sequence other than the target sequence, since under lower annealing temperatures base pair mismatches are possible. By raising the annealing temperature the target sequence is more likely to be the only amplified sequence. Primer set 3 was predicted to generate an amplicon at 138 bp, while primer set 2 should generate a product of 146 bp. Annealing temperatures ranging from 44 °C to 55 °C were tested utilizing the Robocycler machine for these two primer pairs. The cDNA used in the PCR reaction was reverse transcribed from LP-BM5 infected SC-1 cell RNA.

Results showed that PS2 did not amplify cDNA under any of the annealing temperatures tested (See figure 9A). Primer set 3, on the other hand, exhibited increased primer specificity as the temperature increased. The optimal annealing temperature for primer set 3 was chosen to be 55 °C, since there were absolutely no signs of non-specific bands, minimal primer dimer, and an acceptable amount of 138 bp product (See Figure 9B). As a result of these findings, primer set PS2 was discarded from future analysis and primer sets PS1 and PS3 was used from this point forward.

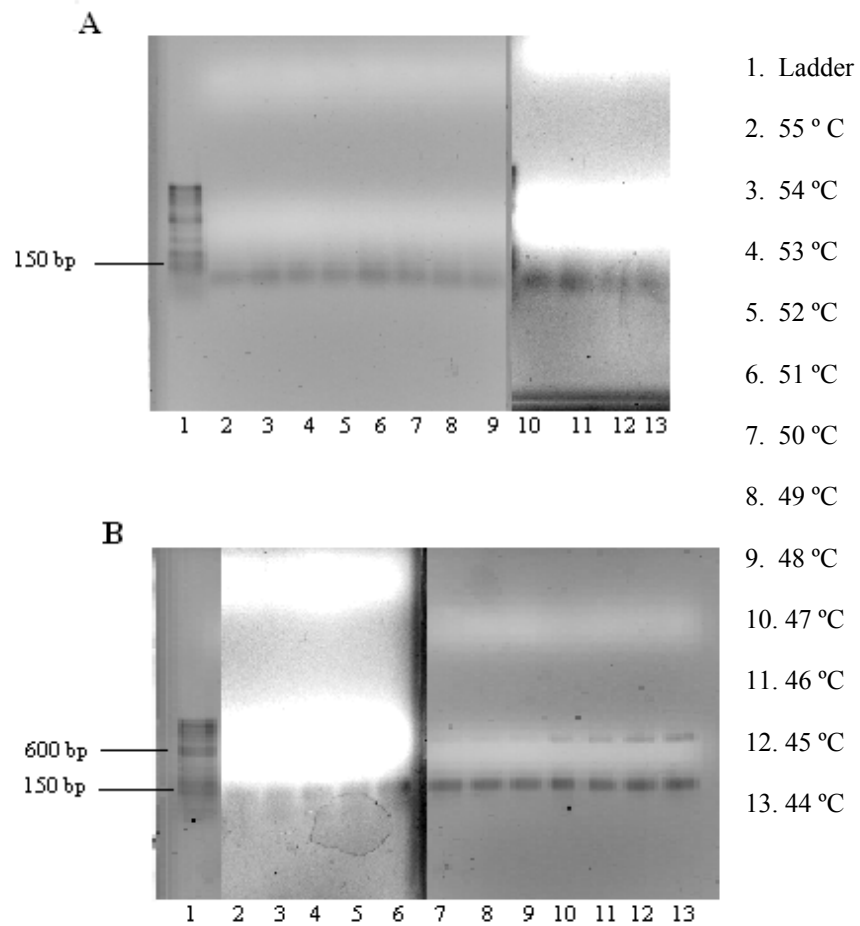


Figure 9: RT-PCR of LP-BM5 infected SC-1 cells using MCF PS2 and MCF PS3 over a range of annealing temperatures. The annealing temperatures ranged from 55 °C to 44 °C. Figure 9A shows PCR products from primer set 2 (PS2), which lacks visible bands at the expected 146 bp. Figure 9B shows PCR products from primer set 3 (PS3), which shows amplicons at the expected 138 bp. As the annealing temperature increases, the bands around 600 bp begin to disappear. The ladder used was a 50bp mini ladder.

C. Evaluation of Species Primer Specificity

To confirm that the two working MCF primer pairs (PS1 and PS3) were binding specifically to the MCF sequences and not other sequences, RNA was collected from 2 species other than the mouse and subjected to the same RT-PCR protocol (see materials and methods). Rat (*Rattus norvegicus*) and fruit fly (*Drosophila melanogaster*) RNA was obtained from the Bacon and Woodard labs of Mount Holyoke College. MCF is not known to exist within the genome of *R. norvegicus* or *D. melanogaster*, therefore amplicons generated within these two strains might suggest that the primer sets are not specifically binding to MCF (Krieg et al., 1992). cDNA was created from the two species and run in a PCR reaction along with cDNA reverse transcribed from LP-BM5 infected SC-1 cell RNA. The positive control LPBM5 infected SC-1 cell cDNA showed specific amplification for both primer sets 1 and 3, as expected. The fruit fly (*D. melanogaster*) cDNA and Rat (*R. norvegicus*) cell cDNA only showed evidence of primer dimer with no amplicon bands (See figure 10).

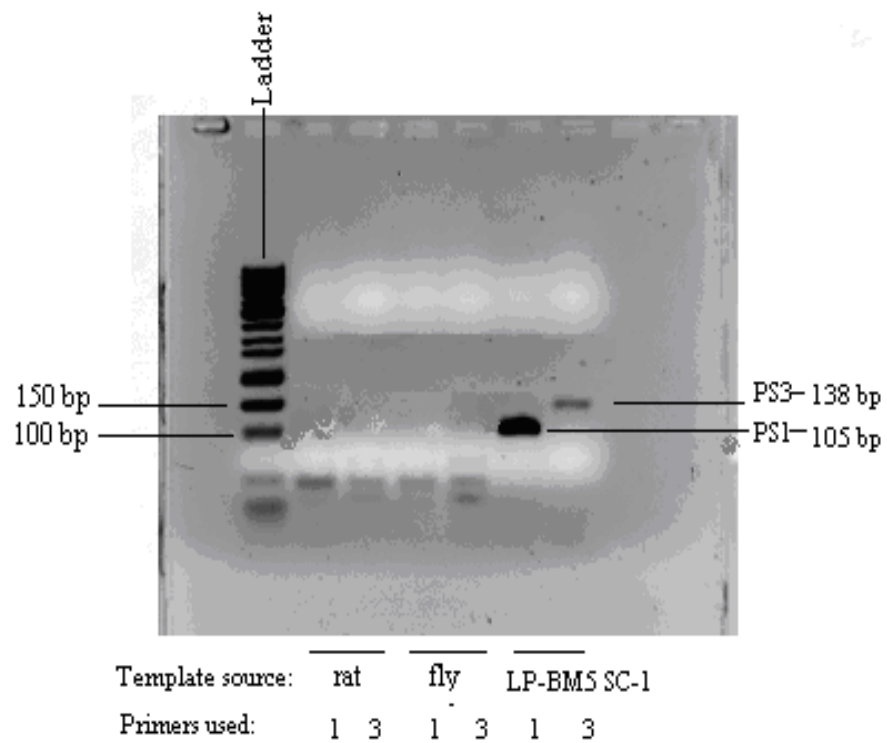


Figure 10: RT-PCR of RNA from three different species (*Rattus norvegicus*, *Drosophila melanogaster* and *Mus musculus*) using MCF primer sets 1 and 3. There are no amplicons visible with PS1 (expected at 105 bp) or PS3 (expected at 138 bp) with rat or fly cDNA. The LP-BM5 infected SC-1 mouse cells did show amplification at 105 bp for PS1 and 138 bp for PS3. The ladder used was a 50bp mini ladder.

Naïve Mouse Genomic DNA

Genomic DNA was tested using PCR to determine if MCF-like sequences exist in the genome of the mice. Figure 11 shows the results of a PCR experiment using both MCF primer set 1 (PS1) and 3 (PS3) to produce MCF specific amplicons from isolated genomic liver DNA of naïve BALB/c (disease resistant) and BL/6 (disease susceptible) mice. LP-BM5 infected mouse fibroblast cDNA was used as a positive control (RT-PCR). It should be noted that the strength of the band intensity could not be directly evaluated since the representation of MCF template in genomic DNA and cDNA are not comparable. Both primer sets generate bands of the expected size from genomic DNA templates of BALB/c and BL/6 mice.

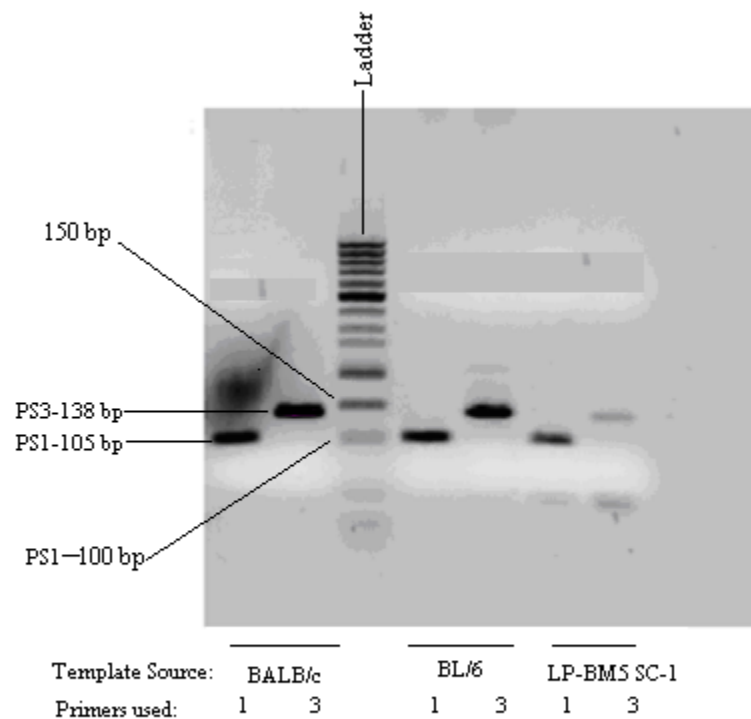
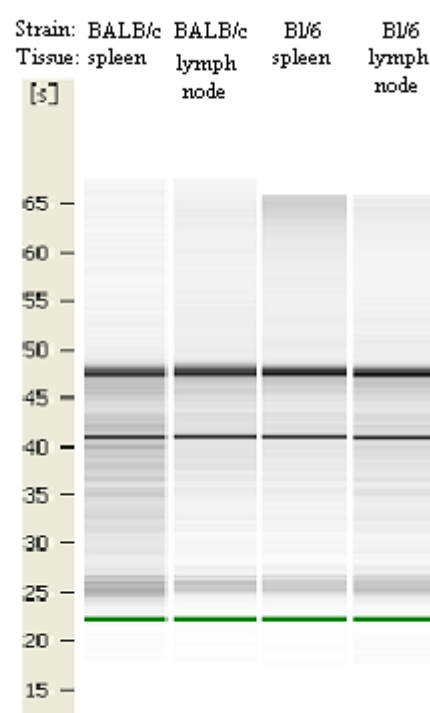


Figure 11: PCR with Genomic DNA isolated from BALB/c (disease resistant) and BL/6 (disease susceptible) mice using MCF PS1 and PS3. RT-PCR of LP-BM5 infected SC-1 cells were used as a positive control. Both mouse strains along with the positive control showed amplicons at the expected molecular weight of 105 bp for PS1 and 138 bp for PS3. The first lane 1 has an artifact in the gel above the band, which does not represent nucleic acid staining. The ladder used was a 50bp mini ladder.

Non-Quantitative RT-PCR

1. Confirming RNA Concentration and Integrity

The Nanodrop and Bioanalyzer (Agilent) were used to determine the concentration and integrity of RNA isolated from disease resistant (BALB/c) and disease susceptible (BL/6) mouse spleens as well as pooled lymph nodes. The absorption reading at 260 nm indicated the concentration of RNA in the sample and the 260:280 absorption ratio indicated level of nucleic acid purity. Table 2 shows the Nanodrop readings for the RNA from the two mouse strains, while figures 12 and 13 shows the gel electropherograms and histograms produced by the Bioanalyzer, respectively. Only RNA samples with a RIN (RNA integrity number), which represents degradation status, above 5 were used. In addition to the mouse strain RNA, the RNA isolated from the LP-BM5 infected SC-1 cells were also analyzed (See figure 14).



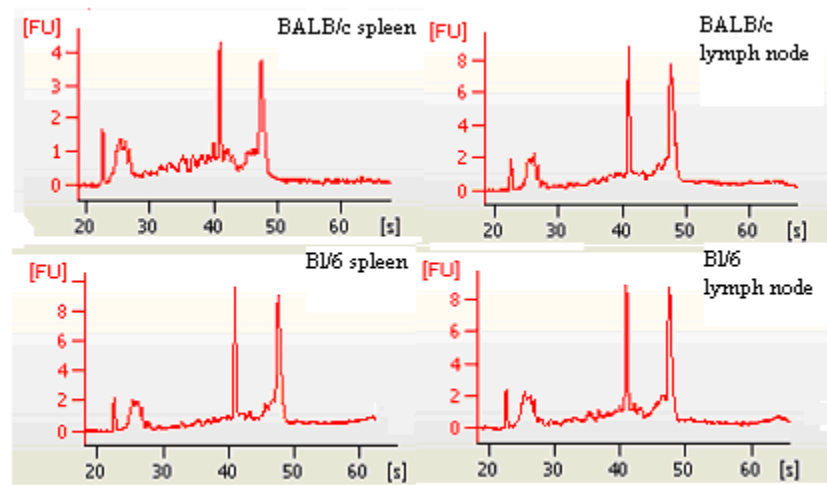
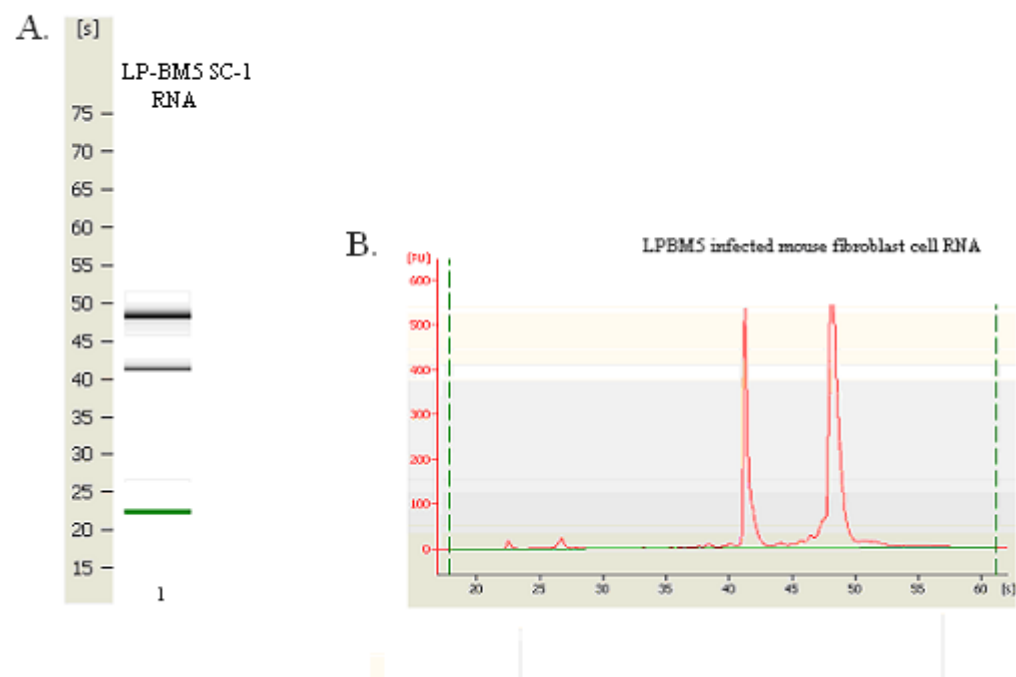


Figure 13: Histograms corresponding to the electrophoretic Nano Chip gel lanes for the naïve disease resistant (BALB/c) and disease susceptible (BL/6) mouse spleen and lymph node RNA.

Table 2: Raw Data Regarding Integrity and Concentration of Naïve Mouse RNA

Strain	Tissue	Concentration (ng/ul)	A260	260:280	RNA Integrity Number (RIN)*
BALB/c	spleen	2113	53	1.96	5.9
BALB/c	lymph node	1147	36	1.95	7.6
BL/6	spleen	2121	53	1.97	8.2
BL/6	lymph node	1353	33	1.98	7

*RIN (RNA Integrity Number) represents the degradation status of an RNA sample on a scale of 1 to 10. A value of 10 designates a perfect sample and 1 is a completely degraded sample. In this experiment values of 5 represent acceptable RNA samples. The RIN allows for comparison of samples and demonstrates repeatability of experiments.



C.

Source	Concentration (ng/ul)	A260	260:280	RIN*
LP-BM5 infected mouse fibroblasts	1126	31	1.89	10

*RIN (RNA Integrity Value) represents the degradation status of an RNA sample on a scale of 1 to 10. A value of 10 designates a perfect sample and 1 is a completely degraded sample. In this experiment, values 5 represent acceptable RNA samples. The RIN allows for comparison of samples and demonstrates repeatability of experiments.

Figure 14: Bioanalyzer results for RNA isolated from LP-BM5 infected SC-1 cells. (A) shows the electrophoretic gel for the RNA 6000 Nano Chip. (B) represents the corresponding histogram for the sample. (C) provides the raw data regarding the concentration, integrity, and purity of the sample.

2. Naïve Mouse RNA

Naïve BALB/c and BL/6 mice were also tested for the expression of endogenous MCF-like sequences. Figure 15 displays the results from the RT-PCR experiment using MCF primer set 1. The positive control (with RT enzyme) LPBM5 infected cell cDNA had a specific band at the correct molecular weight while the negative control (without RT enzyme) LPBM5 infected cell cDNA had no amplification; although primer dimer can be seen at approximately 50 bp.

Both BALB/c and BL/6 mice showed MCF specific amplification of cDNA from the spleen and lymph node tissues. While quantification of amplified product could not be obtained through conventional RT-PCR, a qualitative comparison could be made because identical amounts of starting template were used in all cases. The lymph nodes of the two mouse strains show bands with similar intensity. However, the intensity of the BL/6 spleen band appears to be greater than that of the BALB/c band for this same tissue.

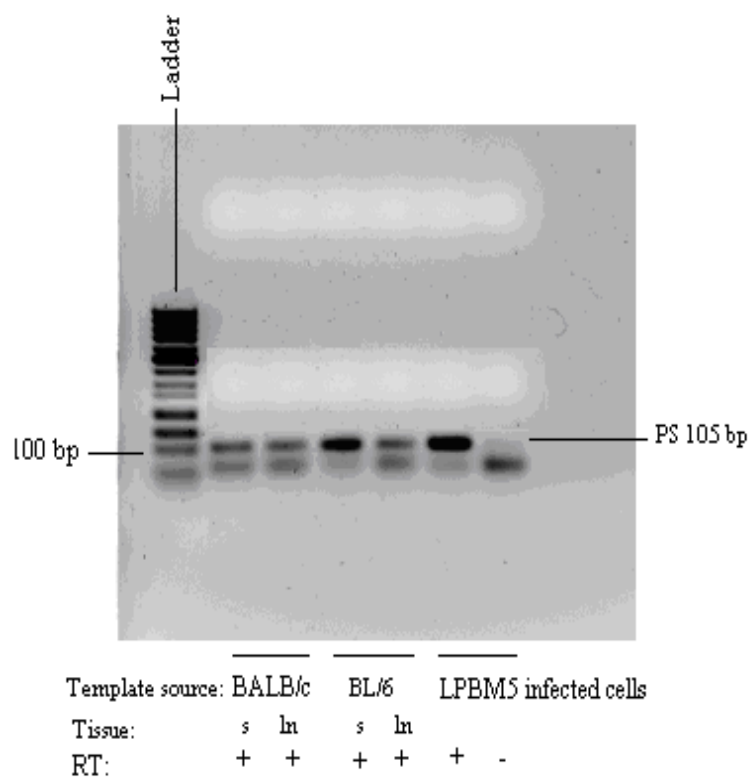


Figure 15: RT-PCR of RNA from disease susceptible (BL/6) and disease resistant (BALB/c) mouse lymph nodes and spleen using primer set 1 (PS1). Both strains in both tissues exhibited bands at the expected size of 105 bp. LP-BM5 infected SC-1 cell RNA was used as a positive control. The RT positive sample had a band at 105 bp while the RT negative sample did not have a band at 105 bp.

The results of RT-PCR with RNA from BALB/c and BL/6 mice using MCF primer set 3 can also be viewed in figure 16. The positive and negative controls were the same as in figure 15. The positive control had amplicons at the desired 138 bp while the negative control did not show cDNA amplification. As with MCF primer set 1, primer set 3 showed MCF specific binding in both BALB/c and BL/6 mouse strains. Once again, a qualitative analysis can be made which suggest that the BL/6 spleen band had a greater intensity than the BALB/c spleen band and the lymph node bands for both strains had similar intensities, which are comparable to the BL/6 spleen band.

In addition a comparison was made between the qualitative data generated from MCF primer set 1 PCR products *versus* MCF primer set 3 PCR products. In general, both primer sets appeared to produce lymph node bands with similar intensities. Also, in both cases, the band specific to the BL/6 mouse spleen was darker than the band of the BALB/c mouse spleen.

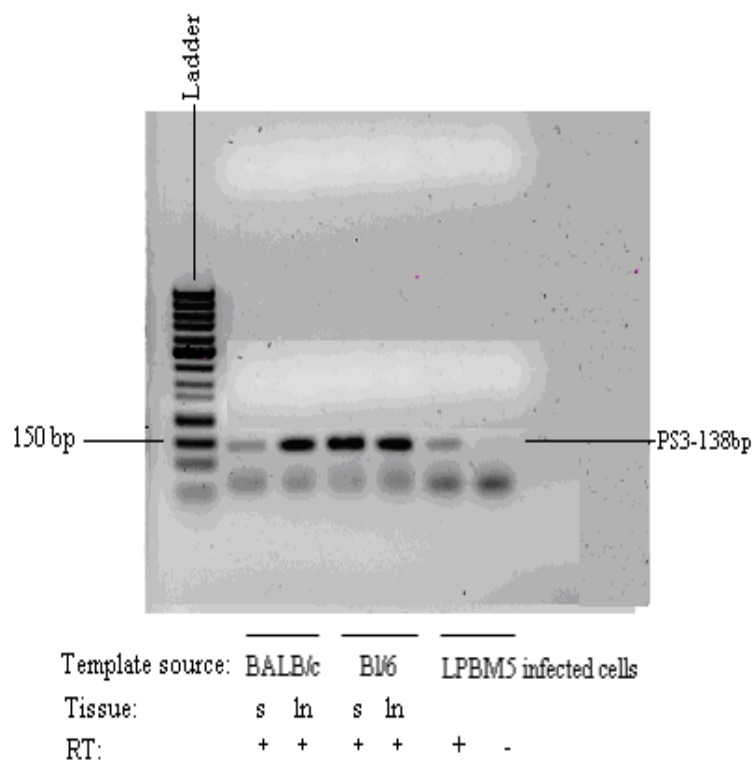


Figure 16: RT-PCR of RNA from disease susceptible (BL/6) and disease resistant (BALB/c) mouse lymph nodes and spleen using MCF primer set 3 (PS3). Both strains in both tissues exhibited bands at the expected size of 138 bp. LP-BM5 infected SC-1 cell RNA was used as a positive control. The RT positive sample had a band at 138 bp while the RT negative sample did not have a band at 138 bp.

REAL TIME PCR

1. Reducing Primer Dimer

When using SYBR Green in qRT-PCR it is important to eliminate primer dimer to reduce fluorescence from double stranded DNA that is not the desired amplicon. For this reason, varying primer concentrations were tested using conventional RT-PCR to minimize primer dimers during PCR. Figure 17 shows that there is very little primer dimer in PCR products using the various primer concentrations tested. Also, 9 μM primer concentrations had the most intense bands and at primer concentrations below 9 μM , product amplification becomes notably decreased. For this reason, 9 μM was selected as the optimal primer concentration for the qRT-PCR experiments.

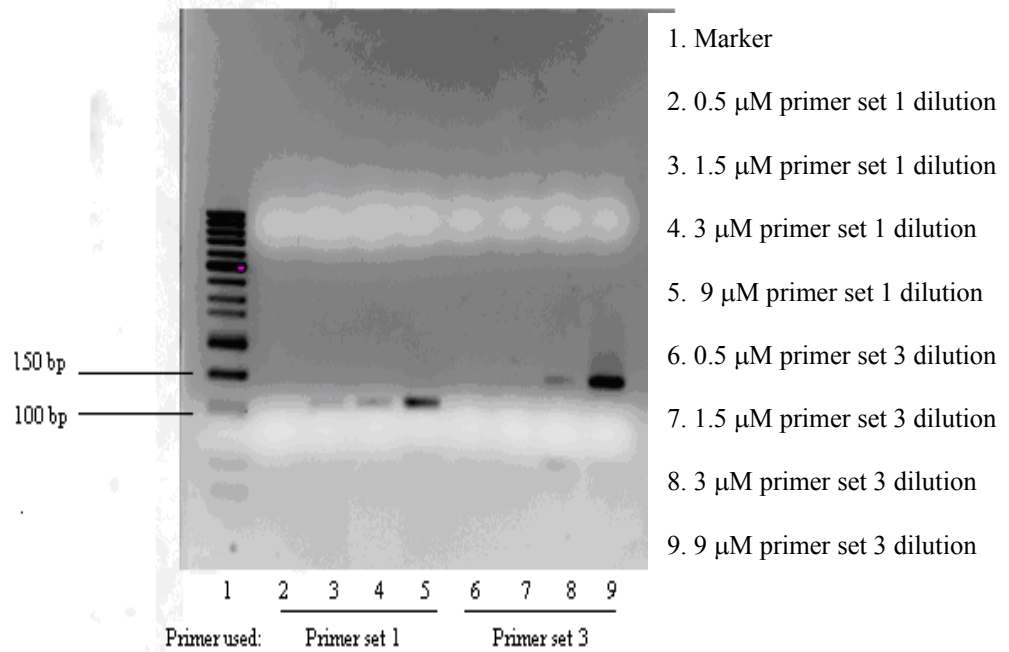


Figure 17: RT-PCR with varying concentrations of reverse and forward MCF primers using LPBM5 infected SC-1 cells cDNA.

Lane 2 did not exhibit a band at the expected size of 105 bp, while lanes 3, 4, and 5 did. Also, lanes 3, 4, and 5 had no primer dimer. Lanes 6 and 7 did not show bands at the expected size of 138 bp. Lanes 8 and 9 have bands at 138 bp with little primer dimer.

2. Real Time RT-PCR Data

Real Time PCR data was collected using the SDS 3000 software and exported into Microsoft Excel for further calculations. The SDS 3000 software provides the cycle number (Ct) at which the fluorescence emitted during PCR crosses the threshold, which can be set automatically or manually. Table 3 shows the analysis of the Ct values collected for the reference gene β -actin, MCF PS1 and MCF PS3 with varying input template concentrations. The Ct values were used to test for efficiency of the primer sets within the SYBR Green qRT-PCR chemistry with a range of template input. A plot was generated of the log template input *versus* the Ct values for the 3 different primer sets: β -actin (figure 18), MCF PS1 (figure 19), and MCF PS3 (figure 20). The slope of the line within each plot was used to calculate the reaction efficiency using the formula: $\text{efficiency} = 10^{(-1/\text{slope})}$. The slope of the line for both β -actin and PS1 was -3.1 and the reaction efficiencies were calculated to be approximately 2.1 . In order to obtain a plausible slope for PS3 a few value had to be dropped, which gave a line with the slope -1.4 . The slope translated into an efficiency of 0.18 . An ideal PCR reaction would double the template cDNA during every reaction cycle. Therefore the efficiency should be 2 with a line of slope -3.33

Table 3: qRT-PCR Validation experiment data. The Ct values of β -actin, MCF PS1, and MCF PS3 were normalized by subtracting the Ct of β -actin from the Ct of the gene of interest. The values for log of the input template are also given.

B ACTIN Avg Ct	MCF ps1 Avg Ct	Delta Ct $\Delta Ct_{ps1} = Ct_{ps1} - Ct_{B-actin}$	MCF ps3 Avg Ct	Delta Ct $\Delta Ct_{ps3} = Ct_{ps3} - Ct_{B-actin}$	LOG input template
17.94	16.45	-1.49	27.41	9.46	0.40
18.66	17.31	-1.34	26.54	7.88	0.10
16.72	15.35	-1.37	26.62	9.90	0.70
16.72	14.39	-2.33	26.27	9.55	1
14.87	13.49	-1.34	26.27	11.40	1.306
13.67	12.22	-1.45	26.53	12.86	1.70
12.91	11.45	-1.46	26.78	13.87	2

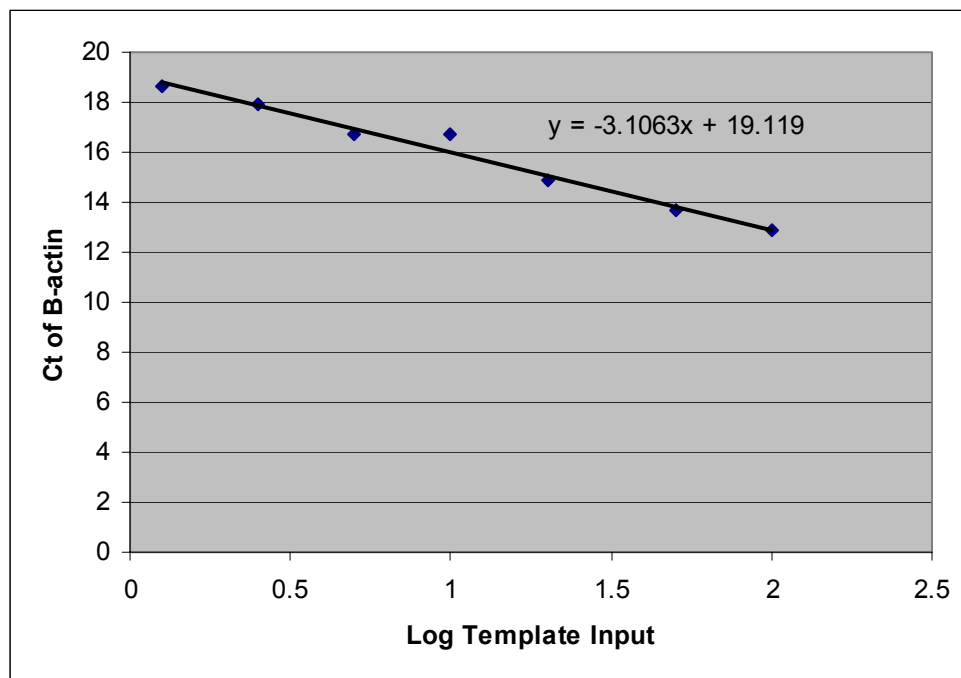


Figure 18: Plot of log template input versus the Ct of β -actin to test for efficiency of primer set. The slope of the line is -3.1 and the efficiency of the reaction is $10^{(-1/\text{slope})}=2.1$. An ideal PCR reaction has an efficiency of 2 and a slope of -3.33.

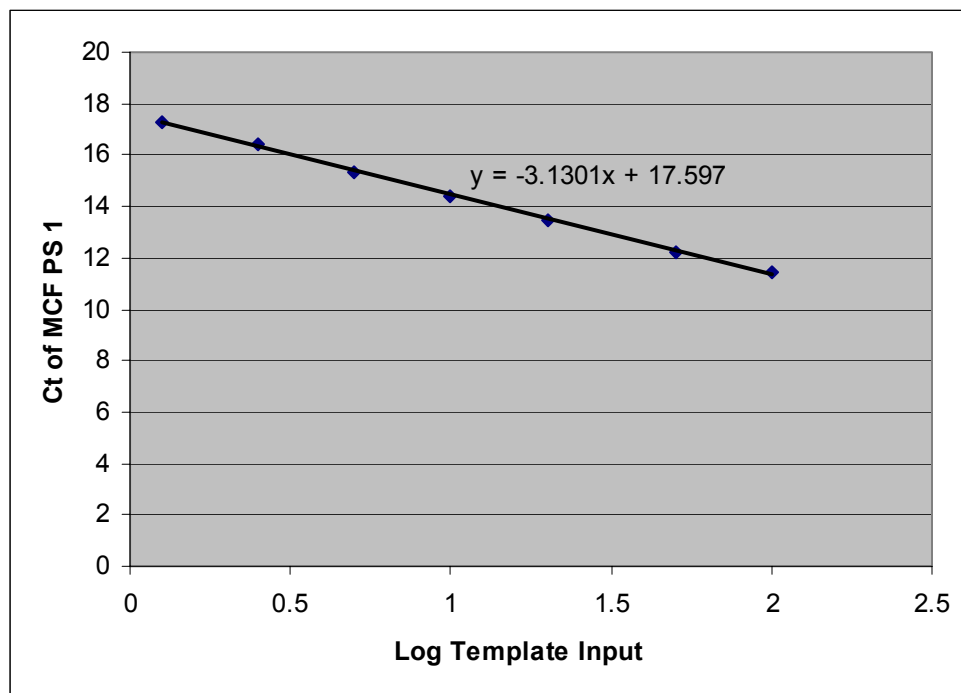


Figure 19: Plot of log input template versus the Ct of MCF PS1 to test for efficiency of primer set. The slope of the line is -3.1 and the efficiency of the reaction is $10^{(-1/\text{slope})}=2.1$. An ideal PCR reaction has an efficiency of 2 and a slope of -3.33.

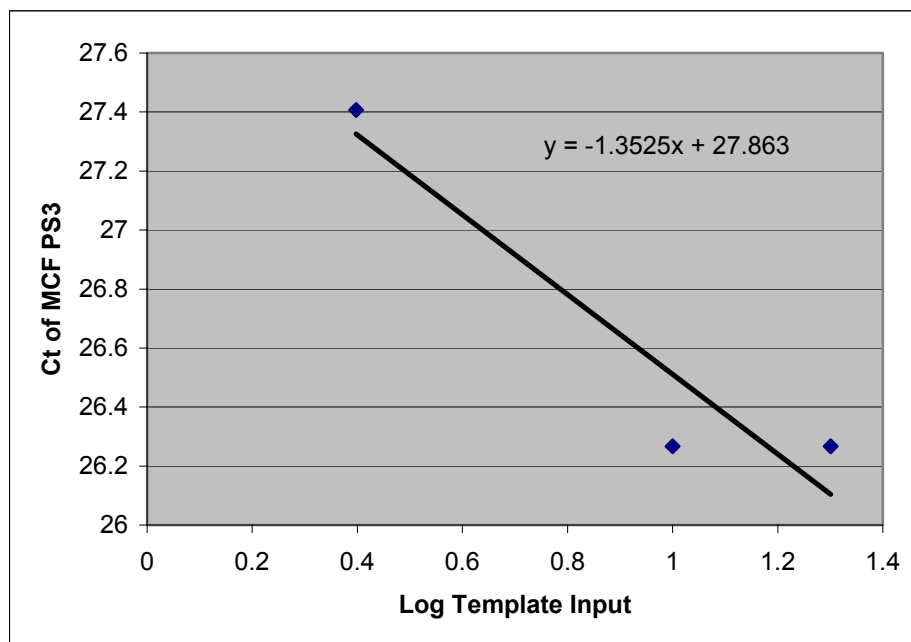


Figure 20: Plot of log input template versus the Ct of MCF PS3 to test for efficiency of primer set. The slope of the line is -1.4 and the efficiency of the reaction is $10^{(-1/\text{slope})}=0.18$. An ideal PCR reaction has an efficiency of 2 and a slope of -3.33.

Figures 21 and 22 show the results of the validation experiment, which compared the primer efficiencies of the reference gene to the primer efficiencies of the gene of interest. The ΔC_t value was generated through normalization of the C_t values by subtracting the C_t of β -actin from the C_t of the gene of interest. The absolute value of the slope for the MCF PS1 plot was 0.02, while the slope for the PS3 plot was 2.9. In order to use the $\Delta\Delta C_t$ method of analysis, the efficiencies of the primer set of the gene of interest must be comparable to the efficiency of the reference gene. Therefore, the slope produced by the line in the validation experiment needs to be less than 0.1. Thus only MCF PS1 can be used to quantitate MCF expression using the $\Delta\Delta C_t$ method.

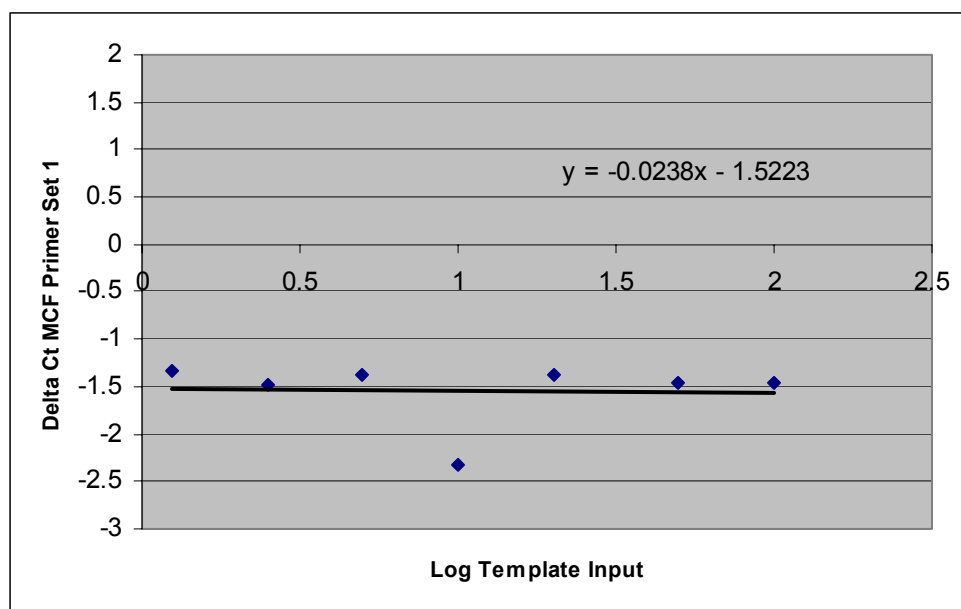


Figure 21: MCF PS1 validation experiment graph comparing normalized Ct values (ΔCt) to a log range of input template values. The equation of the line can be found in the plot ($y=-0.0238x-1.5223$). If the primer set is efficient then the absolute value of the slope will be less than or equal to 0.1

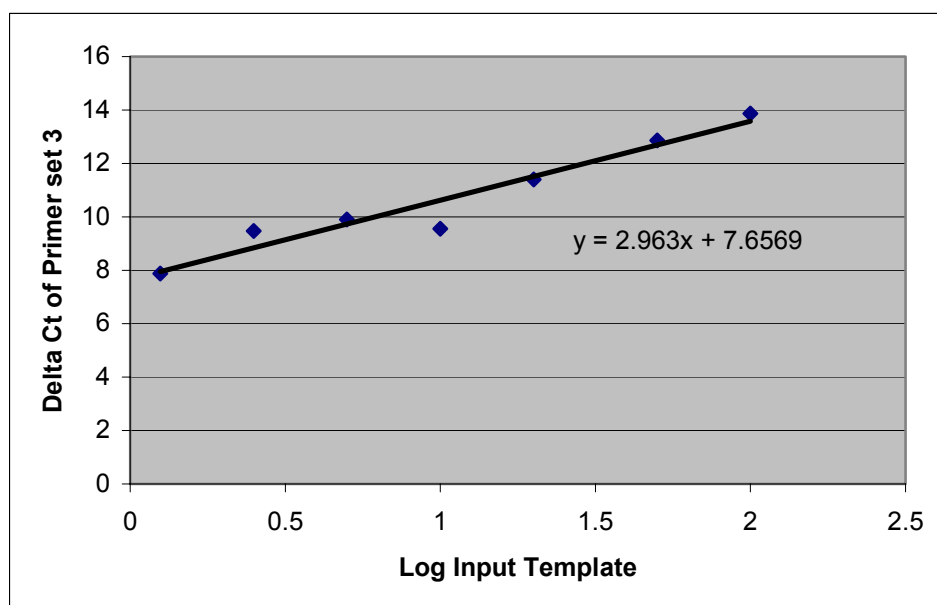


Figure 22: MCF PS3 validation experiment graph comparing normalized Ct values (ΔCt) to the log of input template. The equation of the line is provided on the figure ($y=2.963x+7.6569$). If the primer set is efficient then the absolute value of the slope will be less than or equal to 0.1

Once the validation experiment data was collected, an experimental plate was run to compare the expression of MCF between the two mouse strains. Tables 4 and 5 contain all data and calculations necessary to compare gene expression. First the ΔC_t specific to the gene of interest was calculated by subtracting the β -actin C_t from the MCF PS1 C_t . Then all of the ΔC_t values were calibrated by subtracting the chosen calibrator ΔC_t from all other ΔC_t . The BALB/c spleen was chosen as the calibrator since the C_t of BALB/c spleen was similar to the C_t values of the no template control. Since the no template control had late amplification, which is not ideal, the C_t values of the gene of interest that matched the no template control amplification were considered insignificant. This calibration generates a $\Delta\Delta C_t$ value, which can be used to calculate the fold difference of gene expression.

Table 4: Ct Values for the reference gene used in the experimental plate.

Sample	Detector	Avg Ct
BALB/c Spleen	B ACTIN	21.36
BALB/c LN	B ACTIN	21.35
BL/6 spleen	B ACTIN	20.79
BL/6 LN	B ACTIN	20.57

Table 5: Real time RT-PCR Data using MCF PS1 and MCF PS3. The table lists Ct values, Δ Ct values, $\Delta\Delta$ Ct values and fold expression difference between the two mouse strain's lymph nodes and spleen.

Sample	Detector	Avg Ct	Avg Δ Ct	$\Delta\Delta$ Ct	Fold Expression
			$Ct_{PS1} - Ct_{B_Actin}$	$\Delta Ct - \Delta Ct \text{ (BALB/c spleen)}$	$2^{(-\Delta\Delta Ct)}$
BALB/c Spleen	PS1	28.31	6.95	(calibrator)	
BALB/c LN	PS1	22.66	1.30	-5.65	50.14
BL/6 spleen	PS1	26.13	5.34	-1.61	3.06
BL/6 LN	PS1	23.11	2.54	-4.41	21.20

Figure 23 shows fold difference in expression of MCF within the BALB/c mouse lymph node, BL/6 spleen, and BL/6 lymph node in comparison to the BALB/c spleen calibrator. In these experiments, the BALB/c spleen does not have significant amplification. The other three samples showed a significantly higher level of expression of MCF than the BALB/c spleen. The BALB/c lymph node exhibited the greatest quantity of MCF with a 50 fold higher expression than the calibrator. A 21 fold greater expression of MCF was seen in BL/6 lymph node and a 3 fold higher expression in the BL/6 spleen. The lymph nodes of both mouse strains exhibited the most amplification of MCF, while the spleens had the least amplification.

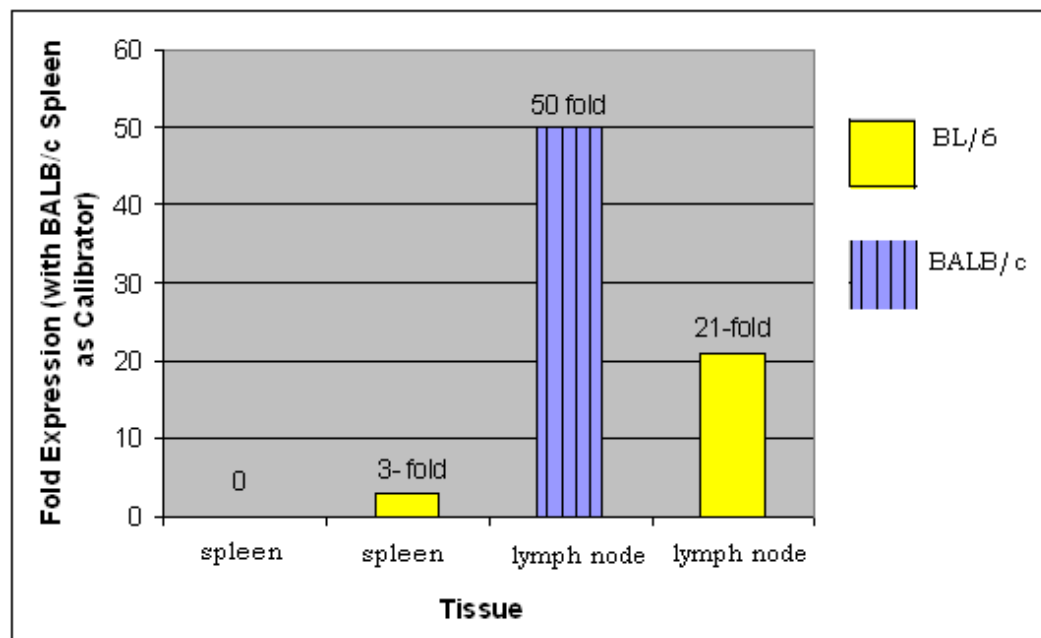


Figure 23: Fold differences in expression of MCF in BALB/c and BL/6 mouse lymphoid tissues. The fold differences of BALB/c lymph node, BL/6 spleen, and BL/6 lymph node are in relation to the calibrator, the BALB/c spleen.

SEQUENCING DATA

. The sequences of the endogenous retrovirus were compared to the sequences of the infectious retrovirus from the LP-BM5 infected SC-1 cells. Figure 24 shows the comparison of the three DNA sequences generated by using the forward primer of MCF PS1. Figure 25 shows the comparison of the three MCF sequences created using the reverse primer of MCF PS1. Many similarities between the two endogenous retroviruses and the infectious retrovirus can be seen closest to the primer sequences (similarities designated by asterisks), while many differences can be seen further from the primer sequence. BALB/c mice exhibited 66% sequence homology using the forward primer and 68% sequence homology using the reverse primer. BL/6 mice only showed only 46% sequence homology using the forward primer and 55% sequence homology using the reverse primer. However, the reverse and forward primer sequence could not be compared due to significant differences between the two sequences despite the fact that they are from the same PCR product.

Figure 26 compares the three MCF sequences that were generated using the forward primer of PS3 and figure 27 compares the three DNA sequences created using the reverse primer of PS3. As seen in figures 24 and 25, the nucleotides of the MCF from the two mouse strains closest to the reverse primer sequence showed more similarities to the infectious MCF sequence. When comparing the three sequences it was found that the BL/6 mice appear to have slightly more sequence homology to the infectious retrovirus than the BALB/c

mice. The BALB/c mice had 70% sequence homology using the forward primer and 54% sequence homology using the reverse primer. However, BL/6 mice exhibited 79% sequence homology using the forward primer and 58% sequence homology using the reverse primer. Once again, the reverse and forward primer sequence could not be compared due to significant differences between the two sequences.

```

      5'
LP-BM5 SC-1 GGC GGG ANG CAG GCC AAC TTA GAG AAA GAT TGA GTC
BALB/c      ** A N* C * G* * C A A * * T T A G ** * * A * G* * T T G G A G C **
BL/6        C C * A A C C T T T A * N A G * * A A G * T T * N * G N T C A * * N G A

LP-BM5 SC-1 A N A G A C A A A A G C T C T T T G A A T C C C A A C A A G G G T G G
BALB/c      * G * * * * * * * * * * * * * * * * * * * * * * N N * * * N
BL/6        C A * A * G G C C T C * * T * * G * * * * * * * * * * * * * * *

reverse primer
      3'

```

Figure 24: Comparison of the sequences generated from PCR products of infectious MCF isolated from LP-BM5 infected SC-1 cells and the endogenous MCF sequences of BALB/c genomic DNA and BL/6 genomic DNA using the forward primer of PS1. The sequences are oriented 5' to 3' and are the reverse complement of the DNA. The reverse complement of the reverse primer is highlighted and nucleotides that are similar between the sequences are designated by an asterisk (*). Ns found within the sequence indicate nucleotides that could not be read during sequencing.

```

      5'
      |
LP-BM5 SC-1 GTN TTG GAN ATC TTT CTC TAG TTT TGG CCA TGC CTA TCC CGT TAC
BALB/c      T *N GG*NTN *NA *C* T** NCNAG**T* GCATG ***** **C ***
BL/6        T *T NG**N* CGN NA*****T CTN TAG *T* GGC CATGCTAT* *CG ***

LP-BM5 SC-1 CAA TCC TGT GTG GCT CGG CATAGAAACAGC AT
BALB/c      *****T *G *****
BL/6        *****TC G*****
                                forward primer
                                3'

```

Figure 25: Comparison of the sequences generated from PCR products of infectious MCF isolated from LP-BM5 infected SC-1 cells and the endogenous MCF sequences of BALB/c genomic DNA and BL/6 genomic DNA using the reverse primer of PS1. The sequences are oriented 5' to 3' and are the reverse complement of the DNA. The reverse complement of the forward primer is highlighted and nucleotides that are similar between the sequences are designated by an asterisk (*). Ns found within the sequence indicate nucleotides that could not be read during sequencing.

Figure 26: Comparison of the sequences generated from PCR products of infectious MCF isolated from LP-BM5 infected SC-1 cells and the endogenous MCF sequences of BALB/c genomic DNA and BL/6 genomic DNA using the forward primer of PS3. The sequences are oriented 5' to 3' and are the reverse complement of the DNA. The reverse complement of the reverse primer is highlighted and nucleotides that are similar between the sequences are designated by an asterisk (*). Ns found within the sequence indicate nucleotides that could not be read during sequencing.


```

      5'
      |
LP-BM5 M1LV ATC GGT CTN GGC CCN GAG CCG GGG GCC CAG GGA NGC TNG
BALB/c      *AN TC*GTT CTG GGC CC* GA* CC* *GG *CC A*G T*G CTN
BL/6        GGG ***GAN ANT GTT CT* G*C T*A *** GG* *CC CAG GT*

LP-BM5 M1LV GAC TAC AGG ATA TCC GNG TTT GGG CCC CNG TCC CAG TAT TNT TCA
BALB/c      ***** **A TAT C*T *GT **G *CC **T GGT C** AGN *****
BL/6        CTN G** CAC *G* *AT CCT G** T** *** *T***** **G*****

LP-BM5 M1LV GCC TTA TTC TTAAAC TAA ACT TCN
BALB/c      *****C
BL/6        *****C
              forward primer
              3'

```

Figure 27: Comparison of the sequences generated from PCR products of infectious MCF isolated from LP-BM5 infected SC-1 cells along and the endogenous MCF sequences of BALB/c genomic DNA and BL/6 genomic DNA using the reverse primer of PS3. The sequences are oriented 5' to 3' and are the reverse complement of the DNA. The reverse complement of the forward primer is highlighted and nucleotides that are similar between the sequences are designated by an asterisk (*). Ns found within the sequence indicate nucleotides that could not be read during sequencing.

DISCUSSION

Until recently, the global gene expression patterns of mice following infection with a retrovirus had not been studied. The microarray, which measures gene expression patterns, has made it possible to study differential gene expression in response to MuLV virus infection in BALB/c (MAIDS susceptible) versus BL/6 (MAIDS resistant) mice early in the immune response. The ultimate goal is to determine what factors confer susceptibility or resistance in the mice and apply the findings to human susceptibility to AIDS. One gene in particular, MCF, was found to be the most highly differential expressed gene between the two mouse strains, exhibiting a 55-fold higher expression in the disease susceptible mice. RT-PCR, Real Time RT-PCR and DNA sequencing were used to further study this gene and explicate its role, if any, in MAIDS disease pathogenesis.

Optimizing RT-PCR Protocol and Primers

In order to perform a successful RT-PCR experiment, high quality RNA along with optimization of the protocol and primers is necessary. The quality and quantity of the RNA isolated from LP-BM5 infected SC-1 cells and the lymphoid tissues of the two mouse strains was inspected using the Bioanalyzer (Agilent) and the Nanodrop. All of the RNA samples chosen for use had little or no degradation, are free of contamination of DNA or protein, and were available in high concentrations.

Three primer sets were then created from a published sequence of MCF. Two of the primer pairs spanned a portion of the oligonucleotide probe that originally detected MCF in the microarray (PS2 and PS3), while one primer set was located upstream of the probe region (PS1). A primer set that contained part of the microarray probe was needed in order to amplify products that were initially detected by the microarray experiment. PS1, which did not contain a portion of the probe, was also created to prove that MCF could be detected using independent sets of MCF-specific primers. Conventional RT-PCR was performed using the three different primer sets and an agarose gel was run to visualize the PCR products. PS1 exhibited a distinct band at the expected molecular weight; therefore the initial PCR protocol was not altered. However, PS2 did not show a band and PS3 produced a band at the expected molecular weight and another band at a high molecular weight (See figure 8).

As a result, the conditions used during PCR were altered in order to induce each primer set to produce one distinct amplicon of the correct size. First, the PCR products were subjected to a wide range of annealing temperatures. Annealing depends directly on the length and nucleotide composition of the primers. Since PS2 did not generate an amplicon, I believed that the annealing temperature was too high, which decreased the primer set's ability to bind to the target sequence. Yet, lowering the annealing temperature increased the probability of the primers annealing to sequences other than the target sequence. This is because at lower temperatures, internal single-nucleotide mis-matches or

even partial annealing of the primers is tolerated. Therefore, having a higher annealing temperature could increase the specificity of amplification. I hypothesized that by increasing the annealing temperature for PS3, the non-specific high molecular weight band would be eliminated. Results showed that PS2 did not work under any annealing temperature tested, but PS3 had more specific binding at higher annealing temperatures. The most specific band was found using an annealing temperature of 55 °C (See figure 9). Therefore, both PS1 and PS3 could be run under the same conditions, which reduced variability between subsequent PCR reactions. Other conditions could have been altered in order to encourage amplification using PS2 (such as altering Magnesium concentrations). However, only one primer set that contained a portion of the microarray probe was needed, so PS2 was abandoned.

The specificity of the remaining primers to the MCF sequence was tested. This was done by using RNA from species which are known not to contain MCF-like sequences in their genome, and subjecting them to the same PCR protocol (see materials and methods and figure 10 in results). Since the primers did not exhibit amplicons in other species they were determined to be specific to MCF.

MCF-like Sequences in the Mouse Genome

To determine whether MCF-like endogenous retroviruses were stable inherited in the genome of the BALB/c and BL/6 mice, PCR experiments with the two working primer sets were performed using DNA isolated from the two strains. Both PS1 and PS3 exhibited MCF specific amplicons in both mouse strains (See figure 11). Therefore, both disease susceptible and disease resistant mice contain MCF-like sequences within their genome.

Expression of MCF-like Sequences

RT-PCR was once again performed using PS1 and PS3, but with cDNA reverse transcribed from spleen and lymph node of naïve, untreated animals from the two mouse strains as the template. Both primer sets showed specific amplification of MCF-like sequences within the BALB/c and BL/6 mice (See figures 15 and 16). Since the presence of MCF-like mRNA is regulated by transcription from DNA, its presence indicates that it is actively expressed in the lymphoid tissues of the two mice.

Although RT-PCR is non-quantitative, the intensity of the bands produced during PCR can be indicative of the abundance of end-point amplicons. A band with high intensity implies that more amplicons are present than in a low intensity band. This is due to the profusion of the protein ethidium bromide (EtBr) in samples with more product present. EtBr, which is used to visualize the bands in a gel, is an intercalator that stability binds to the minor grooves of double stranded

DNA (Wikipedia, 2006). Once the ethidium bromide is exposed to a UV light of a specific wavelength it will fluoresce. The amount of fluorescence is directly proportional to the strength of the band seen and the abundance of product for EtBr.

Amplicons produced using primer set PS1 had varying band intensities. The BL/6 spleen appeared to have a greater concentration of product than the BALB/c spleen, which suggests that the BL/6 spleen has a greater expression of MCF-like RNA than the BALB/c spleen. On the other hand, the lymph nodes of the two mice appear to express a similar amount of MCF-like mRNA. Therefore, more MCF may be expressed in the BL/6 spleen.

The qualitative analysis of MCF expression within BALB/c and BL/6 mice using PS3 also suggests that the BL/6 spleen exhibits greater expression of MCF-like sequences than the BALB/c spleen due to the variation in band intensity. However, the lymph nodes of the two mouse strains had band intensities that were comparative to the BL/6 as opposed to the BALB/c spleen. PS3 data suggests higher expression of MCF in the lymph nodes of both mice and the spleen of the BL/6 mouse, with less expression in the BALB/c spleen. While the qualitative data regarding MCF transcripts in mouse tissues implies levels of expression, pipetting errors or different amounts of starting template could easily alter the results. Therefore, in order to obtain substantial results regarding levels of gene expression a quantitative real time RT-PCR experiment was performed.

It is worth noting that the electrophoretic gels used to visualize the PCR products showed low molecular weight bands around 25-50 bp. These bands are believed to be primer dimer due to their size. Another indication that the bands are primer dimers is that their intensity decreases as the amplicon intensity increases. When more primers are being used to amplify cDNA, less primer pairs are available to bind to each other. Since the presence of primer dimer did not hinder the success of RT-PCR experiments it was not a concern.

Quantitation of MCF Expression using Real Time PCR

While the presence of primer dimer was not a concern during RT-PCR experiments, it is detrimental to Real Time PCR experiments using the SYBR Green fluorescent probe. SYBR Green binds to any double stranded DNA molecule and exhibits fluorescence during qRT-PCR. Since fluorescence of only the target sequence is desired it is important to eliminate all other double stranded DNA. RT-PCR was used with varying primer concentrations with the hopes that by reducing the amount of primer added to the reaction mixture, primer dimer will be reduced. The experiment was successful in producing a band with high intensity and no visible primer dimer using a 9 μ M concentration of each primer (See figure 17).

Once an optimal primer concentration was chosen, a validation experiment was performed to determine the efficiency of the primer sets in amplification of target DNA. The reference gene β -actin and PS1 showed similar acceptable

efficiencies of 2.1. Since an ideal PCR reaction doubles the template during every PCR cycle, the efficiency should be 2. Therefore, β -actin and MCF PS1 have near perfect amplification efficiencies. In order to attempt to salvage the data for generated by comparing the normalized MCF PS3 Ct values and the log template input, certain data points were removed from the data set. A slope of -1.4 and an efficiency of 0.18 were calculated from the revised graph. An efficiency of 0.18 implies that only a small fraction of the template DNA is amplified in the PCR reaction. The poor efficiency of PS3 can be attributed to the fact that each sample crossed the threshold late during the reaction at approximately the same cycle despite the varying levels of starting template.

In order for the $\Delta\Delta C_t$ method of analysis to be used to compare differential expression of MCF, the efficiencies of either MCF PS1 or PS3 need to be similar to the reference gene, β -actin (ABI, 2006). Comparable efficiencies are designated as a slope of less than or equal to 0.1 for the line generated by plotting the log input template against the normalized Ct (ΔC_t) values. Since the absolute value of the slope created when comparing PS1 to β -actin was 0.02, the $\Delta\Delta C_t$ method can be used when analyzing PS1 PCR product amplification. However, the slope for the PS3 plot was 2.9, which indicates that the efficiencies of PS3 and β -actin are very different and qRT-PCR with PS3 cannot be analyzed using the $\Delta\Delta C_t$ method. The data was then normalized in order to account for various errors in the experimental setup such as unequal amounts of starting

template. This was done by comparing the Ct values from the primer sets specific to the gene of interest to the reference gene.

There are various reasons why poor efficiency was associated with primer set PS3. Real Time PCR reactions suggest that the favorable amplicon length is between 100-150 bp. SYBR Green protocols recommend that amplicons should be closer to 100 bp in length rather than 150 bp for optimal reaction efficiency. PS3 amplicons are 138 bp, which may be too long for an optimal Real Time PCR reaction to occur. However, the amplicon length is unlikely to contribute to poor efficiency since the β -actin amplicon is 153 bp and is highly efficient.

Also, it is possible that the high annealing temperature used during PCR affected efficiency. As annealing temperature increases the specificity of binding increases, but the amount of amplification can also decrease. Decreased amplification could result from the increased stringency of binding due to the higher temperatures at which the products can anneal. The previous experiments that tested PS3 using many annealing temperatures (see figure 11B of the results) may have had acceptable amplification at the higher annealing temperatures without non-specific amplification, yet the intensity of the amplicons decreased. The annealing temperature of 55°C was chosen in order to ensure primer set specificity, but slightly lower annealing temperatures may have also worked. Therefore, future qRT-PCR experiments using PS3 could benefit from alterations of annealing temperatures or other parameters such as varying Magnesium Chloride concentrations in the reaction mixture.

Since PS1 was found to be efficient, the $\Delta\Delta C_t$ method was used to compare MCF amplification between the two strains of mice. The fold difference of MCF expression in the BALB/c lymph node, BL/6 spleen, and BL/6 lymph node were compared to the expression of MCF in the BALB/c spleen (calibrator), which was considered to have insignificant amplification. A microarray experiment showed that MCF was highly expressed in the BL/6 mouse lymphoid tissues and found in very low levels in the BALB/c mouse lymphoid tissues. However, the naïve mice showed a different trend of MCF expression levels in the spleen and lymph node of the two strains. As concluded from the qRT-PCR data, the BALB/c spleen does not have significantly high levels of endogenous MCF, but the BALB/c lymph node appears to contain many MCF transcripts with a 50 fold higher expression than the calibrator. The BL/6 mice also showed significant expression of MCF (21 fold higher expression than the calibrator in the lymph node and 3 fold higher expression in the spleen), but in lower levels than in the BALB/c lymph node (See figure 23).

One conclusion that can be drawn from these data is that expression levels of MCF in naïve mice are not the same between the lymph node and spleen. This is very different from the microarray data in which both tissues showed comparable expression of MCF, whether infected with MuLV or mock infected. The injection of the mice with mock supernatant or virus may alter MCF transcription within the two mice. MCF is significantly downregulated or suppressed in the BALB/c lymph node and upregulated in the BL/6 spleen and

lymph node following injection. The cause of the change in expression remains uncertain.

One possible explanation for enhanced expression of endogenous MCF is that it can be induced by stimulation of the immune response or by the activation of nearby genes. Such genes include ones that are involved in the immune response (i.e. Ig molecules or genes encoding lymphocyte antigens) (Krieg et al., 1988; Stevens et al., 1999). The injection of the mice, even with mock supernatant, can be enough of a stimulant to augment MCF in the secondary lymphoid tissues. Mock infection could induce an immune response, due to its components such as penicillin/streptomycin or fetal bovine serum albumin (FBS). FBS originates from an organism other than mouse (cow), therefore its surface molecules and proteins will be recognized by the mouse immune system as foreign and immune response will be mounted. However, the mechanism by which MCF could be suppressed from transcription in the BALB/c mice following injection is unknown. This difference in MCF expression in the two mouse strains could play a major role in MuLV pathogenesis. One research group believes that MCF-like proteins can suppress lymphocyte activation by inducing an inhibitory negative feedback mechanism on the immune system (Krieg et al., 1989; Krieg et al., 1992). Therefore if MCF is downregulated in the BALB/c mice then the immune system will not be inhibited and can mount an effective immune response to virus early during infection. Yet, if the increased transcription of MCF mRNA in the BL/6 lymphoid organs in response to immune

stimuli suppresses the immune system, then the mice will not have the ability to eradicate the virus. As a result, the BL/6 mice would be susceptible to MAIDS, while the BALB/c mice maintain the ability to fight infection.

MCF Sequencing Analysis

MCF specific PCR products were sequenced, which allowed for comparison between the infectious MCF portion of MuLV and the endogenous MCF-like sequences found in the two mouse strains. PS1 amplicons from the BALB/c mouse genome were more similar to the infectious MCF than PS1 amplicons from the BL/6 mouse genome (BALB/c mice exhibited 66-68% homology; BL/6 mice exhibited 46-55% homology). PS3 exhibited the opposite trend (BALB/c mice showed 54-70% homology and BL/6 mice showed 58-79% homology), although the efficiency of the primer pair has been called into question. More notably, each PCR product did not have matching reverse and forward primer sequences, which was unexpected since the forward and reverse primer are both amplifying the same gene region in each respective primer set.

The conclusions that can be drawn from these data indicate that while the MCF primer sets may be specific to MCF, they are amplifying multiple MCF-like sequences that have varying base pairs. If there is more than one MCF-like amplicon within the PCR reaction, which have sequence variation, it is difficult to produce one distinct endogenous MCF sequence. The Ns seen in the sequences from Elim Biopharmaceuticals indicate that the bases at particular locations could

not be read. This could be due to more than one type of nucleotide located at the same position in the PCR product sequence. Strong secondary structures could also account for the unreadable base pairs in these regions.

Interestingly, the most homology between the MCF sequences can be seen at the location of the forward or reverse primers, while the center of the amplicon contains more differences. Presumably, these similarities are what allow the primer sets to bind to all of the multiple MCF sequences. If the variations in bases were increased at the primer binding sites then binding would not occur, resulting in a lack of product amplification. The differences that can be seen at the primer sites are located at the end of the primer sequences not in the middle, so they should not prevent primer binding.

Another reason for variation in the sequences of the PCR products is that PCR amplification, which happens numerous times throughout the reaction, can introduce many mutations in the sequence and Taq DNA polymerase does not have the ability to proofread (Promega, 2006). Future experiments would need to sequence MCF like sequences directly from genomic DNA as opposed to PCR products. Large quantities of genomic DNA would be needed to ensure that sufficient amount of endogenous MCF are present to allow for efficient sequencing. Target regions could also be checked to ensure that they do not have strong secondary structure. However, due to the similarities between all MCF like sequences I do not think it will be possible to create a primer set that is

specific to just one endogenous MCF gene, so problems regarding variability between the sequences might persist.

Future Research

As mentioned previously, the sequencing protocol needs to be altered in hopes of attaining more accurate sequences of endogenous MCF. Also, in order to directly compare expression of endogenous MCF-like sequences to the microarray data, Real Time RT-PCR needs to be performed using the RNA isolated from the spleen and lymph node of the two mouse strains that were either MuLV infected or mock infected. Theoretically, qRT-PCR should support that microarray results that demonstrate a 55 fold higher expression of MCF in BL/6 mice under any conditions. Additionally, determining levels of MCF-like proteins would be valuable to prove the MCF-like mRNA is translated into protein in one or both mouse strains. The next logical step would be to investigate the factors that regulate the expression of MCF and initiate either upregulation or suppression of the endogenous retrovirus post injection. Additionally, duplication of the qRT-PCR experiment using naïve mouse RNA with several biological replicates is important to ensure reproducibility of the aforementioned results.

Since these experiments did not observe MCF expression early during life a conclusion regarding their involvement in development of T cells cannot be made. Therefore, another interesting experiment would include performing

additional RT-PCR experiments using isolated RNA from the thymus of very young BALB/c and BL/6 mice. The thymus is responsible for creating a T cell repertoire that does not include lymphocytes that could recognize self proteins. If MCF-like sequences are present in the thymus of young mice early during T cell development, then MCF could be regarded as self and ignored when the animal is infected with LP-BM5 MuLV.

Conclusions

Since endogenous retroviruses that resemble HIV (HERVS) are present in humans, any knowledge regarding the role of endogenous MCF sequences in MAIDS pathogenesis can help to better understand whether HERVs influence HIV infection. However, studies regarding MCF-like sequences, their different levels of expression and their relationship to disease pathogenesis, are scarce. Further study of MCF could determine its involvement, if any, in increasing the susceptibility of BL/6 mice to MAIDS. If the study of MCF-like sequences can lead to a better understanding of the immune response to HIV, new factors contributing to human susceptibility to AIDS may be discovered. Such progress is important in the eventual production of effective therapeutic agents to control infection or even eradicate HIV.

References

- Applied Biosystems (ABI). Real time PCR: getting started with real time PCR. 2006. Accessed April 1, 2006. <<http://www.appliedbiosystems.com>>.
- AIDS info act sheet: US Department of Health and Human Services. Guidelines for the use of antiretroviral agents in HIV-infected adults and adolescents. 2005. Accessed November 29, 2005. <<http://aidsinfo.nih.gov>>.
- Blatt, C., Mileham, K., Haas, M., Nesbitt, M.N., Harper, M.E., and M.I. Simon. Chromosomal mapping of the mink cell focus-inducing and xenotropic *env* gene family in the mouse. 1983. *Proc. Natl. Acad. Sci.* 80: 6298-6302.
- Chattopadhyay. S.K., Lander, M.R., Rands, E., and D.R. Lowy. Structure of endogenous murine leukemia virus DNA in mouse genomes. 1980. *Proc. Natl. Acad. Sci.* 77: 5774-5778.
- Chattopadhyay. S.K., Sengupta, D.N., Fredrickson, T.N., Morse, H.C., and J.W. Hartley. Characteristics and contributions of defective, ecotropic, and mink cell focus-forming viruses involved in a retrovirus-induced immunodeficiency syndrome of mice. 1991. *J., Virol.* 65: 4232-4241.
- Clark, S., Duggan, J., and J. Chakraborty. Ts1 and LP-BM5: A comparison of two murine retrovirus models for HIV. 2001. *Viral Immunol.* 14: 95-109.
- Cook, J.W., Green, K.A., Obar, J.J., and W.R. Green. Quantitative analysis of LP-BM5 murine leukemia retrovirus RNA using real-time RT-PCR. 2002. *J. Virol. Meth.* 108: 49-58.
- Dorak, M.T. Real-time PCR. 2004. Accessed June 17, 2004. <<<http://dorakmt.tripod.com/genetics/realtime.html>>>
- Fine, H.A., and J.G. Sodroski. Tumor viruses. *Cancer Medicine: cancer entiology.* 1981. 6: 237-250. BC Decker Inc.
- Gardner, M.B., Kozak, C.A., and S.J. O'Brien. The Lake Casitas wild mouse: evolving genetic resistance to retroviral disease. 1991. *Trends Genet.* 7: 22-27.
- Gourley, M.F., Krieg, A.M., and A.D. Steinberg. Preferential nuclear compartmentalization of endogenous mink cell focus-forming-related retroviral transcripts. 1990. *J. Exp. Med.* 171: 1443-1452.
- Jolicoeur, P. Murine acquired immunodeficiency syndrome (MAIDS); an animal model to study the AIDS pathogenesis. 1991. *FASEB J.* 5: 2398-2405.

- Jolicoeur, P., Hanna, Z., Aziz, D., Simard, C., and M. Huang. The murine acquired immunodeficiency syndrome (MAIDS) induced by the Duplan strain retrovirus. 1991. *Amer. Soc. Microbiology*. 113-131.
- Krieg, A.M., Gause, W.C., Gourley, M.F., and A.D. Steinberg. A role for endogenous retroviral sequences in the regulation of lymphocyte activation. 1989. *J. Immun.* 143: 2448-2451.
- Krieg, A.M., Khan, A.S., and A.D. Steinberg. Multiple endogenous xenotropic and mink cell focus-forming murine leukemia virus-related transcripts are induced by polyclonal immune activators. 1988. *J. Virol.* 62: 3545-3550.
- Krieg, A.M., Gourley, M.F., and A. Perl. Endogenous retroviruses: potential entologic agents in autoimmunity. 1992. *FASEB J.* 6: 2537-2544.
- Khan, A.S. Nucleotide sequence analysis establishes the role of endogenous murine leukemia virus DNA segments in formation of recombinant mink cell focus-forming viruses. 1984. *J. Virol.* 50: 864-871.
- Lange, C.G. and M.M. Lederman. Immune reconstitution with antiretroviral therapies in chronic HIV-1 infection. 2003. *J. Antimicro. Chemo.* 51: 1-4.
- Liang, B., Wang, J.Y., and R.R. Watson. Murine AIDS, a key to understanding retrovirus-induced immunodeficiency. 1996. *Viral Immunology*. 9: 225-239.
- Miedema, F., Petit, A. J., Terpstra, F. G., Schattenkerk, J. K., Wolf, F., and B.J. Al. Human immunodeficiency virus (HIV)-infected asymptomatic homosexual men; HIV affects the immune system before CD4⁺ T helper cell depletion occurs. 1988. *J. Clin. Invest.* 82: 1908–1914.
- Morse, H.C., Chattopadhyay, S.K., Makino, M., Fredrickson, T.N., Hugin, A.W., and J.W. Hartley. Retrovirus-induced immunodeficiency in the mouse: MAIDS as a model for AIDS. 1992. *AIDS* 6: 607-621.
- Mosier D. Small animal models for acquired immune deficiency syndrome (AIDS) research. 1996. *Laboratory Animal Science*. 46: 257-264.
- Mosier, D.E., Yetter, R.A., and H.C. Morse III. Retroviral induction of acute lymphoproliferative disease and profound immunosuppression in adult C57BL/6 mice. 1985. *J Exp Med.* 161: 766-784.

- Mosier, D.E., Yetter, R.A., and H.C. Morse III. Functional T lymphocytes are required for a murine retrovirus-induced immunodeficiency disease (MAIDS). 1987. *J. Exp. Med.* 165: 1737-1742.
- Nolan, G.P. Nolan lab tutorials. Retroviral tutorials. 2006. Accessed: April 2, 2006. <http://www.stanford.edu/group/nolan/tutorials/ret_6_gpedesc.html>.
- Obata, M.M., and A.S. Khan. Structure, distribution, and expression of an ancient murine endogenous retroviruslike DNA family. 1988. *J. Virol.* 62: 4381-4386.
- Panoutsakopoulou, V., Little, C.S., Sieck, T.G., Blankenhorn, E.P., and K.J. Blank. Differences in the immune response during the acute phase of E-55+ murine leukemia virus infection in progressor BALB and long term nonprogressor C57BL mice. 1998. *J. Immunol.* 161: 17-26.
- Parham, P. 2005. *The immune system* 2nd ed, Garland Publishing, New York.
- Pogo, B.G., Holland J.F. Possibilities of a Viral Etiology for Human Breast Cancer. 1997. *Biol Trace Elem Res.* 56: 131-42.
- Promega. Abstract for Taq DNA polymerase. 2006. Accessed April 29, 2006. <<http://www.promega.com/tbs/9pim166/9pim166.html>>.
- Risser, R., Horowitz, J.M., and J. McCubrey. Endogenous mouse leukemia viruses. 1983. *Ann. Rev. Genet.* 17: 85-121.
- Sankaran, S., Guadalupe, M., Reay, E., George, M.D., Flamm J., Prindiville, T., and S. Dandekar. Gut mucosal T cell responses and gene expression correlate with protection against disease in long-term HIV-1-infected nonprogressors. 2005. *PNAS.* 102: 9860-9865.
- Seifarth, W., Frank, O., Zeilfelder, U., Spiess, B., Greenwood, A.D., Hehlmann, R., and C. Leib-Mosch. Comprehensive analysis of human endogenous retrovirus transcriptional activity in human tissues with a retrovirus-specific microarray. 2005. *J. Virol.* 79: 341-352.
- Stevens, R.W., Baltch, A.L., Raymond, P.S., McCreedy, B.J., Michelsen, P.B., Bopp, L.H., and H.B. Urnovitz. Antibody to human endogenous retrovirus peptide in urine of human immunodeficiency virus type 1-positive patients. 1999. *Amer. Soc. Microbio.* 6: 783-786.

- Stewart, A.F.R. Identification of Human Homologs of the Mouse Mammary Tumor Virus Receptor. 2002. Arch. Virol. 127: 577-581.
- Stewart, T.H.M., Sage, R.D., Stewart, A.F.R., and D.W. Cameron. Breast Cancer Incidence Highest in the Range of One Species of House Mouse, *Mus Domesticus*. 2000. British Journal of Cancer 82: 446-451
- Taruscio, D., and A. Mantovani. Factors regulating endogenous retroviral sequences in human and mouse. 2004. Cytogenet. Genome Res. 105: 351-362.
- Tepsuporn, S. Strain-specific differential gene expression in a mouse model of AIDS using DNA-microarrays. 2005. Senior Thesis: Mount Holyoke College, S. Hadley MA.
- Tomonaga, K., and J.M. Coffin. Structures of endogenous nonecotropic murine leukemia virus (MLV) long terminal repeats in wild mice: implication for evolution of MLVs. 1999. J. Virol. 73:4327-4340.
- UNAIDS. Joint United Nations Program on HIV/AIDS. Fact Sheet. 2005. Accessed: November 29, 2005. < <http://www.unaids.org/en/media/fact+sheets.asp>>
- Urnovitz, H.B., and W.H. Murphy. Human endogenous retroviruses: nature, occurrence, and clinical implications in human disease. 1996. Clin. Microbiol. Reviews. 9: 72-99.
- Ward, J.M., Parsonneault, E., and D.E. Devor-Henneman. The virtual mouse necropsy: search for the elusive lymph nodes and many mammary glands. 1999. Accessed: March, 25, 2006. <<http://www.geocities.com/virtualbiology/necrops.html>>.
- White, D.E., and F.J. Fenner. 1994. Medical Virology 4th ed, Academic Press, Orlando.
- Wikipedia, the free encyclopedia. Ethidium Bromide. 2006. Accessed February 23, 2006. <<http://en.wikipedia.org>>
- Young, R.A. Biomedical discovery with DNA arrays. 2000. Cell. 102: 9-15.

APPENDIX I

Raw Data from Real Time PCR Validation Experiment. All wells were run in triplicate and the data was averaged.

Well	Sample Name	Detector	Task	Ct	StdDev Ct
A1	2.5	B ACTIN	Unknown	18.18	0.375
A2	2.5	B ACTIN	Unknown	18.14	0.375
A3	2.5	B ACTIN	Unknown	17.51	0.375
A4	2.5	MCF PS I	Unknown	16.6	0.132
A5	2.5	MCF PS I	Unknown	16.41	0.132
A6	2.5	MCF PS I	Unknown	16.35	0.132
A7	2.5	MCF PS III	Unknown	26.73	0.648
A8	2.5	MCF PS III	Unknown	27.47	0.648
A9	2.5	MCF PS III	Unknown	28.02	0.648
B1	1.25	B ACTIN	Unknown	18.81	0.136
B2	1.25	B ACTIN	Unknown	18.56	0.136
B3	1.25	B ACTIN	Unknown	18.6	0.136
B4	1.25	MCF PS I	Unknown	17.36	0.047
B5	1.25	MCF PS I	Unknown	17.26	0.047
B6	1.25	MCF PS I	Unknown	17.32	0.047
B7	1.25	MCF PS III	Unknown	26.53	0.389
B8	1.25	MCF PS III	Unknown	26.15	0.389
B9	1.25	MCF PS III	Unknown	26.93	0.389
C1	5	B ACTIN	Unknown	16.84	0.104
C2	5	B ACTIN	Unknown	16.68	0.104
C3	5	B ACTIN	Unknown	16.64	0.104
C4	5	MCF PS I	Unknown	15.43	0.074
C5	5	MCF PS I	Unknown	15.34	0.074
C6	5	MCF PS I	Unknown	15.28	0.074
C7	5	MCF PS III	Unknown	25.91	0.633
C8	5	MCF PS III	Unknown	26.81	0.633
C9	5	MCF PS III	Unknown	27.13	0.633
D1	10	B ACTIN	Unknown	15.98	0.244
D2	10	B ACTIN	Unknown	15.79	0.244
D3	10	B ACTIN	Unknown	15.49	0.244
D4	10	MCF PS I	Unknown	14.56	0.153
D5	10	MCF PS I	Unknown	14.26	0.153
D6	10	MCF PS I	Unknown	14.35	0.153
D7	10	MCF PS III	Unknown	26.54	0.846
D8	10	MCF PS III	Unknown	25.32	0.846

D9		10	MCF PS III	Unknown	26.94	0.846
E1		20	B ACTIN	Unknown	15.14	0.255
E2		20	B ACTIN	Unknown	14.84	0.255
E3		20	B ACTIN	Unknown	14.63	0.255
E4		20	MCF PS I	Unknown	13.4	0.137
E5		20	MCF PS I	Unknown	13.64	0.137
E6		20	MCF PS I	Unknown	13.42	0.137
E7		20	MCF PS III	Unknown	26.27	0.03
E8		20	MCF PS III	Unknown	26.24	0.03
E9		20	MCF PS III	Unknown	26.29	0.03
F1		50	B ACTIN	Unknown	13.85	0.205
F2		50	B ACTIN	Unknown	13.7	0.205
F3		50	B ACTIN	Unknown	13.45	0.205
F4		50	MCF PS I	Unknown	12.29	0.089
F5		50	MCF PS I	Unknown	12.12	0.089
F6		50	MCF PS I	Unknown	12.24	0.089
F7		50	MCF PS III	Unknown	26.54	0.099
F8		50	MCF PS III	Unknown	26.62	0.099
F9		50	MCF PS III	Unknown	26.42	0.099
G1		100	B ACTIN	Unknown	13.13	0.208
G2		100	B ACTIN	Unknown	12.9	0.208
G3		100	B ACTIN	Unknown	12.71	0.208
G4		100	MCF PS I	Unknown	11.43	0.059
G5		100	MCF PS I	Unknown	11.41	0.059
G6		100	MCF PS I	Unknown	11.52	0.059
G7		100	MCF PS III	Unknown	26.67	0.252
G8		100	MCF PS III	Unknown	26.61	0.252
G9		100	MCF PS III	Unknown	27.07	0.252
H1	NTC		B ACTIN	Unknown	32.37	0.178
H2	NTC		B ACTIN	Unknown	32.63	0.178
H3	NTC		B ACTIN	Unknown	32.29	0.178
H4	NTC		MCF PS I	Unknown	26.85	0.416
H5	NTC		MCF PS I	Unknown	26.29	0.416
H6	NTC		MCF PS I	Unknown	26.04	0.416
H7	NTC		MCF PS III	Unknown	27.38	0.356
H8	NTC		MCF PS III	Unknown	27.12	0.356
H9	NTC		MCF PS III	Unknown	26.68	0.356

Raw Data from Real Time Experiment. All wells were run in duplicate and the data was averaged.

Plate	Well	Sample	Detector	Task	Ct	Ct std err	Avg Ct
Plate3	A1	BL/6 spleen	B ACTIN	ENDO	20.847	0.055	20.792
Plate3	A2	BL/6 spleen	B ACTIN	ENDO	20.737	0.055	20.792
Plate3	A3	BL/6 LN	B ACTIN	ENDO	20.66	0.093	20.567
Plate3	A4	BL/6 LN	B ACTIN	ENDO	20.474	0.093	20.567
Plate3	A5	BALB/c Spleen	B ACTIN	ENDO	21.427	0.071	21.356
Plate3	A6	BALB/c Spleen	B ACTIN	ENDO	21.285	0.071	21.356
Plate3	A7	BALB/c LN	B ACTIN	ENDO	21.586	0.232	21.354
Plate3	A8	BALB/c LN	B ACTIN	ENDO	21.122	0.232	21.354
Plate3	A9	NTC	B ACTIN	ENDO	33.381	0.19	33.19
Plate3	A10	NTC	B ACTIN	ENDO	33	0.19	33.19
Plate3	B1	BL/6 spleen	MCF PS I	Target	25.662	0.466	26.128
Plate3	B2	BL/6 spleen	MCF PS I	Target	26.594	0.466	26.128
Plate3	B3	BL/6 LN	MCF PS I	Target	23.22	0.109	23.111
Plate3	B4	BL/6 LN	MCF PS I	Target	23.002	0.109	23.111
Plate3	B5	BALB/c Spleen	MCF PS I	Target	28.246	0.06	28.306
Plate3	B6	BALB/c Spleen	MCF PS I	Target	28.366	0.06	28.306
Plate3	B7	BALB/c LN	MCF PS I	Target	24.063	1.407	22.656
Plate3	B8	BALB/c LN	MCF PS I	Target	21.249	1.407	22.656
Plate3	B9	NTC	MCF PS I	Target	28.569	0.215	28.785
Plate3	B10	NTC	MCF PS I	Target	29	0.215	28.785
Plate3	C1	BL/6 spleen	MCF PS III	Target	26	0.221	25.779
Plate3	C2	BL/6 spleen	MCF PS III	Target	25.558	0.221	25.779
Plate3	C3	BL/6 LN	MCF PS III	Target	25.275	0.027	25.248
Plate3	C4	BL/6 LN	MCF PS III	Target	25.221	0.027	25.248
Plate3	C5	BALB/c Spleen	MCF PS III	Target	28.598	0.03	28.628
Plate3	C6	BALB/c Spleen	MCF PS III	Target	28.658	0.03	28.628
Plate3	C7	BALB/c LN	MCF PS III	Target	28.019	0.006	28.012
Plate3	C8	BALB/c LN	MCF PS III	Target	28.006	0.006	28.012
Plate3	C9	NTC	MCF PS III	Target	29.7	0.11	29.81
Plate3	C10	NTC	MCF PS III	Target	29.919	0.11	29.81

APPENDIX II

The complete sequence of a PCR product, oriented in the 5'-3' direction using BL/6 mouse genomic DNA and MCF primer set 1 forward. The 3'-5' complement of the reverse primer for MCF primer set 1 is highlighted.

```
NNGCGGGGANGCAGGGGCCCAACCTTTAGNAGAAAAGATTGNAGNTCAGANGACAAAAGGCCTCCT
TTTTGGAATCCCAACAAGGGTGGGANATTTNNNCNTGCMNTNCTTGGAGAAAAGTCCCTCTNTCTCT
CNNTANGACNTNCNTNCNNNNCTNTAGNCNCCTTGGTCNCTCANTNGTCNCTCTNGNAGGCNNTTN
CTCNTTCCCCACNNGNCNTGCCTTCCTCNCATCCNTGCTGGNCNNTGAGNCGNCTTGCNANTGATG
CNTGCTGAGGTACCCCTCGTGATTCCACGTTTCNGNATCNTCNCCNCNCCNNTTGGTGTNGCCCGN
TNCCGNTNNTCTCNCNTCNCCGCCNATGNNTCGCNCCGGTNNTCTGCTNTNTNTTNTCGTTGACTG
NTANTGTGCNCTTTGGTCTCTTTNTTCCATCGCCTCCNTGTGTGTCTGNCGGGCNTTTGTGNGCCT
GCNCNTGNTCCGGCCTCNCATTTNTTCTANATTNTGNCCTGGNNTCCCTCANATNTCTCACCTTCN
GCNCCNTCTATTNCCNTTACNNAGNCNCTNCCCNCTCCTNTTCTNTTTCAGCCTNTCNCNTNCTNCT
TNNANTGNNTCGNTGTCNTCANNANGNCTTCAACTNTGTNTTGNNTGANGTCNTCNTCTNGCNNTN
ACTTTNGTNNNTNTTNNNTNNGTCNGTNNCCCTTNCCTATCTTTNTCNTGACTNCAAANNTNCTTCT
TNNTTTCCTGTNCNCANCTNNNTNCCNNTTCCCTANNTTGTNCTTNTNNNNNTTTTCATNGATTN
NCTNTNACTTTTCCNCCNCTCCCTNTTGGCTTGTGTCNNTGTNNNTNTTTANNNNTNCCCNATCNCCTGTC
TCNCCNNTTCTNNATGNCCTCCNNTTTNTNTNNNNCCCCCTCTTCNNATTACNNTTNGCACTNCTTTNT
NNATTCTTTNNNNATNTTTCTNNTTTNNNNCCATCCATNCCNNTNGNAATTTATTTTAANCTATTT
NTNTTATNCTCTNNTNNTNCTTCCNNTTTTATAATGTTTTTTTTTTTTTCCNCTNTTNTNNG
NNNNNTTTCCCNNTNATATTTCTNTTGNATATCTTTTCTTTATNNTTCNTTNTNNTNTT
NCNTATTNTCCTNCANTNNAATTNTNNTNTNANTNGNTGTTNTNNTTCCNTATNCCCTNNATTCTN
TNTCNTTATTTTTNTNCCCNCNTTTNTTTTNCCTCTTNTNCCCTNTNNNTTNTNGTTTNTTNN
TTTGTNTTTCNCTTTTTTTTTNNNTTTTNTTNCNATTTTCATTTNTATCTNNTNTTNTNNTTCT
TNNTTNTTTTGCCTNTTNTATTNTATCTTNTANNTATTTTCCTTCTNATNNNTTNTATNTNANTN
TTTNTATNTTAGNNTTTNTTTTNTTGGANNTTNTTCTNNTNTNTNTNTGTTNCTCTNNTAT
TATTTNNTNTNTTTTCTTNTTTCNNTNTTCCCTNNNTNNTNTTNTNTNTNTNTNTCTCTCCTN
NNTNNTCTNNTTTNCTTNTNNNNNTCTNTNTNCNTTNTNTTTTTTCTTNTNTNTNTNTTTTCT
TTTN
```

The complete sequence of a PCR product, oriented in the 5'-3' direction using BL/6 mouse genomic DNA and MCF primer set 1 reverse. The 3'-5' complement of the forward primer for MCF primer set 1 is highlighted.

TTTNGGGNNCGNNATCTTCTNTAGTTGGGCCATGCTATCCCGTACCAATCCTGTGTG**GTCGGGCAT**
AGAAACAGCANAGANNNCCTTCNTTTGGGTNNGTGTCNCCTGTCTCCTGCTCCNTGATTTTGCNGN
TCCTCCNCCTTTTCCCGTATGACCTCCTCNANTGNCTATNCNCCNATGGNCNCGGGTGNTNGNNNT
TCNGACGCTGGACCCGCTCCTCCCGCTTTTCGCACCTTNTCNCCGCCCTANNCGGCCCGCNCNGNG
ANGCNTCCTTNTCCCGGCGCCNCATGGNATGNTGTAGTTTTNTACNTGTANCCCTGTANCCNCTGC
TTGCCTCGCNTCNTTCCGNGCCCNCTGCTTGNCTCGNTTCTNTCCGCGCACCNCTATGNGNNNNN
TCNTTGCCTNGNGCTTCNTCTNNGTCNATGCCTTCNCNTGNGANANNCNTGCTTCGNTNGTCCCTA
CNTTGNTTCTCNTCGATCCGTTTCATCCTTCNTCTGTTGCTCCGNTCGNCNTGCNNCTGCCTCTGAT
GCTCCGNTTTCTTCTGCCCCCTGNNCTCTCTTCCCGNCCTCTCCTTAACCCTTCTCNCNGNTTCCC
CCNCCTTCTTACCTGTCNCCTGNTGTTTTNCNNTTTTNTCCCCTGCGTCTCTNNGTCTTTNNCNTN
CNNNTCCNTNGNTNNTCTNGNTGNNTNNTNTTNNNCNTNNTNTTNNNNCTTTTGNTNNNNCNNTTN
NNTCNNTTGTCTCNGNCTNNTCTNTNNCNTTTNNNNCTCNNCTTNTTCTNNTNNTNNTTNTTTGNNN
TTNNNNTTNCNNNNNTNTNTNTGTNTGNNNANCTTTNNNCNNNNGTNNCNNTNTGNNTNTNNTTTC
CNTNGNTCNCNNNNTNCNNTNCNNNNCTTATNNNNTTNTNTNNNANNNNTNTNNTTCTNCTCTTNC
NTTNTNNNGNNNTCNNNNNNNCNNNNNNANCNTNNTNNNNCNTNTNNTTNNNNNTNNNNNNNTNCN
NNTNATNNNNCTNNNNNANNNNTNNTNTNNNNNTNTNTNNTTNTNTNTTTTNTNTNNNNNNNNNN
NTNNTTNTTNGTTNTNTNTNNTTNNANNNNTNNTNTTTNNNNNCCNNTNTNTTNNNNNNTTTT
NNGGNTNNNCNNNNANTNNNTNNTTNNNCNNTCTNNTNNTCTNNTNNTNTNTCNTTTNNNTNTGN
NNTNTCNCNNGTNTCTCNCCTTNTTATNNNCNNCNNTTNNNNNTNNTNNTNNNNNTNNNCNNTC
NCNNTTNNNNNGGGNTNNNNANNNNNNTCNNTNTTNNCACNCNNCNTNNNNNTTNTNNTATNNANN
NNNNNNNNNNNTNTNNNNNTNNNNNNNATNNTNNNNNTNNTTTNNNNN

The complete sequence of a PCR product, oriented in the 5'-3' direction using BALB/c mouse genomic DNA and MCF primer set 1 forward. The 3'-5' complement of the reverse primer for MCF primer set 1 is highlighted.

GAGGCGGGGANGCAGGCCAACCTTAGTAGAAAGATTGGAGCTCAGAGACAAAAGCTCTTTGAATCC
CAACAANNNGTGNAGGGGAATNTGTATAGTGGCCTAAGAGNCCCGTCGCTGGTCNNCGAGTGTNACC
CCGTCCAANNGTCCANGTCANNACTTTCTNCANNNCCTCCNNNTACCACNCCTGCNNTTNTGAANA
NNCNGGCNNNGCCNCCTCNANNTNTTGTAGNGGGGCCNCNCNTNNGNCTCNNTNTGCNACNNCGCT
NNNCACTNACCNCNGGNCCANTNGCNGNTNTNGTTCCNNNAACCTGNNANNANANCCAACGGTNTCN
CCNNNNNTNCNNAGNATNCNACTNCTGNNTTNTCTNCTNCCNTTNTCTCGCCTNNTNGACTGNCTN
CGCCGTTNNCCTACNTTGCTNANCNNNTTNNNNNTCCNAAAGNCNCNTTGNNTTCTNNANCNNAGC
TTCAGNCTNTTCCNANTTACTGAGNNCTGCAATCTCCTAAGNTTNTCAACCCCTCCNTAANNCTT
NTTTTNCNGTTNGCNTNANANTCTCTTNNATNTNNTTTTCANNTTNTNATGNTTNTCNTGACAANT
GAATATCTTNGTTTGTCTNATNCCCACNNNCCGAANTTGNCTTAANNGAATAGTNTCTATNTTNC
NNAANGANTTANCCCNNTTCTNGTATTGTGNAANCTNTTGCCTAAAANCGATTTNTTCTNNTTGT
NNNCNGNNTTNNANTNNNNTTNAGCGTTCNTGNTTANNANTCANNATNNGTNATNCANTTANNGA
TGNGGTNGNTTCNNGTCTCCNATGTCCTTCAANAANNTTTTANNTNNNCNCCNCCNNGNNNNATTN
CNNTNNTGNTANTTTNNGTAANGNCCNNNATAGNNTTGAAGAGATTNNTTTAAACNNNNNTNNN
ANTAATNGNNTNTCNNTCTCCTTATCCGNAATTTNNATTGTNNTNTACTNTNTTGGCNTTCTNNN
CNTATTAAANTANTCTTCTATNGGNTNNATTTCAAACCCTTNCTTNATNATTGCTAAANTTTCTGC
ATCCCTATNATNNAANTTCNTANNATTTTNTTNCNTNGTTGGTAATTNTTCTNGNATCTNNTCC
TATNTTNATTGNANANNNTTTNNAATCCGCATNNTNTAGAATTGTTNNTTATNNNTATTTNNATA
TANGNAANNTNNTTGATTGNATNTTCCNNTTCTTCCCCTATANTAGNTTTTCTACNCNNAATNC
TNTNNTGTTTTNNGNNNNATTNTNNTTTTNTCNTCATNTNTATTTAAGNCTTCTTGNGNAANNTT
TCTAGNNTAAACTGNTNAGATTATAATGNATAATNTNATGNGNTNTNTTTATTATNTNATANCNN
CTCTCGTCTTTANANNTAATTCNCNGTTGNTATNTTCTCTGTNTTTTATAGATTCCCTTCTCTCT
TNGTNTCANNTTNTNTTNTNTCCTCTTCTCACTNAATTTNTTNNCCNNTNGTATGTGTTTATTGC
CATAGTGTNNTCTCNTNTTGTNNNTAGTNCNTNTTAANCATT

The complete sequence of a PCR product, oriented in the 5'-3' direction using BALB/c mouse genomic DNA and MCF primer set 1 reverse. The 3'-5' complement of the forward primer for MCF primer set 1 is highlighted.

GTTTTTNGGGNTNNCAANATCTTTCNCNAGTTTGGCCATGCTATCCCGCTACCAATCCTGTGTTGG
TCGGCATAGAAACAGCATTAANACTCTNNTTGGCAGAGGTGGGCGGATATCENNNGCTACTCTTANNT
TGNCTCCATAGTCNTCNGGTTCAANTGTNNAANGATACTCCAGCACNTATTCCCCANTGATTACNAG
NANCTGGTGACCNNNNCAGTNGGAGNGGNTGNCNCCANCTTCANANGCACCNCNCGNACCNGANGC
ANANGCCCCNTGAGTACNGCCNTACTNCGCCCCCAAATGCATTGCGACGATTTTCCAGNTGTATCN
TTGNCTCGAAAGTNAGCTNNCGNNNTCCTNTNGCCGCTGCTTGCCTCGCTGTCTTTCCGGGCNCC
CTCGATGCCATGCNTTTNAAGCNTCANNNGCATANCTGNNTAGTCTTNAGCTTGNGNANACNNCA
TCNTTATGGCATCNACTGTGATTTTCTTGNTGTNTTCATCNGTNNATTTTNTCTCATCGTCNNGA
ANGACNTACATCTGANGTNCCGTATAGGTCATGNANCTGACCCCNATTNTNCGNTTCTTNCGANNC
CTTCNCTANTCTTNCCCATCNGCAACANTATCNATTCACCACAGGTNNGANNNTCANTGCCNCTTA
NGTAAANTGNTTTNNTTCGTTTTNANTCCCATGCNCANCTTCGANNCGTNGCTAANNNGTTTTNAN
CAATAANTTGAACNATTNTNATNNTCAATATNNTTNNAANNTCTCENNNGGNANTATTNNNGNCNCT
GTNTTNNNTTTNTTTTGANTNGTCNNTTNNANNTTGCCAGAGANNTNNCNNATNTNTGANNTNANT
TATNNTCNTTTNTCCNATTGTATNNTTTNGTNGTNNCCCCNNANGNNNANNCTGCAATNTTCNNT
GNTTNACAANNCAANTTTNNGNGNTTACTTTNGTNNAGANTCTTAATTTCTNCANNTNANTTNAATN
NTGTCANTTAGGTTNGTNNNANNTCNCNTNNAGTTNNAGNNANNNNAANGAGNTNCCNTCAGNTTNN
TCGGNTNNTTNATNCAATTNNNTGGGTNAAGNAGGTTTGTNTTNNTTCTNACCAATAATTTT
NNCAAGATTNAAGTNGATNTTAGGNTNCCAATCTTNTGTATANTTATGNTCNAACNNNTTNAGN
NGNATGGANNTCTNTCNTTATNTNTTANANAAAATACTTCANNNANTNTNTAANNNATNNACCTGA
GCNNNANNNNAATNAGTNCNANTTCNTNNAATNTTTCTGTTTTTATAGATTATNATATTCACTTCGC
TCCTAGNNTTGNTGNATCTCTNTNCTTNTTGGTNTGNTNTCANNTTGAGNNGTGCGATGNNTTAN
NCTCTCTTANTTGTGTCNTTNTTGTAGTNNNTNTTNTTNAACANN

The complete sequence of a PCR product, oriented in the 5'-3' direction using LP-BM5 infected SC-1 cell cDNA reverse transcribed from RNA and MCF primer set 1 forward. The 3'-5' complement of the reverse primer for MCF primer set 1 is highlighted.

GGCGGGANGCAGGCCAACTTAGAGAAAGATTGAGTCANAGACAAAAGCTCTTTGAATCCCAACAAG
GGTGGAGNNAATNTCNTGNGGACAAAGCCCNNNTCCNCANNNNTNGAGTNTCTGGCGTNCAGCGCCN
GNCNGCACTNANCCCCNGCCTCCAGATCCANAGATGCNTNNNCCAANANANTGGCCNCGGNGNCNNC
CANAATTTTCNANGAGGGATNCTCGTCATNGTTNNNTNTGTTCTTNCCCTNNACCNTNCNNNNGGCCC
GATGNNGATNNCGNNCATNNNANTGANNTNNANNAGCGCATACAGTGNTGNCTTANNNTANNAGTG
ANANTNANTGCTGGNTTGTTCATATTNTTCATTNTCNGCCTNGCGNTCNGGCCNNGCCTTNNNCNTN
NNNTGNNATCNCGACCTTTNTCATTCTNNNTAANNTCNNGATNGANNTCCTNTCAGTNTNACGNN
TCAGNNTTNGTANNTNCGNTTGAANANNGTACTACANNNNTNNNTTGTCTTTTGCANCNTTTCTA
NNNGCNNANCTTATANTNCNGTAAATGNNNTNNNATTNNCCTTNATTNTCNGNNCNTTTCNATTTTTN
GCTTNTNTNTNTGANCANNNNTNCNNTTNTATNGGNTTACNNNNCGNTNTCAATATNCNNCTAN
TTNTNCANTNGNNTAAGNAATTNTCNCTNCCTTTTNTNTANNTGATCNTGNAATGATNCCNCNANT
CTNTCCGNTGTNTTNGNNNNCTATCCNTCATCTNTGNANNTNNNTNGNTNAGNANNTTCANCTNCGC
NNNACCNATNTCGTNNTGTTTNCNGNNNATNTGANCANTTNTCCATNTNNGCNAANATTNNNTNN
NATAATTTGGNATATAAGAGTNNGNTGGCCTCTCTNTANNANTNTTTAGTTATAGNANNATCTTAA
NTNNATTNACTTCATNATAANCNTNCNNTNNNTANTTCNCCACTNNCAGTTCATNTTGANTNTNTN
TNNNAANNTTNTNTTNTNATANATNTTACGGTNTGTCCACTTTCNAGATTTTNTATGNNNTTTAT
NTTNCNATNNNTNNNTNTANTATATNTNNNTNTTNTCTATNGANTNATNGGNTTNCGTAATNTT
NCGTNTCTNAANATTTTTAATCGTTNGNNNATNCTCCTCTTTTTNTTAGTNNATTAAATTTNACTCT
NNNTGNNNTNGNTGTTTCATCTANNCTTNCCTNNNTATTNNNTNNNTNATTTGNTNTTNTNGGNTTTTT
AAATTNNNTNCNTATTCNAACTNNNAAANNNNNNTTTTNTNNNNNTCAGNNTCCNTTTTNTNTGCTN
NNATNTTTTTTCCACTTACTTTTTCTATNTNTTGTATCCTNAGTTTNTCTCTNTCTTCTTATANN
TNNANCCCTTNTTNGGANAANCCTCTTNTNTNTTGTNTTTTNTATNTTNTNTGNTNNGNNNTTCT
GTATTCNCATTTANTCTTCTATNTGNATTANTTCNNTCTNNTTANNATTTNTACTCTTTTCTGNA
TNNNTATTNNNTNCCCNCACTNGTCTTGTCTANNTTCTNTACTNTTTGNNNTNTTATCNNNNNTNGA
TGNCNNATTCACTTNTCTTATACNATTCTCTGTTATTATTGNCTTANTCTCTTTTTNTTTTG

The complete sequence of a PCR product, oriented in the 5'-3' direction using LP-BM5 infected SC-1 cell cDNA reverse transcribed from RNA and MCF primer set 1 reverse. The 3'-5' complement of the forward primer for MCF primer set 1 is highlighted.

TTTTTNGGAAGTNTTGGANATCTTTCTCTAGGTTTGGCCATGCCTATCCCGTTACCAATCCTGTGT
GGCTCGGCATAGAAACAGCATTAACAGNCTCTTAGTTNAGAGANNACGNTCNTCTNGNATNGNTGCT
ACNNNGTNNNNCCTACGTCATCAGNTCTTCGGTGGTATNNNCCTCNTNCANTNGNCTTNNCNCNG
NGTNNGCCGGNNTATCTTGGTGANNNNNGCAAGTGNGAGNGGGCTGGNNNNTGTTTCAGAAACCTC
TCCNCTCGCGGNTAGNNNANGCNCGNNGCAGTGNNNGCCNTNCNCNTTCCCGANNNANNATNNNG
GCANTNGCTTATNNTATTNCATTGTNNTNGTNTGGAACGNTNAGTTGGTCTNCNNGTCCATTNNTN
CNGCNGNNTGCCTGTCATNTTGNCNGNCCNGACCNANCNNCACNTGCTNTTCCAGTNTTTNGACGT
CGCAANCATCTGCACTGATNTGTNGCCTTGGGGTNNGTGNACGNGTCNCTNTNNTCTTTCTTGAA
TTNATTTTTCAGTNTTNCNTNGANTCNNNNANATNNTTTNNGGCATCNAATGTNCNTCACANCTNN
TGGNNNCNATTTNTNGNNNTNNTCCNTGANNNNCGTACNNTNCNNNTNTCTCNNNCNNTNNNNTTA
NACNNATCTTCCNCGANNCCNATNNTTCTNACNATNTNCCNGTCNCCTTGNTNTNTCATTNANT
NANNTTTGNACNTNTGANNTATNNTNTNAGTNNTTNCNNCTTTNNCTCACNTTCGCCTGTATTTTN
TGCNNGAGTANGAAAATATTTNANTTNAANTNTCCNTNATTTTTTNNTGTTNNNCAANAATNCNTGN
GANNCCANATNNGATNATTANTTNAAANTCNTCTNNGTCNNNNNGTGNTTTNTNNNAGNTANTN
TGANACNTAACNANNNGCNCATTANNAATNAGATCANNACANAATNNTNATNANTNNCTNTTNCTG
NNTANTTNATNCNNANNTATGGTATGATTCAATNTTNNTTNNCNCNANNATNAAANNANNGTTATG
ATAGNCNCTTNAAGGANTNNNNTCGTTNTTTNNGGNATNCCNNNTNATTGTGANATTTNGNAT
TNANANACGNNTTANNCGNNTNNNNANTACTNANNTTNANNTATTNTNAAGGTNCTTNNANNNAAA
NCGTNTTNTANNTNGNGNCNTCCNCNNGTGTAATNTCTTTNTTATTNNNATNATTTGTANTNTTA
ANATGAGTANCTATTNTTCCNTGTGTTNNAANCNNTNNGTNNNATGAGGNATTANNTNTNGTGTAT
NNAGNNTNCGTCCNATTNNTTNACNGTTTGTNGNTTCACTCATANTTNAATTNANNTCGGTGTNTA
ACNATCNTTNNGNCNNNGGTCANNNNNNGGCATNATNNTGTGCTTTTNNTTTTNAN
TGNNTANNANTNTANANGTTGATAAGNGATNTGAGNTTGCTATTTNGTNANGCTNTTATNTNTTNA
NATNTATTNCNCTACACNNNTATNTNTTGTNTNNNTATTACTCTNCTTCTTNNCNGCTCGGATANG
NTGTNGGNNTGCGTGCTGTNTTGATTNNGTNTNCTANNTNNNGTNTNTTTCTNTATNCTTNATT
TNTGNCATTA

The complete sequence of a PCR product, oriented in the 5'-3' direction using BL/6 mouse genomic DNA and MCF primer set 3 forward. The 3'-5' complement of the reverse primer for MCF primer set 3 is highlighted.

```
ANTGGGNAGGTGCCAACAGGAATATCTGTGGTCNAGCACCTGGGCCCCGGNCTCAGGGCCAAGAAC
AGATGGTACTCAGATAAAGCGAAACTAGCAACAGTTTCTGGAGGCTTNTCGCCGCTTGANGCCTG
GTCNAANCAGTNTCCTCAAGCCATGNGCCTTCATTANNTGCNTTANCAAACANNGTGGCCTANGCG
NCCNCCANGATGCTNGTGNGGACTNCTCNNAAGAGNCANTCTGCNCCCNCNNACNACCNNNTG
GCCCCNTCTNGATNTCGNGCTNNCNCTGAANTAAGTANGNNCNTACNGGTTTNCNTATNTTATTNG
NNAANNTNAATGTCGNNTTNGCTNNTATNCNNTNNCTNTCTTGTGGGCNNTCNNCTCNTNGNAGNC
TACNNTCGNNCNGTTCCCTTTTTTCATTNNNTTAAGGTCANATGNNCTTCCTNNNACCATTCACTNNT
CNTCACNNGTNATTTTCGCTTGANNAGTNCCTTNNCTGTTGNTTCTATTNNNTCCTTTACNNA
NACNTCNNTNATTTTCCTNGTNAGTTCATTAGTCNTGTCCTTGCANNTTCTGTTNTTATCNNTTTN
GNGTNCATCNTNNNTGTTGTANCNTNCNTNNTTTATTCTATNTTNTGNGNAGNNATTTATNTNC
AATNNNCCTTTGTCATGCACTNCTNCTTNTNTNTTTTNCNANTNNTNATCTTANNTCNTCT
TNACGATNTGTGTGNANNNNTTNANNTTGTGTNNNATTTTATCCTATTAAANNTTNACTTNCCA
TNANCCTTTGCTTNATNATTGTTTTATTCTNNCTTACNNNNNTCCATTTANTCTANTNTTATCAGA
ATATTTNTNTNGANNANCTTTTNAATAATATTNNNTTGNNNACTCNNTTNNNNATTNTNTTTNNA
TATTTCTNTNNNTNTTTTCCACTNCANANCTTNTATGAANNNTNCTANTANACTGTTGTATTTNTA
TTTTCTCTTNTCTGTNTNTTTCNCNGAATTTGTTNTATTTTTTATTTTTTCTGTCNTTCTTTNANN
GNCNNNTATTTNCTTTCTNNANTTTGTNNTNNAANTTNCNTTCCANTTNAACTNCCACATTTTNT
NTTNCNCTTNANNTNNCAATANNNNATNATAANNNTCNNACTTNTTTTGTTTNTNTCACTTNNC
CTNNTNATTTTNCNNTTANCNTNTTTTTTNTNANTCNCTTTCNATTTCTTNTTTATTNTCTATTN
ATATACATATTTCTNTNCATTGTTGTTCTNTTTTNTTTTTTCTNNTTNTTNTCCATNTTTTTAAT
ATNNNTNTTTCTNCTTAATTTTNTATTCTTTNCCTATTATATNTTNTNACACTCTTTTCGANTNANC
NTNCNNTATANTNCATTNNTNTTTNTNNTNNTNTNTNAAANNNTTTNTTTTCTNGTNTTNCCTC
TTTACNCTATANATTANCTTCTCTTTNGANTNTANTTCNNTGTCTTCNTNNNTTTNTAAATTTCC
TTTATACTNCTATATTNTGTNTTTTGTNTNTTTNTTTTNTCCTNNNTTANNTTNTTCTCTCTA
TCNANTNCTTNTCTTTATTNNTTCTCTNTACTTTTTTNT
```

The complete sequence of a PCR product, oriented in the 5'-3' direction using BL/6 mouse genomic DNA and MCF primer set 3 reverse. The 3'-5' complement of the forward primer for MCF primer set 3 is highlighted.

```
NGGGGGTGANANTGTTCTGGCCTGAGCCGGGGCCAGGTGCTNGACCACAGATATCCTGTTTGGCC
CCTGTCCCAGTATTGTTCAGCCTTATTCTTTAACTAACTTCCAGATCNGCTGNTTGAANCTAANC
CNGCACCNATTNNCNAATGACCACCAGAANTGGNGANCGANNGATTGGAANGGGTGGNGCCATCTT
CAGANGCGTGGCCGGCNCCAAAGGCAAANGCACCTTGNGNACGCCATAGGANGGNCNNAAGTGCA
ATGCTTAATTTNCCAGGTGTAGCNNTGCAACGTAAGTTAGATACCGNTAANCCNANAGCNGCNGCT
TGCCTCGCTTCNNTCCGGGCANNCTGCATGCTCATGNTTTNGNGCCGCNAACCCGAATGTGTTTA
GTCTTTTAGCTTGAAAAACAGCATCNTNANTGGCNTNAGCNNNGATANNCTAGATGCGATCGANNGT
NAANTNTTTNGCATCAAATGNGAACAACCTTCANNNNGGATGTTCAGNAAANNCATGNAACTGANN
NCCATTTCATCGTTNNNATNCGGACNCTNATNTNTNNTCNCANCCGNANACGTTNNCCANNANCNCN
GGTNNACCAGANGNTACTCNNTCNTGTGAACTGGNATTNATTTNAGNTNAGATGCACATGCGANAT
ANACGGTAANAACANACAAANTCCATCGCNNTNGNAGNGNTANANCAATNTGGTTNAANN
GGNNANNGANCGTNTNGGTANTAAATAGNNCNGTGCNNCGTTATAGGNTTNAATCNGAGNATGN
GTNNNTAATNNATNTGATNANNNAANNAANNTGNGTANCANAANGAAANAANCNTGAANNAANGA
GGNNAANTAGANGNGTGNNTCNCCACGANNANANGNATAANNGANNNTNATGACNNGAGNNANATG
AGAAGAATTANNANCNTAGTAAAAAAGNNCTTNNNANAGNNTTNCNNNNNNNAATANNATTGTNAG
NATNNATANANNANAATAAACANTNNNNGGGAAATGNNACNANTCCNNNANNTCAAATNAACANTA
NAAGGTCCAAATANAGANNAGTTAATNTNNATGATNNNNNTANGATCAANANNGNANAATNAGGAAN
TATNNACAATTTGNTTAACTNTAANNTAANTNNCAGNTATNNATGTNNGANCGATNTNGGANNNNNA
ANGNACANCCNTTGNGANANGTTNNANNTGAANCATNGANGTAAGNNNATATNNGANNAANNTNT
GGAANATGGNNANCCANNANGANTATNGGATGTTNTNTGAGCTTCATNATNTCNCNNANAATNGAA
GTNNGNNAAATCTANACATTNNNNCCNGTNTTATTTNANNGTGAANTTANTTANGNAATNGGNATN
NNNGAATANTAAATATNTNGANNTGTNTTTTNCN
```

The complete sequence of a PCR product, oriented in the 5'-3' direction using BALB/c mouse genomic DNA and MCF primer set 3 forward. The 3'-5' complement of the reverse primer for MCF primer set 3 is highlighted.

```
NAACTGGGNAGGGGCCAACAGGGATATCTGTGGTCNAGCACCTGGGCCCCGGCTCAGGGCCAAGAA
CAGATGGTACTCAGATAAAGCGAAACTAGCAACAGTTTCTGGAATGNTATCCCCCTCTTTTGCCTNT
CNNAACTTTTTCCNATNCNTTCCATTACCANGCCTNCTNTTNTGAATANTNTGGACNTGGCNCCCN
CNATANNTTNTAGGGGNGCTNCNNGTANTNCTNTTCTGNTCCTGNGNNCNTCACNACCCNCTNGC
CNNNTGTNGTNTTNGTTCTTCAACNNAAGAANAANGCCGCAACGCNNTCNCCTTATTNTNTCTNA
TANNATGTCNTCTTGGTTNCNCTTNTACNNNTTTCCTCCTNGTCTCANNGTCCNTNNNTNATTCTT
ANTTNGNTGAGTANNNTNNCATTTCCTTCNNTTCGCNTTNAATTTCCTTNATNTNACGNNTCANNNA
ATTTCTCGCTTAAAGAGNNACTNNAATNTNNTNATATNTTANCNNNTCNTTANNNNCTTTATNNC
CTNNTTNNCTTNTGTCTCTTCNNAATTTGTTCCNNNCATGCNNTCNAAACTTTACANTTNNCNNNCN
TTCTNNNGNTTNTNTNNTACATNTNTCCNNNTTGNTTNNNTAANANCTTNNCCNNCNTTNTTNT
NGANATNTCTTNTCTCTCANTNTCTNANTNTGANCATTNTTNCANTTATTTTCGATTTTNTANCTTG
TNAAATNTATCCACGATCTNTTTTGNANCNATTATTATTTATTTTNTNNNNNTTNCCTACGATATG
TTTNTTNCNNTTNNATNTNCCNTGNCNNNNNNNAATTNAAATTTGANNCNTNNTTNNAATTNCTTT
NNCTAATCTTTTATGNTANTTTCCAATTCNGACTTNNNCNTATTTNANTTATTNNTTCTGTTNTAA
TCATTTCTNTGTNTNTNNTCCNCNAANNTTNTGANGTTTTATTCTCTGACCNNCCTTATGNTATT
NNANTTTTTTNTNTNNTNNCTTTNNCTATNTTNTTCTATTANNTTATTNTTTTGNCCNCTTNNCT
TTNGTTCTTACTTCTTNTNATTNTNNATCTGNTNNNTTNTNCTTTNTCNCATNTCCNCNNTTNTNT
NACTNTNNTANGNNTTNTTTTNNCTNNCTTTANNTTGNTTNNNTATNNCCCTCTTTAAATATTCAAN
TATTTAGTTTGTATTNNNTTANNTNNCCTATTTNTCATTTCNNCTCTATTTCTNTTTGNCCTCTTA
TNAAATCTTTTCNTCTTTCCTTNTGTNTNNCCCTTTTAACTANTTCTTCNTCTNGTCATNTTT
NTTTTNTNATCTNTTTTANTNNNCTTNTCTTTATTTANATTNCTCCTATCNNNTNANTAANTTTT
ATNTNTCCTTANATTNNATNTACTTTTCATATTATCTTTTCNCTTTNTNCTCANTTNTTCTTTNTCC
NCTTNTATTNTNNATTTANNTCTCTTNGTGACNTTNTNNTATNTTTTCNTCTTTATTTNTTNGTC
CTTTTTTTTG
```

The complete sequence of a PCR product, oriented in the 5'-3' direction using BALB/c mouse genomic DNA and MCF primer set 3 reverse. The 3'-5' complement of the forward primer for MCF primer set 3 is highlighted.

```
NGGGAANTCTGTTCTGGGCCCCGAGCCGGGGCCCAGGTGGCTNGACCACAGATATCCTGGTTTGGC
CCCTGGTCCCAGNTATTNTTCAGCCTTATTCTTTAACTAAACTTCCAGNTGNTCGNGGTTNACCCT
AGAGCCTCAGCENNAGCTGNCGAATGACNTCCAGNGNNGNNGNCGNACNGAGNNGAAGNGATGGTGC
CGCNTNCAAAGGANGNGCCNGCACCANNGGCAAAGGCACCTNGNGTACNNCAGNGNNGGCCCNAT
GAGCACTGCTTACTNCNCAGGAGAAGCNTTGCNNGGTTAGNNAGNTNTNGCNANGCCTCGANNGG
CAGNTNGCNTCGGNTCTNTCCNNGCTGNCNGGNTGGCATGNTNTAGAGCNGCGNNCTGGGANNNG
TNNAGGCNTTAGGNNGAANNACTGCANNGTCNGNGGCNTGAGGAAGNGNGATGNTTGANGNGATCA
GCCGTGANNTTCTTGNCAGCCATCNTNTGGNNACCNTATNTCGGGGNGNCNAAAAGACNNCNCAAC
TGNGGANCNGTNCNCNNNATGCNNNTGTNCNACTAGTCANAGCTTCTTCCGANNCCTTNTCTATCT
NCCNCGAACNGCACCATNCGNCTACNACCTGGGGGANCGNANNNANTACNTNNNTAGACCNANGGN
NTTTNNGNCGGTNTAANACNATGCACCTCGCGGAAGGNNGGAAAGANGAGANAGTNNAATAANNNGN
NANAANNAGGNTGAANGATAGTTGGGNCCNGTNNNANGNNAANNTGGANNNANNNNTANGNGGACA
NNNGNANANCNGAANGAANANNNNGNNGAGANNNNGNCNNANNNNNNAAATNTNTANGGAGGT
ANNAGNTTANTNNNNCTTNGANNTAANAGCCNCTAAGGGGAAACNGAGCNAAGATCGGNGGANNNN
AATCGTGATTGGGGGTNNNNANGTAAANANAACNCGANNTTNTGTNGGTAAAANAGNAAGNNNTGN
NNTGGNGNAAANNAAAAACNNNNGGNAGGANCNGNNNAANANNAANANCNNNTNNATNGGNAGNTT
NATNAAANNATTTANANTAGGGGATGANTNNGGGTGAATAAGTATGTNNAGANNANTNNNAAAGNT
ATGGGGATANTGTNNANTATTTNGGGNGNNNACATGGTGGGGNNANGNGAAANCCCNAGNAGNAAA
AANNTAANAANNTNNNTTGN CNATGNAAATCNGAATAANTNATGTTGANGGTAANGNGNGTAACGN
ANGNAATAGNNCNGNAAAGNNANNNACTCTNTNNNANTANNNGNANGAATNGCNANATGGANNATN
GGNNGAATATGNTACATATGTNTGANATCAACNNGGNGGNGNNCGNNNGTNTNGNTNNCTNNGTG
TGNGTATTATANNNTNNGNANCTNNTANNGA
```


The complete sequence of a PCR product, oriented in the 5'-3' direction using LP-BM5 infected SC-1 cell cDNA reverse transcribed from RNA and MCF primer set 3 forward. The 3'-5' complement of the reverse primer for MCF primer set 3 is highlighted.

[illegible]

The complete sequence of a PCR product, oriented in the 5'-3' direction using LP-BM5 infected SC-1 cell cDNA reverse transcribed from RNA and MCF primer set 3 reverse. The 3'-5' complement of the forward primer for MCF primer set 3 is highlighted.

GAGNAATCGGTCTNGGCCCNAGACCGGGGGCCAGGGANGCTNGGACCACAGGATATCCGNGTTTG
GGCCCCNGTCCCAGTATTNTTCA**GCCTTATTCTTTAACTAACTTCN**NGANNNNNNNNGNNNGNNN
NANNGNNNNNGGANNNNNNNNNGGNNNGNNNNNNNGNNNNNNNGGNGNNNNNNNGNNNNNNNNAN
NGGNNNNNGNNNNNNNGNNNNNNNNNNNNNGNNNNNNNNNNNNNGNNNNNNNNNNANNNNNNNNN
NNNNGGNGNNNNNNNNNGNNNNNGNNNGNNNNNNNGNANNNNNNNNNNNNNNGGNGGNGNGNN
NNNNNNNGNNNNNNNGNNNNNNNNNNNGNNNNNNNNNNNGNNNNNNNNNNNNNNNNNNNNNNNN
NNNNNNNNNNNNNNNGNNNGNNNNNNNNNNNNNNNNNNNNNNNGNNNNNNNGNNNNNNNNNNNN
NNNNNNNNNNNNNNNGNNNGNNNNNNNNNNNNNNNNNNNNNNNGNNNNNNNGNNNNNNNNNNNN
NN
NN
NNNNNNNNNNNGNN
NN
NN
NN
NN
NN
NN
NN